

Aus dem Forschungszentrum Borstel
Leibniz-Zentrum für Medizin und Biowissenschaften
Abteilung Immunchemie und Biochemische Mikrobiologie
Leiter: Prof. Dr. Dr. h.c. Ernst Theodor Rietschel

Mechanismen der Granulomnekrose bei mykobakteriellen Infektionen

Inauguraldissertation
zur
Erlangung der Doktorwürde
der Universität zu Lübeck
- Aus der Technisch-Naturwissenschaftlichen Fakultät -

Vorgelegt von
Sahar Aly
aus Alexandria/Ägypten

Lübeck, 2006

Erstberichterstatter:
Prof. Dr. Dr. h.c. Ernst Theodor Rietschel
Zweitberichterstatter:
Prof. Dr. med. Jürgen Westermann

Tag der mündlichen Prüfung:
Lübeck, den 12. Juni 2006

From the Research Center Borstel
Leibniz-Center for Medicine and Biosciences
Department of Immunochemistry and Biochemical Microbiology
Head: Prof. Dr. Dr. h.c. Ernst Theodor Rietschel

Mechanisms of granuloma necrosis in mycobacterial infections

Inaugural Dissertation
for
Obtaining the Doctorate Degree
of the University of Lübeck
- From the Faculty of Science and Technology -

Submitted by
Sahar Aly
from Alexandria/Egypt

Lübeck, 2006

First examiner:
Prof. Dr. Dr. h.c. Ernst Theodor Rietschel
Second examiner:
Prof. Dr. med. Jürgen Westermann

Day of the oral examination:
Lübeck, the 12th of June 2006

Contents

Title	Page
List of abbreviations	IV
List of figures	IX
List of tables	XI
1. Introduction	1
1. 1. Epidemiology of tuberculosis	1
1. 2. Immunology of tuberculosis	3
1. 3. Protection and pathology of tuberculosis	7
1. 4. The animal model	10
1. 5. IFN- γ -mediated mechanisms of necrosis	11
1. 6. The physiology of mycobacterial lesions	12
1. 7. Aim of the work	13
2. Materials and Methods	15
2. 1. Materials	15
2. 1. 1. Chemicals	15
2. 1. 2. Reagents and media	17
2. 1. 3. Kits	19
2. 1. 4. Antibodies	21
2. 1. 5. Equipment	21
2. 1. 6. Bacteria	22
2. 2. Experimental animals	23
2. 2. 1. Immunocompetent mice	23
2. 2. 2. Immunodeficient mice	23
2. 3. Methods	23
2. 3. 1. Mice	23
2. 3. 2. Bacteria	24
2. 3. 3. Infection of mice	24
2. 3. 4. Infection of guinea pigs	25
2. 3. 5. Organ dissection	25
2. 3. 6. Homogenization	26
2. 3. 7. Bacterial load	27

2. 3. 8.	Histology	27
2. 3. 8. 1.	Paraffin sections	27
2. 3. 8. 2.	Haematoxylin-Eosin (HE) staining	27
2. 3. 8. 3.	Ziehl-Neelsen (ZN) staining	28
2. 3. 8. 4.	Frozen sections	28
2. 3. 9.	Immunohistochemical analysis	28
2. 3. 9. 1.	Hypoxia and HIF-1 α	28
2. 3. 9. 2.	iNOS and HIF-2 α	29
2. 3. 9. 3.	Endomucin	29
2. 3. 9. 4.	Counter-staining	30
2. 3. 10.	Enzyme Linked Immunosorbent Assay (ELISA)	30
2. 3. 11.	RNA preparation	31
2. 3. 12.	Ribonuclease Protection Assay (RPA)	31
2. 3. 13.	Affymetrix gene expression micro-arrays	32
2. 3. 14.	Oxygen measurement	34
2. 3. 15.	Statistics	35
3.	Results	36
3. 1.	Mouse model of mycobacteria-induced granuloma necrosis	36
3. 2.	Absence of granuloma necrosis in IFN- γ deficient mice	37
3. 3.	Granuloma necrosis in IL-18 deficient mice	38
3. 4.	Absence of granuloma necrosis in mice deficient for the IFN- γ signaling molecules STAT-1 and IRF-1	41
3. 5.	Granuloma necrosis in IFN- α/β -receptor deficient mice	43
3. 6.	Differential gene expression in wild-type versus IFN- γ deficient mice	44
3. 7.	Differential expression of angiogenic and angiostatic factors in wild-type versus IFN- γ deficient mice	47
3. 8.	Granuloma vascularization in wild-type and IFN- γ deficient mice	50
3. 9.	Vascularization and granuloma necrosis in CXC-receptor-3 deficient mice	51
3. 10.	Hypoxia in pulmonary granulomas of <i>M. avium</i> -infected mice	53

3. 11.	Hypoxia in pulmonary granulomas of <i>M. tuberculosis</i> -infected mice	56
3. 12.	Pulmonary oxygen concentrations in <i>M. tuberculosis</i> -infected mice	57
3. 13.	Hypoxia in granulomas of guinea pig lungs infected with <i>M. tuberculosis</i>	59
4.	Discussion	61
4. 1.	Signaling pathways downstream of IFN- γ	62
4. 1. 1.	Type I and II interferon systems	62
4. 1. 2.	IFN- γ -mediated mechanisms	64
4. 2.	Angiostasis and vascularization	70
4. 2. 1.	Imbalanced angiogenesis in <i>M. avium</i> -infected mice	70
4. 2. 2.	CXCR3-mediated angiostasis in <i>M. avium</i> -infected mice	73
4. 3.	Oxygen concentration inside granulomas	74
4. 3. 1.	Non-replicating persistence	74
4. 3. 2.	Anaerobic respiration	74
4. 3. 3.	Evidence for hypoxia	78
4. 3. 4.	Consequences for TB treatment	80
5.	References	82
	Appendix 1	i
	Appendix 2	ix
	Appendix 3	xii
	Summary	xiv
	Zusammenfassung	xv
	Acknowledgement	xvi
	Danksagung	xvii
	Curriculum	xviii
	Lebenslauf	xx

List of abbreviations

Name	Abb.
α -Crystalline	Acr
Adenosine triphosphate	ATP
Analysis of variance	ANOVA
Antigen presenting cell	APC
Bacterioferritin	BfrB
Biological safety level	BSL
B-lymphocyte chemokine (CXC-ligand-13)	BLC (CXCL13)
CC-ligand	CCL
CC-receptor	CCR
Centimeter	cm
Cluster of differentiation	CD
Coenzyme A	CoA
Colony forming unit	CFU
Complement factor	C
Complement receptor	CR
Complementary desoxyribonucleic acid	cDNA
Complementary ribonucleic acid	cRNA
Count per minute	cpm
Cubic feet per hour	CFH
CXC-ligand	CXCL
CXC-receptor	CXCR
Cytidine triphosphate	CTP
Degree Celsius	°C
Delayed type hypersensitivity	DTH
Dendritic cells	DC
Desoxyribonucleic acid	DNA
Directly observed treatment short-course	DOTS
Double-distilled water	Aqua bi-dist.
Enzyme Linked Immunosorbent Assay	ELISA

Epstein-Barr virus-induced molecule 1 ligand chemokine	ELC
Expected proportion of false positives when calling an effect significant	q-value
Fc-family of receptors	FcR
Figure	Fig.
Flavin-adenine dinucleotide	FAD
Fold change	FC
Glycine dehydrogenase	GcvB
Gram	g
Granulocyte colony-stimulating factor	G-CSF
Guanosine triphosphate	GTP
Haematoxylin-Eosin	HE
Hour	h
Human immunodeficiency virus	HIV
Hypoxia inducible factor	HIF
Hypoxic response element	HRE
Immunoglobulin G	IgG
Inducible nitric oxide synthase	iNOS
Interferon	IFN
Interferon regulatory factor	IRF
Interferon-alpha activated factor	AAF
Interferon-alpha/beta-receptor	IFN- α/β -R
Interferon-gamma activated factor	GAF
Interferon-gamma activated site	GAS
Interferon-gamma-inducible protein-10 (CXC-ligand-10)	IP-10 (CXCL10)
Interferon-inducible T-cell chemoattractant (CXC-ligand-11)	I-TAC (CXCL11)
Interferon-stimulated gene factor 3	ISGF3
Interferon-stimulated response element	ISRE
Interleukin	IL
Interleukin-1 β converting enzyme	ICE
Isocitrate lyase	Icl
Isoniazid	INH

Abbreviations

Janus kinase	Jak
Kilogram	kg
Knock-out	KO
Lipopolysaccharide	LPS
Lipopolysaccharide-induced CXC chemokine	LIX
Lipoteichoic acid	LTA
Lymphotactin	Ltn
Macrophage inflammatory protein	MIP
Major histocompatibility complex	MHC
Mannose receptor	MR
Messenger ribonucleic acid	mRNA
Micro-Curie	μCi
Microgram	μg
Microliter	μl
Micrometer	μm
Micromolar	μM
Milligram	mg
Milliliter	ml
Millimeter	mm
Millimeter of mercury	mmHg
Millimolar	mM
Minute	min
Molar	M
Monoclonal antibody	mAb
Monocytes chemoattractive protein-1	MCP-1
Monokine induced by interferon-gamma (CXC-ligand-9)	MIG (CXCL9)
Multidrug-resistant tuberculosis	MDR-TB
Mycobacterium	<i>M.</i>
<i>Mycobacterium avium</i> complex	MAC
Mycobactin	MbtB
Mycolic acid cyclopropane synthase	PcaA
Myeloid differentiation primary response gene 88	MyD88

Nano-Ampere	nA
Nanogram	ng
Nanometer	nm
Natural killer	NK
Nicotinamide-adenine dinucleotide	NAD
Nicotinamide-adenine dinucleotide phosphate	NADP
Nitrate reductase	NarG
Nitric oxide	NO
Non-replicating persistence	NRP
Nuclear factor-kappaB	NF-κB
Oxygen	O ₂
Partial oxygen pressure	pO ₂
Per cent	%
Phosphorus-33	³³ P
Pimonidazole	PIM
Platelet endothelial cell adhesion molecule-1	PECAM-1
Potenz Hydrogen (hydrogen concentration)	pH
Probability that the proven effect is true	p-value
Purified protein derivatives	PPD
Reactive nitrogen intermediate	RNI
Reactive oxygen intermediate	ROI
Reduced flavin-adenine dinucleotide	FADH ₂
Reduced nicotinamide-adenine dinucleotide	NADH
Reduced nicotinamide-adenine dinucleotide phosphate	NADPH
Regulated upon activation normal T-cell expressed and secreted	RANTES
Ribonuclease Protection Assay	RPA
Ribonucleic acid	RNA
Rifampin	RMP
Robust multi-array average	rma
Room temperature	RT
Round per minute	rpm
Scavenger receptor	SR
Scavenger receptor class A	SR-A

Abbreviations

Second	sec
Secondary lymphoid-tissue chemokine (CC-lygand-21)	SLC (CCL21)
Signal transducer and activator of transcription	STAT
Standard deviation	SD
Streptavidin-conjugated phycoerythrin	SA-PE
Table	Tab.
T-Cell activation gene 3	TCA3
T-helper 1	Th1
Toll-like receptors	TLR
Toxoplasma	<i>T.</i>
Transfer ribonucleic acid	tRNA
Tuberculosis	TB
Tumor necrosis factor	TNF
Type I IFN receptor	IFNAR
Type II IFN receptor	IFNGR
Tyrosine kinase	Tyk
Unit	U
Uridine triphosphate	UTP
Vascular cell adhesion molecule	VCAM
Vascular endothelial growth factor	VEGF
Water	H ₂ O
Wild-type	WT
World Health Organization	WHO
Ziehl-Neelsen	ZN

List of figures

Title	Page
Figure 1: Estimated TB incidence rates in 2003 show that TB constitutes a global emergency	1
Figure 2: Mice infected with <i>M. avium</i> by aerosol develop granuloma necrosis	36
Figure 3: Bacterial load is increased in IFN- γ -KO mice infected with <i>M. avium</i> by aerosol	37
Figure 4: IFN- γ -KO mice infected with <i>M. avium</i> by aerosol do not develop granuloma necrosis	38
Figure 5: IFN- γ is reduced but not absent in IL-18-KO mice infected with <i>M. avium</i> by aerosol	39
Figure 6: Bacterial load is slightly increased and survival time is prolonged in IL-18-KO mice infected with <i>M. avium</i> by aerosol	40
Figure 7: IL-18-KO mice infected with <i>M. avium</i> by aerosol resemble wild-type mice in terms of granuloma necrosis	40
Figure 8: Bacterial load is higher in STAT-1-KO mice infected with <i>M. avium</i> by aerosol at 14 weeks post-infection	41
Figure 9: STAT-1-KO and IRF-1-KO mice infected with <i>M. avium</i> by aerosol do not develop granuloma necrosis	42
Figure 10: Bacterial load is identical in IFN- α/β -R-KO and wild-type mice infected with <i>M. avium</i> by aerosol	43
Figure 11: IFN- α/β -R-KO mice infected with <i>M. avium</i> by aerosol resemble wild-type mice in terms of granuloma necrosis	44
Figure 12: Genes are differentially expressed in the lungs of wild-type versus IFN- γ -KO mice	45
Figure 13: IP-10 is absent in the lungs of IFN- γ -KO compared to wild-type mice	47
Figure 14: Chemokines are up-regulated in the lungs of infected compared to uninfected mice	48

Figures

Figure 15:	Angiogenic mediators are down-regulated in the lungs of infected compared to uninfected mice	49
Figure 16:	Capillary network is almost intact in IFN- γ -KO mice but rarefied in granulomatous lesions of wild-type mice	50
Figure 17:	Bacterial load is identical in both CXCR3-KO and wild-type mice infected with <i>M. avium</i> by aerosol	52
Figure 18:	Capillary network is similarly rarefied in granulomatous lesions of CXCR3-KO and wild-type mice	52
Figure 19:	CXCR3-KO mice infected with <i>M. avium</i> by aerosol resemble wild-type mice in terms of granuloma necrosis	53
Figure 20:	Marked staining for HIF-1 α and faint staining for HIF-2 α is evident in the lungs of C57BL/6 mice infected with <i>M. avium</i> by aerosol	54
Figure 21:	Marked staining for hypoxic cells is evident inside lung granulomas of C57BL/6 mice infected with <i>M. avium</i> by aerosol	55
Figure 22:	Hypoxia is absent and blood vessels are present in the lungs of C57BL/6 mice infected with <i>M. tuberculosis</i> by aerosol	56
Figure 23:	Experimental setup for direct oxygen measurement in infected mouse lungs <i>in vivo</i>	57
Figure 24:	Partial oxygen pressure is reduced in the lungs of C57BL/6 mice infected with <i>M. tuberculosis</i> by aerosol	58
Figure 25:	Hypoxia is evident in lung granulomas and lymph nodes of guinea pigs infected with <i>M. tuberculosis</i> by aerosol	60
Figure 26:	Both type I and type II interferon systems are involved in the IFN- γ -signaling pathway	63
Figure 27:	Genes (with annotations) are differentially expressed in the lungs of wild-type versus IFN- γ -KO mice	i

List of tables

Title	Page
Table 1: Some genes are regulated higher than 10-fold in the lungs of wild-type versus IFN- γ -KO mice	46
Table 2: Genes that are reported to be regulated by IRF-1 are also found to be regulated in IFN- γ -KO compared to wild-type mice as shown by micro-array analysis	65
Table 3: Balance is shifted towards angiostasis in wild-type mice compared to IFN- γ -KO mice as shown by RPA	72
Table 4: Some genes are regulated higher than 2-fold in the lungs of wild-type versus IFN- γ -KO mice	iv
Table 5: Some genes are regulated higher than 4-fold in the lungs of wild-type versus IFN- γ -KO mice	ix
Table 6: Some genes are regulated higher than 5-fold in the lungs of wild-type versus IFN- γ -KO mice	xii



1. Introduction

1.1. Epidemiology of tuberculosis

‘If the importance of a disease for mankind is measured by the number of fatalities it causes, then tuberculosis must be considered much more important than those most feared infectious diseases, plague, cholera and the like. One in seven of all human beings dies from tuberculosis. If one only considers the productive middle-age groups, tuberculosis carries away one-third, and often more.’ [1]

The situation described by Koch in 1882 has not really improved since. Nearly one third of the world population is infected with the causative agent *Mycobacterium tuberculosis*, almost 8 million new individuals develop active tuberculosis (TB) and 2 million die of the disease each year [2]. The TB epidemic is worse now than at any other time in history, and there is no vaccine that prevents infection entirely [3].

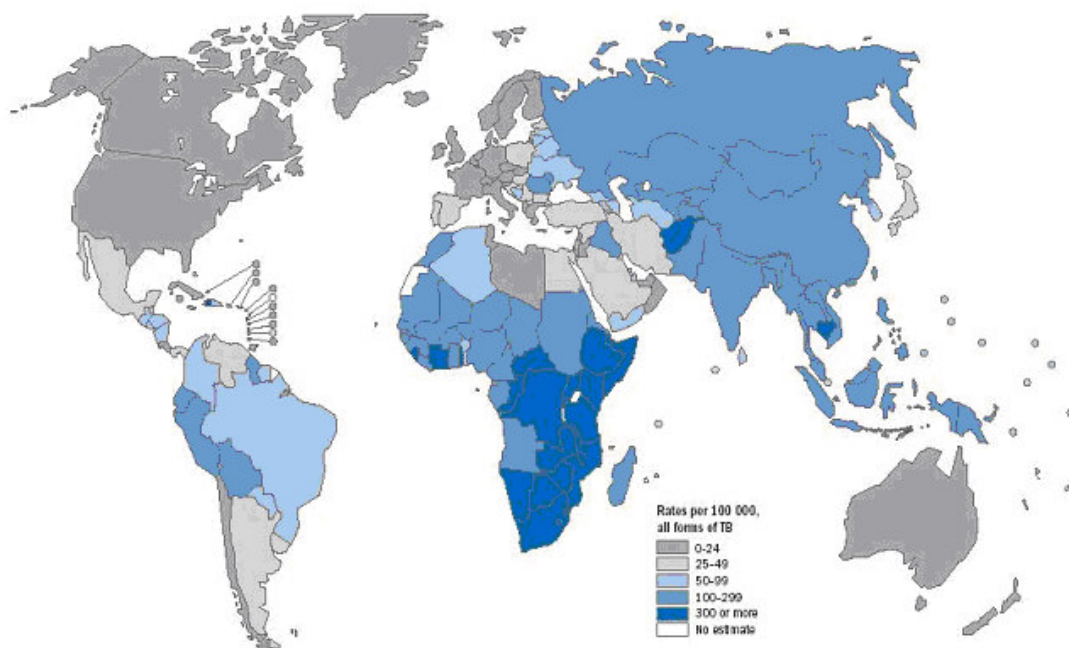


Figure 1: Estimated TB incidence rates in 2003 show that TB constitutes a global emergency. The 22 countries shown on the map are the high-burden countries accounting for 80% of the TB cases in the world [4].

The incidence of tuberculosis infection has increased due to several factors:

- the health system in Eastern Europe and in some regions of the former Soviet Union has collapsed as a result of political and economical problems;
- TB control efforts have been constricted, as tuberculosis was not heading the budgetary list of the Western European and the North American countries [5-7];
- in countries like the Sub-Saharan Africa and South Africa, where the incidence of human immunodeficiency virus (HIV) is high, infection with HIV increases the susceptibility of those individuals to TB [8, 9];
- poverty, crowded homing conditions, homelessness and unemployment in many parts of the world, are often associated with malnutrition and low hygiene, the main risk factors for increased susceptibility to TB [1, 3];
- multidrug resistance has emerged not only in Eastern Europe and the former Soviet Union, but also in Central and South-East Asia, especially India and China, as well as the Western Pacific and South Africa [10, 11];
- although tuberculosis has been the focus of medical research for more than 100 years, *M. bovis* BCG, the only vaccine developed and used for the last 70 years is not completely satisfactory due to great variation in its efficacy [12-16].

In 1993 the World Health Organization (WHO) declared TB a global emergency. The internationally recommended strategy for TB treatment and control, which was developed by the WHO, is known as directly observed treatment short-course (DOTS). By the end of 2000, 148 of 210 countries were implementing the DOTS strategy that has produced an average cure rate of 80% where it was used [17].

Increasing the cure rate is getting problematic due to the emergence of multidrug-resistant tuberculosis (MDR-TB). When patients, after treatment with the standard regimens, are not cured and their mycobacteria show *in vitro* resistance to at least the two most powerful anti-tuberculosis drugs, rifampin (RMP) and isoniazid (INH), they constitute the group of multidrug-resistant tuberculosis patients. Drug-resistant tuberculosis arises from inconsistent or partial treatment, due to a lack of medical care and an adequate follow-up system [18].

There is an urgent need to improve TB treatment, not only to overcome MDR-TB, but also for the eradication of latent TB infection. This is an asymptomatic infection with TB at continued risk for activation of the disease, when the immune system of the host weakens due to old age, immunosuppressive treatment, or immunocompromising co-infections [19, 20]. In order to find a rapid solution allowing the implementation of an alternative

therapeutic scheme, new drugs had to be administered together with old tuberculostatics [21]. Potential new tuberculosis drugs can be subdivided into two categories, off-the-shelf drugs and novel compounds. Off-the shelf drugs are fluoroquinolone compounds like levofloxacin, moxifloxacin, gatifloxacin [22-24], long-acting rifamycins like rifapentine, rifabutin, rifalazil [25-27], and oxazolidinone compounds [28], while novel compounds are nitroimidazopyrans [29, 30]. Over the last 30 years, only one new class of antibiotics has been introduced, the oxazolidinones [31].

The recently sequenced genome of *Mycobacterium tuberculosis* and the number of bacterial genes identified by DNA sequencing projects and bioinformatic analysis provide a pool of new targets for novel drugs [32]. Thus, the process of drug discovery can not be considered successful, as the number of bacterial targets actually utilized is less than 0.1% of the potential targets [31].

The lifestyle of *M. tuberculosis* inside the host is still under investigation and not yet fully understood. Elucidating the host-pathogen interaction during the course of infection, especially that arising at the site of infection, could provide insight into the complex mechanisms governing the different stages of infection. Unveiling the physiologic status of a latent tuberculous lesion could help in the discovery of new targets for drug development and vaccination.

1. 2. Immunology of tuberculosis

M. tuberculosis is a slow-growing, facultative intracellular pathogen that can survive and multiply inside macrophages and other mammalian cells. It is Gram-positive, non-spore-forming, and aerobic. It shares with other members of the *Mycobacterium* genus a cell wall of unique composition due to the dominant presence of mycolic acids that make up more than 50% of its dry weight. It is the cell wall that gives *M. tuberculosis* its acid fastness, enabling it to retain basic dyes in the presence of acid alcohol [33, 34].

Mycobacterium avium and *Mycobacterium intracellulare* are biochemically and phenotypically related microorganisms, often referred to as the *Mycobacterium avium* complex (MAC). *M. avium* is a non-spore-forming, slow-growing, acid-fast bacterium [35, 36] that is typically non-pathogenic and readily cleared via innate and adaptive host defenses [37]. It is in general an opportunistic mycobacterium infecting immunocompromised individuals, especially HIV-patients, but it can also induce chronic

infections in immunocompetent individuals with a similar clinical picture as in *M. tuberculosis* infections [38, 39].

Resident alveolar macrophages and dendritic cells in the lung are the first line of defense against invading mycobacteria. Ingestion of *M. tuberculosis* by phagocytes depends on the engagement of surface receptors on those cells that mediate the binding of the mycobacterium to the phagocyte [40, 41].

Among complement receptors (CR), CR1 and CR3 are the major CR expressed on monocytes, whereas CR4 is the receptor predominantly found on tissue macrophages, including alveolar macrophages. CR1, CR3, and CR4 are the major CR mediating uptake of *M. tuberculosis* [42].

CR recognize opsonins on the surface of the mycobacterium, facilitating thereby its phagocytosis [43]. Opsonization via C3 involves part of the complement activation cascade. Opsonized mycobacteria bind directly to C2a, followed by the generation of the split product C3b, which is necessary for binding to the complement receptor CR1 [44]. In contrast, CR3 is involved in the nonopsonic uptake of mycobacteria [45].

The importance of complement factors and receptors is evident from *in vitro* experiments. Blocking multiple CR classes using mAb revealed a marked inhibition of phagocytosis. The combination of a mAb against CR1 and a mAb against CR3 yielded a strong inhibition of about 50-70%. A combination of two different mAb against the CR3 receptor, each recognizing a different epitope, yielded an inhibition of *M. tuberculosis* phagocytosis of about 70-80% by human macrophages and monocytes [46, 47].

The mannose receptor (MR) on macrophages recognizes mannose and fucose on the surfaces of pathogens and mediates phagocytosis of the organisms [47-49]. Interestingly, virulent strains of *M. tuberculosis* are phagocytized through the mannose receptor, while attenuated strains are not [47]. This indicates that phagocytosis through the mannose receptor might be of advantage for the mycobacterium.

The scavenger receptors (SR) are a family of structurally diverse phagocytic receptors having broad ligand specificity [50] that includes the recognition of anionic polymers and acetylated low-density lipoproteins [51]. Class A scavenger receptors (SR-A) have been shown to participate in phagocytosis of apoptotic cells [52] and as they recognize lipopolysaccharides (LPS) of Gram-negative and lipoteichoic acids (LTA) of Gram-positive bacteria [53, 54] they might play a role in host defense mediating the clearance of pathogens [55]. If CR and MR uptake are blocked, macrophages can still internalize *M. tuberculosis* through SR-A [56].

Fc γ -receptors, in contrast, seem to play a minor role in the protection and eradication of tuberculosis [57]. Fc γ -receptor-mediated phagocytosis of *M. tuberculosis* induces an inflammatory response, while complement-receptor-mediated phagocytosis does not [58]. The Fc γ -receptors are phagocytic receptors that recognize antibodies of the immunoglobulin G class coating an antigen, thereby facilitating phagocytosis [58]. Antibodies represent an intersection between adaptive and innate immunity. They recognize their ligands on infectious agents with high specificity but are bound and internalized through their Fc-domain by the Fc-family of receptors (FcR) [59-61].

Toll-like receptors (TLR) are a family of pattern recognition receptors which not only recognize distinct molecular patterns associated with microbial pathogens [62, 63] and enable macrophages and dendritic cells to recognize bacteria [64], but also play a crucial role in the function of the innate immune system by activating NF- κ B and other signaling pathways to produce inflammatory cytokines [65]. Signal transduction by members of this family requires an adapter molecule, MyD88 [63, 66]. The activation of the innate immune system by TLRs in turn influences the development of adaptive immune responses. In certain model systems, for example, MyD88-deficient animals do not exhibit adequate effector responses when stimulated with TLR ligands [66, 67]. These animals are highly susceptible to infection with a wide variety of different pathogens, including *Staphylococcus aureus* [68], *Listeria monocytogenes* [69, 70], *Toxoplasma gondii* [71], and *Mycobacterium tuberculosis* [72, 73].

Mycobacterial antigens induce through TLRs the production of IL-12, a strong proinflammatory cytokine [74], as well as tumor necrosis factor (TNF)- α [75], thus ensuring an appropriate immune response is initiated to defend against the particular pathogen causing infection [76-79].

At the same time, dendritic cells migrate to the draining lymph node, where they mature into highly effective antigen presenting cells (APC). On encountering antigen-specific lymphocytes in the lymph node, APCs activate them to proliferate into effector cells [80], resulting in a specific cell-mediated Th1-immune response, characterized by IFN- γ -producing CD4+ and CD8+ T-lymphocytes that express adhesion molecules on their cell surface facilitating their migration to the site of infection [81-84]. Mycobacterial antigens processed in the phagolysosome by the antigen presenting cells are presented to antigen-specific CD4+ T-cells by MHC class II molecules, while MHC class I molecules present mycobacterial antigens to antigen-specific CD8+ T-cells [85]. Secretion of IL-12 by

antigen-presenting cells is essential for the induction and generation of Th1-immune responses [86], as well as local environmental signals like TNF- α or IFN- γ [84, 87] that induce a Th1-cytokine and chemokine response [88-90].

The bacteriostatic function of macrophages is not expressed in the lungs until *M. tuberculosis* specific CD4+ and CD8+ T-cells extravasate from blood into alveoli and large numbers begin entering the site at which *M. tuberculosis*-infected macrophages reside [33]. Immunity is mediated predominantly by CD4+ Th1-cells with the aid of CD8+ T-cells [16, 83]. CD8+ T-cells can kill infected macrophages and the bacteria within them using perforin and granulysin [91]. The protective role of CD4+ T-cells, and most likely CD8+ T-cells, is based on their ability to synthesize and secrete the key Th1-cytokine, IFN- γ that enables the macrophage to proceed with phagosomal maturation [92] and activates the mycobacteriostatic function of macrophages at sites of infection [83, 93].

IFN- γ activates macrophages and dendritic cells (DC) to produce CXCR3-ligands like MIG, IP-10 and I-TAC to recruit CXCR3+ T-lymphocytes and natural killer (NK) cells [94, 95] that in turn augment the IFN- γ effect at the site of infection [96] and potentiate an up-regulation of the CXCR3-ligands leading to a chronic Th1-inflammation [97]. The high influx of macrophages and lymphocytes to the site of infection is not only associated with CXC-chemokines, but also CC-chemokines are involved [84, 98].

Inside the phagolysosome of activated macrophages several mechanisms are involved in its bacteriocidal function. These mechanisms include the production of reactive oxygen intermediates (ROI), like superoxide and hydrogen peroxide [99] as well as reactive nitrogen intermediates (RNI), like nitric oxide and its metabolites [100-103]. In addition, apoptosis of phagocytic cells reduces the viability of intracellular mycobacteria [104, 105]; therefore, pathogenic strains of *M. tuberculosis* reduce host cell apoptosis more than related attenuated strains [106]. This is achieved in part by inducing IL-10 that decreases TNF- α activity resulting in reduced apoptosis of infected cells [107].

One of the major anti-microbial defense mechanisms of macrophages is nitric oxide and its metabolites. It is generated from L-arginine by action of the inducible isoform of nitric oxide synthase (iNOS). Macrophages become partially activated by ingesting *M. tuberculosis*, but do not become fully activated and produce iNOS unless they are stimulated with IFN- γ . When Th1-immunity is expressed in the lungs, most of the iNOS synthesized in the lungs is present in *M. tuberculosis*-infected macrophages at sites of infection [33].

As immunity to tuberculosis is cell-mediated, antibodies are believed to be of minor importance in the host defense [108, 109], although antibodies circulate in the blood and might easily access the site of infection [110, 111] and plasma cells exist in tuberculous lesions [112]. Antibodies are carried by the blood circulation and, hence, can rapidly interact with invading bacteria and their antigens to activate a complement cascade [113, 114] producing C5a, which is a strong chemoattractant for granulocytes and monocytes [115].

Complement activation induces in vascular endothelial cells the secretion of chemokines and the up-regulation of their adhesion molecules for leukocytes [116]. Cytophilic antibodies possess the ability to activate macrophages [117, 118] to release permeability factors [119] and cytokines [119-121]. Thus, antigen-antibody reactions accelerate the cell-mediated immunity to tuberculosis by rapidly bringing the expanded antigen-specific T-cells to the site of infection [122]. When mycobacterial antigens combine with circulating and cytophilic antibodies, chemotaxins are produced that cause a rapid accumulation of macrophages and antigen-specific T-lymphocytes at the site of infection. The infiltrating cells produce cytokines like MCP-1, IL-1, TNF- α and IFN- γ , which activate the accumulating macrophages and recruit further cells to the site of infection [122]. However, B-cell depletion in experimental systems had no effect on bacterial load or disease progression [123, 124].

1. 3. Protection and pathology of tuberculosis

Although the host uses all its immune defenses against *M. tuberculosis*, the pathogen can survive inside the host evading its anti-bacterial effector mechanisms. The host therefore aims to locally entrap mycobacteria at the site of infection within granulomas, highly organized structures containing differentiated macrophages and lymphocytes. Tuberculous granulomas are characterized by the presence of a central core of caseous necrosis, a region of acellular debris surrounded by epithelioid cells, which are activated macrophages rich in lysosomal and mitochondrial enzymes like β -galactosidase, acid phosphatase, β -glucuronidase, cytochrome oxidase, and succinic dehydrogenase [125].

The phagocytized bacteria, however, inhibit the phagosomal maturation by preventing its fusion with the lysosome into a phagolysosome [126]. Thereby they reduce the maximal acidification of the phagosomal interior, they resist the anti-microbial defense mechanisms

and evade an unfavorable environment [127] that is damaging to DNA and cell-membranes. Replication and survival is achieved despite deficiency in carbohydrates, iron and oxygen. The availability of fatty acids provides an alternative energy source [128].

The highly activated macrophages localized at a site of infection are associated with the destruction of bacteria, while epithelioid cells do not develop nor do their enzymes increase in areas devoid of bacteria [125]. The center of a granulomatous lesion is mainly occupied by a dense accumulation of epithelioid cells [129, 130], which are activated macrophages that fuse to form multinuclear giant and foamy cells [131]. Destruction is not confined to macrophage, but the tissue around them becomes destroyed as well [132-134]. Removing dead cells and replacing them with newly recruited activated macrophages is a dynamic antigen-stimulated T-cell-mediated process [135].

TNF- α is a major proinflammatory cytokine that has immunoregulatory functions [136, 137] and plays an important role in granuloma formation [138, 139] as well as macrophage activation [136, 137]. In chronic infections, TNF- α is responsible for maintaining the granulomatous structure and confining the mycobacteria locally [140]. TNF contributes to the tight organization of a granuloma [141] and is essential for the differentiation of macrophages into epithelioid cells. Anti-TNF antibodies neutralizing the TNF activity in mycobacteria-infected individuals results in reactivation and dissemination of *M. tuberculosis* [140, 142-144].

IL-18 is a pro-inflammatory cytokine that shares many properties with IL-1 [145] and synergizes with IL-12 [146]. It plays a protective role as well, evidenced by the high susceptibility of IL-18-KO mice to *M. bovis* BCG and *M. tuberculosis* [147].

IL-12 is the main Th1-inducing cytokine that is produced upon *M. tuberculosis* infection mainly by phagocytic cells like activated macrophages and dendritic cells [148-150]. IL-12 is the main inducer of IFN- γ production [146], playing thereby a protective role confirmed by the high susceptibility of IL-12-KO mice to mycobacterial infections [93, 151, 152].

Chemokines and cytokines organize and direct infiltrating cells to sites of infection, thereby playing crucial roles in granuloma formation and maintenance. The production of cytokines participates to a greater or lesser degree in shaping local chemokine expression [153]. The Th1-response is associated with CXC-chemokines, like MIP-2, LIX, MIG, IP-10, I-TAC, as well as CC-chemokines, like MIP-1 α and MIP-1 β , co-expressed with IFN- γ and associated with NK-cells, CD8⁺ T-cells and Th1-cells [89].

The IFN-induced CXC-chemokines MIG, IP-10 and I-TAC were described as angiostatic chemokines. They share a common functional receptor, named CXC-chemokine receptor (CXCR)₃, that is expressed on endothelial and infiltrating inflammatory cells, especially Th1-cells. CXCR₃ is associated with the late phase of the endothelial cell cycle. Thus, endothelial cells express CXCR₃ only if they become activated and especially when they exhibit a high proliferation rate. Consequently, MIG, IP-10 and I-TAC, which bind CXCR₃ with high affinity, act as effective inhibitors of endothelial cell proliferation. This explains the angiostatic activity of those chemokines [154].

A variety of activated immune cells are recruited to a site of infection, where anti-microbial defense mechanisms are induced to arrest and confine replicating mycobacteria invading the lung tissue. This results in granuloma formation, which is a protective hallmark of mycobacterial infections during early stages. But at late stages it is associated with a severe form of pathology, the T-cell-mediated granuloma necrosis, also called the Koch phenomenon. Granuloma necrosis consists of a center of dead caseous tissue packed in a tuberculous granulomatous infiltrate of viable macrophages, lymphocytes, plasma cells and fibroblasts [155].

Robert Koch observed a severe skin lesion at the site, where he injected tuberculin intradermally into *M. tuberculosis*-infected patients, as well as an aggravated immune response at the original site of infection. This feature is called delayed type hypersensitivity (DTH) reaction and did not arise in uninfected controls [156]. For the diagnosis of TB, purified protein derivatives (PPD) of *M. tuberculosis* are still used by intradermally injecting PPD into tested individuals. The delayed reaction peaks after 48-72 h [157].

The number, size and location of caseous foci in the lung determine the extent of damage, as destruction and displacement of large parts of the lung tissue result in a loss of pulmonary function [157, 158]. Alternatively, the caseous center may liquefy and rupture, spreading the contained bacterial load into the bronchi, resulting in intrapulmonary dissemination and transmission of tuberculosis in the population [159].

Local proteinases like cathepsin D, as well as nucleases and lipases are involved in the liquefaction of pulmonary caseation, as they can hydrolyze and digest the solid caseous material [112, 160, 161]. Emptying of the softened material into the bronchi releases the mycobacteria into an oxygen-enriched environment that allows an outburst of mycobacterial growth [155, 162]. A cough would discharge the softened caseum and its large mycobacterial content to the outside allowing a new active transmission.

As evident from the preceding section, immunity to tuberculosis represents a dilemma, as it is protective as well as destructive. It was speculated that low concentration of mycobacterial antigens would stimulate a protective immunity in macrophages, while high concentrations destroy macrophages leading thereby to caseation and tissue injury [125]. The pathogen not only evades the mycobacteriostatic functions of the immune response, but also promotes the immune response towards pathology. The cells and mediators that have an anti-mycobacterial protective function become consequently responsible for tissue destruction. Since the times of Robert Koch, it has been the aim of infection immunology to differentiate between the protective and the destructive pathways of pathogen control in order to enhance the former and inhibit the latter.

1. 4. The animal model

In order to dissect the molecular mechanisms involved in pathogenesis, an animal model is needed. Indeed, four different animal models are mainly used for this purpose.

Rhesus macaques and cynomolgus macaques are susceptible to *M. tuberculosis* infection and develop a clinical picture that is similar to the infection in human beings from the immunological and pathological point of view [163-165]. Granulomas arising in the lungs of macaques are structurally similar to those developing in humans [131]. Although the proportion of macaques that develop active disease is higher than in human beings, about 40% of macaques infected with a low dose of *M. tuberculosis* were able to contain the infection in a state that resembles latency in humans [163, 165]. This indicates the possibility to use this animal model to study latency [163, 165] and reactivation [163] of tuberculosis. From the ethical point of view, it is difficult to use this animal model.

Rabbits develop disease similar to humans and lung granulomas formed during the disease show the same progression, involving caseation, liquefaction and cavitation as observed in advanced cases of human TB [112]. The disadvantages of rabbits are the lack of inbred strains, reagents for this animal model and the high costs of maintenance [166].

Guinea pigs are very sensitive to *M. tuberculosis* infection. The course of disease progression and the early stages of granuloma formation in this animal model resemble those in humans [167]. Necrotic lesions, a pathology that arises during the infection with tuberculosis in humans, are also observed in guinea pigs [168]. Unfortunately, there is a

lack of inbred strains as well as reagents for this animal model. The maintenance costs are also high [166].

Mice are the most frequently used *in vivo* model, because of their well-studied genetics, the existence of immunocompetent and immunodeficient strains, as well as susceptible and resistant strains, the availability of reagents to measure and detect cytokines and chemokines, as well as low maintenance costs in comparison to other animal models [167]. Mice infected with *M. tuberculosis* do not develop the same pathology as humans; instead, a severe form of interstitial fibrosis occurs with complete destruction of the lung architecture [169, 170].

However, a mouse model of aerosol infection with a high-dose (10^5 CFU) of *Mycobacterium avium* (TMC724) shows a lung histopathology which strongly resembles the centrally caseating necrosis in lung granulomas of humans [171, 172]. Using this model system, CD4⁺ T-cells and IFN- γ were identified as the major factors inducing granuloma necrosis. The downstream mechanisms induced by interferon-gamma, which mediate tissue destruction, however, remained unknown.

1. 5. IFN- γ -mediated mechanisms of necrosis

For a better understanding of the host immunopathology, the tissue-destructive mechanisms mediated by IFN- γ need further investigation. Regarding IFN- γ signaling, it proceeds via two interconnected pathways, where a variety of molecules is involved. There are molecules exclusively involved in the type II IFN signaling like IFN- γ , STAT-1 and IRF-1 as well as molecules that are involved in the type I IFN signaling like IFN- α/β , STAT-2 and IRF-9 [173].

Previous studies [174] reported that *M. tuberculosis* infection induces a rapid activation of IFN- β that stimulates the type I IFN receptor. The IFN-stimulated gene factor (ISGF)3 inducing IRF-7 and the STAT-1 homodimer inducing IRF-1 are both essential molecules that play a regulatory role. IRF-1 could cooperate with IRF-7 in regulating IFN- α as well as reinforcing IFN- β .

The IFN- α/β pathways have not been examined for possible involvement in the development of granuloma necrosis. However, IFN- γ was previously reported to be crucial for granuloma necrosis [171, 172]. IFN- γ is a main inducer of a variety of molecules and is involved in several cellular immune mechanisms. Cells that accumulate at the site of

infection are attracted by specific chemokines. In order to unveil the cells that are mainly associated with tissue destruction, it was important to analyze the chemokines, especially those induced by IFN- γ and that dominate at the site of infection. Thus, the following hypothesis was proposed: IFN- γ induces angiostatic chemokines that cause a reduced vascularization leading to hypoxia. Cells under oxygen starvation die and result in a necrosis.

1. 6. The physiology of mycobacterial lesions

Mycobacterium tuberculosis is able to reside and proliferate inside host macrophages despite the mycobacteriostatic activity of these cells. The continued intracellular multiplication of bacteria might lead to the lysis of the infected cell, the extracellular bacteria are ingested by other immature macrophages and monocytes attracted to the site of infection [158].

Surviving mycobacteria are thought to adapt to an intracellular lifestyle of non-replicating persistence (NRP) [175, 176], in which they are largely resistant to known bacteriocidal mechanisms of macrophages and many anti-microbially active drugs [177]. *M. tuberculosis* is able to regain growth when pressure from the host's immune system subsides due to old age, immunosuppressive treatment, or immunocompromising co-infections, and the most prevalent form of tuberculosis in industrialized countries is reactivation TB [178].

One of the environmental factors inducing NRP is the severe hypoxia presumed to be present within granulomatous lesions. Here, mycobacteria are located within macrophages that are walled off by a fibrous capsule, or they reside within necrotic tissue, so called caseum, that has no obvious supply of oxygen [159]. Persistence, and even susceptibility to certain drugs – such as metronidazole – under anoxic conditions, has been demonstrated in an *in vitro* model developed by Wayne and co-workers [179].

In that model, *M. tuberculosis* experiences a shift in its metabolism during anaerobiosis, characterized for example by the utilization of nitrate respiration for energy production and by the transcriptional activation of fatty acid-degrading enzymes and DNA-repair proteins as well as by remodeling for iron acquisition [128]. Several mutants, inactivated at gene loci demonstrated to be mostly activated by anoxic stress, are indeed attenuated during the chronic phase of infection in mouse models of infection; however, others, most notably

those in the *dosR* regulated gene cluster thought to be exquisitely responsible for the anoxic stress response, are paradoxically not affected at all or are hypervirulent in the mouse model [180-182].

Although hypoxia was always assumed to exist in granulomas *in vivo*, this assumption was never directly examined in animal or human tissues. The physiologic state of a necrotic or non-necrotic granuloma has not yet been determined, neither in humans nor in animal models infected with tuberculosis.

1.7. Aim of the work

One of the major obstacles for eradicating TB by chemotherapy is the fact that *M. tuberculosis* can persist within chronic, granulomatous, and even calcified lesions for the lifetime of human beings. Conventional drugs are ineffective against latent bacteria inside those lesions. Therefore, describing the biochemical and biophysical nature of the chronic granulomatous lesion as well as the lifestyle of the mycobacterium inside this lesion may identify a baseline that could help in discovering new targets for TB drug development.

The mechanisms that lead to granuloma necrosis are still unknown. Minimizing this severe pathology can only be achieved by identifying effector molecules critically involved in the development of granuloma necrosis. This might provide the possibility to block the development of necrotic foci at a point that would not negatively affect the protective role of granulomas, while hindering the progress into necrosis, which is the first step on the way to a new active transmission.

We used the mouse model infected with a high-dose of *Mycobacterium avium* by aerosol to answer the following questions:

- Which molecules involved in the IFN- γ signaling pathway are associated with the development of granuloma necrosis?

To answer this question, we used mice deficient for key molecules like IL-18, IFN- γ , IFN- α/β -receptor, STAT-1 and IRF-1, infected them with *M. avium* and compared lung histopathology with infected wild-type mice.

- Does a misbalance between angiogenic and angiostatic mediators affect vascularization and result in granuloma necrosis?

To answer this question, we analyzed gene expression by micro-arrays, angiogenic mediator expression by Ribonuclease Protection Assay, capillary density by immuno-

histochemistry in wild-type mice infected with *M. avium*. In addition, mice deficient for CXCR3, infected with *M. avium* were compared with infected wild-type mice in terms of pulmonary granuloma development.

- Are pulmonary granulomas in mice infected with *M. avium* and in mice infected with *M. tuberculosis* hypoxic?

To answer this question, we used a biochemical method injecting a hypoxia marker that becomes reduced under oxygen starvation, binds to local thiol-containing proteins and can be detected by an antibody. In addition, we used a biophysical method inserting a flexible Clarke-type catheter micro-electrode for oxygen into the visibly altered lesions of the lung to directly measure the oxygen concentration in infected mice and compare them with uninfected mice as well as with hypoxic tumors. In comparison, the oxygen status in the lungs of infected guinea pigs was also analyzed biochemically.

Our overall goal was to analyze the physiology of granuloma necrosis using a combination of biochemical and biophysical methods and to conduct a comparative study between the outcomes of the mouse model infected with *M. avium* versus the guinea pig and the mouse model infected with *M. tuberculosis*.

2. Materials and Methods

2.1. Materials

2.1.1. Chemicals

Chemical	Abbreviation used in text	Source
Acetone		Merck, Darmstadt, Germany
Agarose		Invitrogen, Karlsruhe, Germany
Aluminium sulphate		Sigma, Deisenhofen, Germany
3-Amino-9-ethylcarbazole	AEC	Sigma, Deisenhofen, Germany
3-Amino-9-ethylcarbazole substrate	AEC substrate	Sigma, Deisenhofen, Germany
Ammonium persulphate (10%)	APS	BioRad, München, Germany
Aqua double distilled	Aqua bi-dist.	Deionisation facility, Research Center Borstel, Germany
Avidin horseradish peroxidase	Av-HRP	BD Pharmingen, Heidelberg, Germany
Boric acid		Merck, Darmstadt, Germany
Bovine serum albumin	BSA	Sigma, Deisenhofen, Germany
Brain heart infusion agar		Difco, Heidelberg, Germany
Brome phenol blue		Serva, Heidelberg, Germany
1-Bromo-3-chloro-propane	BCP	Sigma, Deisenhofen, Germany
Buraton		S&M, Norderstedt, Germany
Carbol fuchsine		Merck, Darmstadt, Germany
Chloroform		Merck, Darmstadt, Germany
Citric acid monohydrate		Merck, Darmstadt, Germany
Diethyl-pyrocabonate	DEPC	Ambion, Huntingdon, England
N,N-Dimethylformamide		Sigma, Deisenhofen, Germany
Disodium hydrogen phosphate		Merck, Darmstadt, Germany
Dithiothreitol	DTT	BD Pharmingen, Heidelberg, Germany
Entellan		Merck, Darmstadt, Germany
Eosin		Merck, Darmstadt, Germany
Ethanol (for molecular biology)		Merck, Darmstadt, Germany
Ethidium-bromide		Sigma, Deisenhofen, Germany
Ethylene-diamino-NNN',N'-tetraacetic acid	EDTA	ICN Biomedicals, Eschwege, Germany
Ethylenglycol		Sigma, Deisenhofen, Germany
Foetal calf serum (heat inactivated)	FCS	Biochrom, Berlin, Germany
Formalin (37%)		Merck, Darmstadt, Germany
Glacial acetic acid		Merck, Darmstadt, Germany
Glycerine		Merck, Darmstadt, Germany

Materials and Methods

Guanidine-isothiocyanate	GUTC	Merck, Darmstadt, Germany
Haematoxylin		Merck, Darmstadt, Germany
Hydrochloric acid	HCl	Merck, Darmstadt, Germany
Hydrogen peroxide	H ₂ O ₂	Merck, Darmstadt, Germany
Isoamylalcohol		Merck, Darmstadt, Germany
Isopropanol		Sigma, Deisenhofen, Germany
Kaiser's glycerine gelatine		Merck, Darmstadt, Germany
N-Lauroylsarcosine		Sigma, Deisenhofen, Germany
Löffler's methylene blue		Merck, Darmstadt, Germany
β-Mercaptoethanol	M-EtOH	Sigma, Deisenhofen, Germany
Middlebrook 7H10 agar		Difco, Heidelberg, Germany
Middlebrook 7H9 medium		Difco, Heidelberg, Germany
Oleic acid, albumin, dextrose, catalase	OADC	BD Pharmingen, Heidelberg, Germany
Paraffin (Paraplast Plus)		Sherwood Medical, St. Louis, USA
Pentobarbital		University Clinic, Lübeck, Germany
PeqGOLD TriFast™	Trizol	PeqLab Biotechnologie, Erlangen, Germany
Phosphoric acid	H ₃ PO ₄	Merck, Darmstadt, Germany
Pimnidazole hydrochloride		Chemicon, Hampshire, United Kingdom
Potassium chloride	KCl	Merck, Darmstadt, Germany
Potassium dihydrogen phosphate	KH ₂ PO ₄	Merck, Darmstadt, Germany
Pronase		Fisher Scientific, Schwerte, Germany
Pyruvate		Sigma, Deisenhofen, Germany
RNase-Inhibitor	RNasin	BD Pharmingen, Heidelberg, Germany
Rotihistol		Roth, Karlsruhe, Germany
Rotiphorese acrylamide with bisacrylamide	Gel 40	Karl Roth, Karlsruhe, Germany
Sigmacote		Sigma, Deisenhofen, Germany
Sodium acetate anhydrate		Merck, Darmstadt, Germany
Sodium carbonate	Na ₂ CO ₃	Merck, Darmstadt, Germany
Sodium chloride	NaCl	Merck, Darmstadt, Germany
Sodium chloride solution (isotonic)		Braun, Melsungen, Germany
Sodium citrate		Merck, Darmstadt, Germany
Sodium citrate dihydrate		Merck, Darmstadt, Germany
Sodium hydrogen carbonate	NaHCO ₃	Merck, Darmstadt, Germany
Sodium hydroxide	NaOH	Merck, Darmstadt, Germany
Sodium iodide		Sigma, Deisenhofen, Germany
Sodium pyruvate		PAA, Pasching, Austria
Streptavidin horseradish peroxidase	St-HRP	Dako Cytomation, Hamburg, Germany
TEMED		Karl Roth, Karlsruhe, Germany
Tissue freezing medium	Tissue Tec	Leica, Nussloch, Germany

Tris-(hydroxymethyl)-amino-methane	Tris	Serva, Heidelberg, Germany
Trisodium citrate dihydrate		Merck, Darmstadt, Germany
Tris-saturated Phenol		Sigma, Deisenhofen, Germany
Tween-20		Sigma, Deisenhofen, Germany
Tween-80		Sigma, Deisenhofen, Germany
Urea		BioRad, München, Germany
Uridine-5'-Triphosphate α - ³³ P	(α - ³³ P)-UTP	MP Biomedicals, Eschwege, Germany
Water (sterile, pyrogen-free)		Braun, Melsungen, Germany

2. 1. 2. Reagents and media

Reagent	Amount	Concentration	Components
Bacterial cultures			
OADC-supplemented Middlebrook 7H9 medium			
	2.0 ml		Glycerine
	4.7 g		Middlebrook 7H9
	0.5 ml		Tween-80
	100 ml		OADC
	900 ml		Aqua Bi-dist.
OADC-supplemented Middlebrook 7H10 agar			
	5.0 ml		Glycerine
	19.0 g		Middlebrook 7H10
	100 ml		OADC
	900 ml		Aqua Bi-dist.
Pyruvate-supplemented Middlebrook 7H10 agar			
	5.0 ml		Glycerine
	19.0 g		Middlebrook 7H10
	0.75 ml		Pyruvate
	900 ml		Aqua Bi-dist.
Animal treatment			
Anaesthetic			
	1.0 ml	53.3 mg/ml	Pentobarbital
	7.0 ml	0.9%	NaCl
Hypoxia marker			
	0.1 g		Pimonidazole hydrochloride
	8.62 ml	0.9%	NaCl
Immunohistology			
Phosphate buffered saline PBS			
100 mM pH 7.4			
		2.7 mM	KCl
		1.5 mM	KH ₂ PO ₄

Materials and Methods

		137 mM	NaCl
		9.0 mM	NaH ₂ PO ₄
		in	Aqua Bi-dist.
Fixative			
		4%	Formalin
		in 10 mM	PBS
Decolorizer			
		0.5%	HCl
		in 96%	Ethanol
Haematoxylin-Eosin stain			
Eosin			
		1%	Eosin
		in	Aqua Bi-dist.
Haematoxylin			
	6.0 g		Haematoxylin
	0.6 g		Sodium iodide
	52.8 g		Aluminium sulphate
	250 ml		Ethylenglycol
	60 ml		Glacial acetic acid
	690 ml		Aqua Bi-dist.
Non-specific blocking agent			
		5%	FCS
		in 10 mM	PBS
Citrate buffer			
10 mM pH 6.0			
		1.8 mM	Citric acid monohydrate
		8.3 mM	Sodium citrate dihydrate
		in	Aqua Bi-dist.
Peroxidase blocker			
		3%	H ₂ O ₂
		in	Aqua Bi-dist.
Acetate buffer			
40 mM pH 4.7			
	22.2 ml	200 mM	Glacial acetic acid
	52.8 ml	200 mM	Sodium acetate anhydrate
	300 ml		Aqua Bi-dist.
3-Amino-9-ethylcarbazole AEC solution			
	1.0 g		3-Amino-9-ethylcarbazole
	200 ml		N,N-Dimethylformamide
3-Amino-9-ethylcarbazole AEC substrate			
	150 ml	40 mM	Acetate buffer (warm)
	7.5 ml		AEC solution

	0.07 ml	30%	H ₂ O ₂
	3 volume		AEC substrate
ELISA			
Coating buffer			
0.1 M pH 9.5			
		100 mM	NaHCO ₃
		34 mM	Na ₂ CO ₃
		in 1 litre	Aqua Bi-dist.
Washing buffer			
		0.05%	Tween-20
		in	PBS
Stop solution			
		1 M	H ₃ PO ₄
Molecular Biology			
GUTC buffer			
pH 7.0			
		4 M	GUTC
		25 mM	Sodium citrate
		1%	N-lauroylsarcosine
		100 mM	M-EtOH
		in 0.1%	DEPC water
Electrophoresis			
TBE buffer			
pH 8.0			
		900 mM	Tris
		900 mM	Boric acid
		20 mM	EDTA
		in	Aqua Bi-dist.
Loading buffer			
pH 7.6			
		400 mM	Brome phenol blue
		5 mM	Tris
		60 mM	Glycerine

2. 1. 3. Kits

Kit	Working concentration	Source/Components
Immunohistology		
Sigma Fast TM 3,3'-diaminobenzidine DAB		Sigma, Deisenhofen, Germany
	1 volume	3,3'-Diaminobenzidine
	1 volume	Urea H ₂ O ₂
	5 ml	Aqua Bi-dist.

ELISA		
OptEIA		BD Pharmingen, Heidelberg, Germany
	1:250	Capture antibody
	1:250 or 1:500	Biotinylated detection antibody
	10 ng/ml	Standard (recombinant murine antigens)
	1:250	Av-HRP
Assay diluent		BD Pharmingen, Heidelberg, Germany
Avidin-Biotin block		Vector Laboratories, Burlingame, USA
	ready	Avidin
	ready	Biotin
3,3',5,5'-Tetramethylbenzidin TMB		BD Pharmingen, Heidelberg, Germany
	1 volume	Reagent A
	1 volume	Reagent B
Molecular Biology		
RiboQuant Template Sets		BD Pharmingen, San Diego, USA
RiboQuant <i>In Vitro</i> Transcription Kit		BD Pharmingen, San Diego, USA
	61 μ M	UTP
	2.75 mM	GTP
	2.75 mM	ATP
	2.75 mM	CTP
	100 mM	DTT
	5 \times	Transcription buffer
	40 U/ μ l	RNasin
	20 U/ μ l	T7 RNA polymerase
	1 U/ μ l	DNase
	2 mg/ml	yeast tRNA
	20 mM	EDTA
	4 M	Ammonium acetate
RiboQuant RPA Kit		BD Pharmingen, San Diego, USA
	1 \times	Hybridization buffer
	80 ng/ μ l	RNase A
	250 U/ μ l	RNase T1
	1 \times	RNase buffer
	10 mg/ml	Proteinase K
	1 \times	Proteinase K buffer
	2 mg/ml	yeast tRNA
	4 M	Ammonium acetate
	1 \times	Loading buffer

2. 1. 4. Antibodies

Immunohistology				
Mouse antigen	Primary antibody	Host, Source	Secondary antibody	Host, Source
iNOS	1:800 in 5% FCS/PBS	Rabbit, Upstate	1:500 in 5% FCS/PBS	Goat, Dianova
Endomucin	undiluted	Rat, Prof. Vestweber Münster	1:500 in 5% FCS/PBS	Goat, Dianova
Pimonidazole derivative	1:50 in 1% BSA/PBS	Mouse, Chemicon	-	-
HIF-1 alpha	1:100 in 1% BSA/PBS	Mouse, Novus	-	-
HIF-2 alpha	1:1000 in 5% FCS/PBS	Rabbit, Novus	1:500 in 5% FCS/PBS	Goat, Dianova
ELISA				
Antigen		Host	Source	
IFN- γ		Rat IgG1	BD Pharmingen	
TNF- α		Rat IgG1	BD Pharmingen	
IL-12p40		Rat IgG1	BD Pharmingen	

2. 1. 5. Equipment

Apparatus	Description	Source
96-well-plates	Maxisorb	Nunc, Roskilde, Denmark
Aerosol	Exposure-Inhalation-System 099 C A4224	Glas-Col, Indiana, USA
Autoclave	Vakulab HP	Münchener Medizin Mechanik, Stadlern, Germany
Autotechnicon	Hypercenter XP	Shadon, Pittsburgh, USA
Centrifuge	Heraeus Biofuge pico	Heraeus instruments, Hanau, Germany
Clarke-type electrode (for oxygen)		Licox, Integra Neurosciences, Plainsboro, USA
Cooling centrifuge (refrigerated)	5417R	Eppendorf, Hamburg, Germany
Cryotome	CM1850	Leica, Nussloch, Germany
Electrophoresis power supply (computer controlled)	Model 3000xi	BioRad, Richmond, USA
ELISA reader	Sunrise	TECAN, Crailsheim, Germany
Gel blotting paper		Whatman, Dassel, Germany
Gel dryer	Slab Gel Dryer UniGelDryer 4050	UniEquip, Martinsried/Munich, Germany
Glass slides	SuperFrostPlus	Langenbrinck, Emmendingen, Germany

Materials and Methods

Histogrids		Simport, Bernard-Pilon, Canada
Homogenizer	Potter S	Braun Melsungen AG, Melsungen, Germany
Imaging plate		Raytest, Straubenhardt, Germany
Light microscope		Zeiss, Oberkochen, Germany
Liquid scintillation counter	1414 Wallac Win-Spectral α/β	PerkinElmer, Boston, USA
Paraffin dispensing station	EG1140C	Leica, Nussloch, Germany
Paraffin stretching bath	Type 12 Nr. 2049	Medax Nagel GmbH, Kiel, Germany
Paraffin wax dispenser	MH 8523B/E	Electrothermal, Essex, U.K.
Pestles (Teflon)		Rettberg, Göttingen, Germany
pH-Meter	HI 8418	Hanna instruments, Kehl am Rhein, Germany
Phosphor imager	Typhoon 8600 Variable Mode Image	Molecular dynamics, Sunnyvale, USA
Rotary microtome	RM 2155	Leica, Bensheim, Germany
S2 Large glass plate special		Biometra, Göttingen, Germany
Sequencing Gel Electrophoresis Apparatus	Model S2	Life Technologies, Karlsruhe, Germany
Serum separation tubes		BD Pharmingen, Heidelberg, Germany
Slide drying bench	MH 6616	Medax, Kiel, Germany
Spectrophotometer	UV-120-02	Shimadzu, Kyoto, Japan
Speed vac plus	SC 110 A	Savant Instruments, Farmingdale, New York, USA
Thermomixer	Eppendorf 5436	Eppendorf-Netheler Hinz GmbH, Hamburg, Germany
Universal vacuum system plus with vapor net CFC free	UVS 400 A	Savant Instruments, Farmingdale, New York, USA
Ventilator	HSE-Harvard MiniVent	Hugo Sachs Elektronik-Harvard Apparatus, March-Hugstetten, Germany
Vortexer	Heidolph Reax 2000	Heidolph Instruments, Kehlheim, Germany
Water bath	GFL1052	GFL, Burgwedel, Germany
XAR film		Kodak, New York, USA

2. 1. 6. Bacteria

Pathogen	Strain	Source
<i>Mycobacterium avium</i>	TMC724	Division of Molecular Infection Biology, Research Center Borstel, Germany (originally obtained from the Trudeau Institute)

<i>Mycobacterium tuberculosis</i>	H37Rv	Division of Molecular Infection Biology, Research Center Borstel, Germany (originally obtained from the Trudeau Institute)
-----------------------------------	-------	--

2. 2. Experimental animals

2. 2. 1. Immunocompetent mice

Strain		Source
C57BL/6		Charles River, Sülzfeld; Germany
C57BL/6 J		The Jackson Laboratory, Bar Harbor, USA

2. 2. 2. Immunodeficient mice

Strain	Background	Source
IL-18-KO	C57BL/6	S. Akira, through Free University of Berlin, Berlin, Germany
CXCR3-KO	C57BL/6	B. Lu and C. Gerard, Boston, USA
IFN- γ -KO J	C57BL/6	The Jackson Laboratory, Bar Harbor, USA
IRF-1-KO J	C57BL/6	The Jackson Laboratory, Bar Harbor, USA
STAT-1-KO	C57BL/6	T. Kolbe, Vienna, Austria
IFN- α/β -R-KO	C57BL/6	U. Kalinke, Frankfurt, Germany

2. 3. Methods

2. 3. 1. Mice

Selectively gene-deficient (knock-out, KO) mice that were backcrossed for at least 10 generations to a C57BL/6 background were used with age- and sex-matched C57BL/6 (wild-type, WT) mice. All mice were free of viral mouse pathogens and common bacterial or parasitic diseases. For the course of *M. avium* infection, age- and sex-matched groups of

mice were housed in isolator cages under barrier conditions in the animal facilities at the Research Center Borstel, and for the course of *M. tuberculosis* infection, age- and sex-matched groups of mice were housed in individually ventilated cages in the animal rooms of the biological safety level (BSL) III facility at the Research Center Borstel. Mice were infected at 8 weeks of age. All mouse experiments were approved by the Schleswig-Holstein Ministry of the Environment, Nature and Forestation, and an independent Institutional Review Board (Nr. V252-72241.123(40-4/01), Nr. V252-72241.123-3(45-5/02) and Nr. V362-72241.123-3(43-5/05)).

2.3.2. Bacteria

M. tuberculosis H37Rv and *M. avium* TMC724 were passaged in C57BL/6 mice and cultured in Middlebrook 7H9 medium supplemented with oleic acid, albumin, dextrose, and catalase to a late logarithmic phase. The absence of contaminating bacteria was examined by applying the culture material on brain heart infusion agar as well as by a Ziehl-Neelsen staining. Aliquots were frozen at -80°C until needed. In order to determine the number of colony forming units (CFU) in the cultures, serial 10-fold dilutions of the bacterial suspension in distilled water with 0.05% Tween-80 were prepared and plated on nutrient Middlebrook 7H10 agar supplemented with pyruvate for *M. avium* or supplemented with oleic acid, albumin, dextrose, and catalase for *M. tuberculosis*. Bacterial colony numbers were determined after 21 days of incubation at 37°C in humidified air and calculated for each culture.

2.3.3. Infection of mice

In a respiratory infection model, mice were exposed to an aerosol containing *M. avium* TMC724 or *M. tuberculosis* H37Rv using an aerosol inhalation device calibrated to deposit 10^5 CFU *M. avium* or 100 CFU *M. tuberculosis* in the lungs of mice, as described [170, 171].

Briefly, a 6.0 ml inoculum of bacteria was prepared by thawing several aliquots, washing them by centrifugation at 16,000 rpm for 15 min, and pooling the pellets in distilled water. 0.5 ml of the inoculum was used to confirm the actual bacterial concentration after 21 days of incubation at 37°C in humidified air. Mice were exposed for 40 min to an aerosol

generated by nebulizing the 5.5 ml of the bacterial inoculum containing 2×10^6 CFU/ml *M. tuberculosis* H37Rv or 10^9 CFU/ml *M. avium* TMC724. Aerogenic infection was performed in a closed Glas-Col aerosol infection device, using the following parameters: 900 sec pre-warming time, 2400 sec nebulizing time, 2400 sec suction time und 900 sec decontamination time. During the aerosol infection the vacuum was kept constant at 60 cubic feet per hour (CFH) and on starting the nebulization the pressure of the compressed air was set at 10 CFH. The inoculum size (~ 100 CFU/lung) for *M. tuberculosis* or ($\sim 10^5$ CFU/lung) for *M. avium* was checked 24 h after infection by determining the bacterial load in the lungs of infected mice. To this end, mice were sacrificed and lungs were dissected and homogenized in 2 ml sterile water with 0.05% Tween-80 to determine bacterial loads by plating serial 10-fold dilutions of whole lung homogenates on appropriate media.

2. 3. 4. Infection of guinea pigs

Female outbred hartley guinea pigs 500g in weight (purchased from the Charles River Laboratories, North Wilmington, USA) were held under barrier conditions in a biological safety level (BSL) III animal laboratory at Colorado State University.

In collaboration with Ian Orme, Colorado, USA, a Madison chamber aerosol generation device (University of Wisconsin College of Engineering Shops, Madison, USA) was used to expose guinea pigs to an aerosol of *M. tuberculosis* H37Rv and was calibrated to deliver approximately 20 bacteria into the lungs, as described [183].

30, 60 and 90 days after infection guinea pigs were sacrificed. Sedated guinea pigs received 60 mg/kg body weight pimonidazole by the intraperitoneal route, and were euthanized 2 h later to harvest tissues. Lungs and lymph nodes were dissected, injected with fresh 4% formalin and positioned into a histogrid. The closed histogrid was immersed into fresh 4% formalin in PBS, pH 7.4 for fixation. After 24 hours of fixation in 4% formalin, the organs were dehydrated and embedded in liquid paraffin. Paraffin blocks were sent from USA by express mail to be further processed in Borstel.

2. 3. 5. Organ dissection

Data for different KO mouse strains were obtained in separate experiments, each having its own control group. The natural course of infection and the kinetics of granuloma formation

in C57BL/6 mice infected with *M. tuberculosis* H37Rv and *M. avium* TMC724 were described previously [170, 171]. Between 11 and 20 weeks post-infection, *M. avium*-infected mice were sacrificed. *M. tuberculosis*-infected mice were sacrificed at day 345, 404 and 522 post-infection.

Mice were scored as moribund when weight loss was in excess of 25% compared with age-matched uninfected controls. Groups of 4–5 mice were anaesthetized by a narcotic overdose and euthanized at indicated time points to follow the course of infection. Blood was withdrawn from the vena cava inferior into serum separation tubes. By centrifugation for 10 min at 6000 rpm serum was obtained and stored for analysis at -80°C . For genotyping of mice, 1 cm of the tail was cut and stored at -80°C . The lung was dissected, weighed and divided. The right lower lobe of the lung was weighed and homogenized in appropriate volume of distilled water for the determination of bacterial load as well as for cytokines determined by ELISA. The right upper lobe of the lung was dissected, injected with fresh 4% formalin and positioned into a histogrid together with a part of the liver and spleen. The closed histogrid was immersed into fresh 4% formalin in PBS, pH 7.4 for fixation. The left lower and middle lobe of the lung were weighed and snap-frozen in GUTC buffer with 100 mM β -mercaptoethanol and stored at -80°C for RNA preparation. The left upper lobe of the lung was dissected, injected with Tissue Tec diluted 1:3 in 10 mM PBS and snap-frozen in a piece of aluminium foil stored at -80°C for frozen tissue sectioning.

As a positive control in experiments determining tissue hypoxia, C57BL/6 mice were subcutaneously injected with different concentrations (1×10^5 , 3×10^5 , and 1×10^6) of MB49 tumor cells. Following macroscopically visible necrotization, usually after 3-5 weeks, the tumor was dissected [184].

2. 3. 6. Homogenization

Dissected lungs were homogenized in 2 ml sterile water with 0.05% Tween-80 (for bacterial load) or in 3 ml 10 mM phosphate-buffered saline with protease inhibitor (for ELISA) or in 1 ml GUTC/M-EtOH (for RNA) using a tissue homogenizer and sterile frozen pestles.

2. 3. 7. Bacterial load

The bacterial load was determined by plating serial 10-fold dilutions of whole lung homogenates on nutrient Middlebrook 7H10 agar supplemented with pyruvate for *M. avium* or supplemented with oleic acid, albumin, dextrose, and catalase for *M. tuberculosis*. Bacterial colony numbers CFU were determined after 21 days incubation at 37°C in humidified air. Considering the weight of the homogenized lung lobe, CFUs were calculated for the whole lung.

2. 3. 8. Histology

2. 3. 8. 1. Paraffin sections

Fixation of organ tissue was performed over night. After 24 hours of fixation in 4% formalin, the organs were dehydrated using an Autotechnicon in the following sequence: 45 min 50% alcohol, 45 min 70% alcohol, 45 min 95% alcohol, 2¼ h 100% alcohol, 2¼ h intermedium, 2 h 65°C hot paraffin. After dehydration organs were embedded in liquid paraffin at 65°C using a paraffin dispensing station. Paraffin blocks were stored at 4°C. 2 µm sections were cut on a rotary microtome, stretched in a cold then in a 37°C warm water bath, and mounted on glass slides. Sections were left to dry at least for 2 h at 37°C on a slide-drying bench. Slides were stained with standard Haematoxylin-Eosin stain for overview, as well as with a trichrome stain for collagen detection.

2. 3. 8. 2. Haematoxylin-Eosin (HE) staining

For histopathological examinations, paraffin sections were deparaffinized with rotihistol, rehydrated and stained with Gill's haematoxylin giving the chromatin a blue color. Excessive color was removed under running tap water. Subsequently, an Eosin counter stain was used to color the cytoplasm as well as intracellular substances in pink. Aqua bi-dist. in turn removed excessive color. At the end, tissue sections were dehydrated and retreated with rotihistol to be covered in entellan. After drying, microscopic examination of the tissue sections was performed using a light microscope.

2. 3. 8. 3. Ziehl-Neelsen (ZN) staining

For histological staining of mycobacteria in infected tissues, paraffin sections were deparaffinized with rotihistol, rehydrated and covered with carbol fuchsine. The slides were heated to boil several times. The bacterial cell wall stains in red color. After cooling down to RT, slides were washed in aqua bi-dist. and bacteria inside the tissue sections were placed in an acidified ethanol solution. As mycobacteria are acid fast, they do not decolorize in contrast to other bacteria. After washing the tissue sections in aqua bi-dist., they were counter-stained with Löffler's methylene blue and washed again in aqua bi-dist. to remove excessive color. At the end, tissue sections were dehydrated and retreated with rotihistol to be covered in entellan. After drying, microscopic examination of the tissue sections was performed using a light microscope.

2. 3. 8. 4. Frozen sections

Frozen organs were allowed to thaw from -80°C to -20°C inside the cold chamber of a cryotome. $5\ \mu\text{m}$ sections were cut on a cryotome and mounted on glass slides. Slides were left to dry for 15 min at RT under a sterile bench, then sections were fixed in 100% acetone for 20 min followed by 20 min in 100% chloroform. After fixation slides were allowed to dry for 20 min at RT.

2. 3. 9. Immunohistochemical analysis

2. 3. 9. 1. Hypoxia and HIF-1 α

$1\frac{1}{2}$ and 3 h prior to dissecting the lung as well as the tumor, mice were intravenously injected with the hypoxia marker pimonidazole hydrochloride at a dose of 60 mg/kg weight of mouse. $2\ \mu\text{m}$ sections of paraffin-embedded tissues were deparaffinized on superfrost slides. Antigen retrieval for hypoxia was carried out on deparaffinized tissues with pronase for 40 min at 40°C , while antigen retrieval for HIF-1 alpha was carried out in a 10 mM sodium citrate buffer for 45 min. Subsequently, reduction of endogenous peroxidase activity was achieved with 0.03% hydrogen peroxide for 5 min at room temperature. The anti-hypoxia antibody Hypoxyprobe-1mAb1 (Chemicon, Hampshire,

United Kingdom) or the anti-HIF-1 alpha antibody (Novus-Biologicals, Littleton, USA) was labeled with a biotinylation reagent for 15 min, followed by incubation with a blocking reagent for 5 min (Dako ARK peroxidase, Hamburg, Germany) in order to block non-specific binding. The reaction was visualized using a streptavidin conjugated to horseradish peroxidase (Dako ARK peroxidase, Hamburg, Germany) followed by its substrate 3,3'-diaminobenzidine (Dako ARK peroxidase, Hamburg, Germany).

2. 3. 9. 2. iNOS and HIF-2 α

2 μ m sections of paraffin-embedded tissues were deparaffinized. Antigen retrieval was carried out in a 10 mM sodium citrate buffer for 45 min. Subsequently, the slides were allowed to cool to room temperature, followed by reduction of endogenous peroxidase activity with 3% hydrogen peroxide in 10 mM phosphate-buffered saline for 30 min at room temperature. Non-specific binding was blocked with 5% fetal calf serum in 10 mM phosphate-buffered saline, pH 7.4, for 50 min. Tissue sections were incubated for 1 h with appropriately diluted anti-iNOS primary antibody (Upstate, Lake Placid, USA) or with the anti-HIF-2 alpha antibody (Novus-Biologicals, Littleton, USA), followed by incubation with biotinylated goat F(ab')₂-Fragment anti-rabbit IgG (Dianova, Hamburg, Germany). After that tissue sections were incubated for 30 min with a peroxidase conjugated streptavidin (Dako Cytomation, Hamburg, Germany).

2. 3. 9. 3. Endomucin

As previously described [185], 2 μ m sections of paraffin-embedded tissues were deparaffinized. Antigen retrieval was carried out in a 10 mM sodium citrate buffer for 15 min. Subsequently, the slides were allowed to cool to room temperature, followed by reduction of endogenous peroxidase activity with 1% hydrogen peroxide in 10 mM phosphate-buffered saline for 40 min at room temperature. Non-specific binding was blocked with 5% fetal calf serum in 10 mM phosphate-buffered saline, pH 7.4, for 50 min. Tissue sections were incubated for 1 h with anti-endomucin primary antibody (obtained as tissue culture supernatant from D. Vestweber, Münster, Germany), followed by incubation with affinity-purified peroxidase-conjugated rabbit anti-rat IgG (dilution 1:100; Dianova, Hamburg, Germany), and goat anti-rabbit IgG (dilution 1:50; Dianova, Hamburg,

Germany). The reaction was visualized either with 3-amino-9-ethylcarbazole (AEC) giving a red staining or with 3,3'-diaminobenzidine (DAB) giving a brown staining for endomucin.

2.3.9.4. Counter-staining

After visualizing the reaction with 3,3'-diaminobenzidine, tissue sections were counterstained with Mayer's haematoxylin and mounted. All reactions were performed in a humidified chamber, and, for control purposes, the primary antibody was either omitted or replaced by an irrelevant mouse antibody of the same isotype.

2.3.10. Enzyme Linked Immunosorbent Assay (ELISA)

Levels of IFN- γ , TNF- α and IL-12 (BD Pharmingen, San Diego, USA) proteins in the lung homogenates were measured with commercial OptEIA Cytokine ELISA kits according to the sandwich technique. Lungs were harvested 14 and 20 weeks post-infection with *M. avium* and homogenized in 10 mM phosphate-buffered saline with protease inhibitor before ELISA measurement. 96-well-plates were coated with capture antibody (diluted 1:250) over night at 4°C in a wet chamber. After discarding the supernatant and washing the plates 3 \times with washing buffer, they were blocked with assay-diluent for 1 hour at RT. Subsequently, the supernatant was discarded and the plates were washed 3 \times with washing buffer. Serial dilutions of standard, samples and controls were applied on the plates and incubated for 2 hours at RT in a wet chamber. After discarding the supernatant and washing the plates 5 \times with washing buffer, the endogenous biotin was blocked using an avidin block for 15 min at RT followed by a biotin block for another 15 min at RT. Plates were washed 1 \times with washing buffer between the avidin and the biotin blocking, while washed 3-5 \times after biotin blocking. The detection antibody (diluted 1:500 for IFN- γ and TNF- α , 1:250 for IL-12) was incubated on the plate for 1 hour at RT, then plates were washed 6 \times with washing buffer. The enzyme reaction took place by applying an avidin-HRP-solution (diluted 1:250) for 1 hour at RT, followed by the TMB substrate reagent, which incubated in the dark for 30 min at RT. Plates were washed 6 \times with washing buffer between the enzyme and the substrate reagent. The enzyme-substrate reaction was stopped by 1 M H₃PO₄ after color development. Absorption was measured at 450 nm against a 620

nm reference wavelength by an ELISA Reader. The cytokine concentration was evaluated using Magellan software (TECAN) and calculated for total organ weight.

2. 3. 11. RNA preparation

Total cellular RNA was isolated from lungs snap-frozen in a GUTC buffer with 100 mM β -mercaptoethanol and stored at -80°C . After homogenizing the tissue, a phenol/chloroform extraction was performed using Trizol diluted with 10 mM PBS and 1/10 volume BCP. The RNA was precipitated using isopropanol, washed with 75% ethanol, air-dried and dissolved in DEPC water. The quality of the isolated RNA was evaluated by agarose gel electrophoresis and RNA was quantified by spectrophotometric analysis at a wavelength of 260 nm.

2. 3. 12. Ribonuclease Protection Assay (RPA)

The Ribonuclease Protection Assay (RPA) was performed according to the Pharmingen standard protocol using the Riboquant *in vitro* transcription kit and the RPA kit in collaboration with Tamás Laskay, Lübeck, Germany. For the synthesis of a radio-labeled anti-sense RNA probe set, a reaction mixture (10 μl) was prepared containing 100 μCi (α - ^{33}P)-UTP, UTP (61 μM), GTP, ATP, CTP (2.75 mM each), DTT (100 mM), RNase inhibitor (40 U/ μl), transcription buffer (5 \times), T7 RNA polymerase (20 U/ μl) and the commercial template sets mAngio-1 and mCK-5c, SLC was inserted into the mCK-5c kit, SLC and the KM-2 kit were obtained from T. Laskay as described [186]. After incubation at 37°C for 1 h, the reaction was terminated by adding DNase (1 U/ μl) for 30 min. The probe was extracted by phenol/chloroform and precipitated with ethanol. Air-dried radiolabeled anti-sense RNA probe was dissolved in hybridization buffer and 2 μl of diluted probe (2×10^5 cpm/ μl for chemokines, 3.5×10^5 cpm/ μl for angiogenic factors) was added to each RNA sample (8 μg each). The samples were overlaid with mineral oil, heated at 90°C for 3 min and subsequently hybridized at 56°C for 12-16 h. After hybridization, the samples were treated with RNases A (80 ng/ μl) and T1 (250 U/ μl) for 45 min at 30°C to digest single stranded RNA. Proteinase K (10 mg/ml) and yeast tRNA (2 mg/ml) were added and samples were incubated for 15 min at 37°C . Finally, RNase-protected probes were purified by extraction/precipitation as described above and separated

on a 5% acrylamide sequencing gel containing 8 M urea in 0.5×TBE buffer. For autoradiography, dried gels were exposed to XAR film at room temperature. For quantitation of radiation intensity of RNA bands, which correlate with chemokine mRNA expression, gels were placed on imaging plates and images were analyzed using a Phosphor-Imager and Image Quant 5.2 software (Molecular dynamics). Chemokine mRNA values were expressed as a ratio to the mRNA values of the corresponding house-keeping gene L32 (% of L32 mRNA expression) in order to normalize for possible differences in gel loading [186].

Chemokine	Abbreviation
ABCD-1	
Angiopoietin	
B-lymphocyte chemokine	BLC
Endoglin	
Eotaxin	
Epstein-Barr virus-induced molecule 1 ligand chemokine	ELC
FLT1	
FLT4	
Interferon-gamma-inducible protein-10	IP-10
Lymphotactin	Ltn
Macrophage inflammatory protein-1 α	MIP-1 α
Macrophage inflammatory protein-1 β	MIP-1 β
Macrophage inflammatory protein-1 γ	MIP-1 γ
Macrophage inflammatory protein-2	MIP-2
Monocytes chemoattractive protein-1	MCP-1
Monokine induced by interferon-gamma	MIG
Platelet endothelial cell adhesion molecule-1	PECAM-1/CD31
Regulated upon activation normal T-cell expressed and secreted	RANTES
Secondary lymphoid-tissue chemokine	SLC
T-cell activation gene 3	TCA3
Thrombin	
TIE	
TIE2	
Vascular endothelial growth factor	VEGF
Vascular endothelial growth factor C	VEGFC

2. 3. 13. Affymetrix gene expression micro-arrays

For biotin-labeled target synthesis starting from 5 μ g of total RNA, reactions were performed using the Affymetrix One-Cycle target labeling and control kit as described by the manufacturer (Affymetrix, Santa Clara, USA) in collaboration with Roland Lang,

München, Germany. Briefly, 5 µg total RNA were converted to double stranded cDNA using a T7(T)24 primer containing a T7 promotor. The cDNA was then used directly in an *in vitro* transcription reaction in the presence of biotinylated pseudouridine ribonucleotides. 12.5 µg of the cleaned and biotinylated cRNA preparation were fragmented and placed in a hybridization cocktail. Samples were then hybridized once to an identical lot of Affymetrix Mouse 430A_2 (total of 22 690 probe sets) for 16 h at 45°C. After hybridization, the gene chips were washed, stained with SA-PE (Vector Laboratories, Burlingame, USA), and read using an Affymetrix gene chip fluidic station and scanner.

Affymetrix CEL files were processed for global normalization and generation of expression values using the robust multi-array average (rma) algorithm in the R affy package (www.bioconductor.org) [187]. The resulting log₂ expression values were transformed into linear values.

Micro-array data from infected mice were normalized and fold change (FC) was calculated relative to baseline controls of uninfected mice. A two-way ANOVA was performed to test the significance of the difference between infected wild-type and infected IFN-γ deficient mice, considering the combined influence of the co-variants infection and the deficiency in IFN-γ. Two-way ANOVA calculation was done using the ANOVA function in R (Version 2.1.1). The resulting p-values were subsequently corrected for multiple testing using the algorithm proposed by Benjamini and Hochberg [188], implemented in the R (www.R-project.org) multi-test package (output: q-values) [189].

The gene expression analysis was filtered for regulated genes that employed the following stringent criteria to define genes as significantly regulated: q-values below 0.01, indicating the level of significance of the difference between infected wild-type and infected IFN-γ deficient mouse strains based on a two-way ANOVA; a FC above 2 or below 0.5, signifying the change in expression level for a transcript between infected wild-type and infected IFN-γ deficient mouse strains. Significantly regulated genes were clustered according to similar regulation patterns. Statistical evaluation and clustering were carried out in collaboration with Jörg Mages, München, Germany.

The cut offs were selected to be FC in expression for infected wild-type versus infected IFN-γ deficient mice above 2 or below 0.5, above 4 or below 0.25, above 5 or below 0.2, and above 10 or below 0.1 using Microsoft Office Excel 2003 for Windows.

2.3.14. Oxygen measurement

Mice were anaesthetized by intraperitoneal injection of pentobarbital at 30 mg/kg body weight. The dose was reduced depending on disease progression and physiological state (ranging from 30 mg/kg to 13 mg/kg body weight). The operation was performed under anaesthesia in collaboration with Klaus Wagner, Lübeck, Germany. Following tracheotomy, a fixed cannula was coupled via sterile tubing to a mouse ventilator, which was set at a rate of 90-120 strokes/min with a stroke volume of 200-300 μ l adjusted to the animal body weight. A flexible Clarke-type catheter micro-electrode (Tip diameter 0.5 mm, probe REF CC1.R, program plug 8400) was used for oxygen partial pressure measurement. By design, the oxygen sensitive area of the probe was positioned 1 mm below the probe tip. Thus, the oxygen pressure readings were not confounded by compression artifacts from insertion of the probe into the tissue. Each oxygen probe was calibrated in a heated (37°C) PBS filled chamber against compressed air and pure nitrogen until stable readings were obtained. Zero current of the probe was <3 nA. Each tissue measurement was preceded and followed immediately by a calibration as described above. Of note, there was no zero current drift of the probe observed and compressed air current drift was below 0.05%. Lung tissue temperature was obtained at the end of each O₂ measurement sequence (Philips thermocouple type k, tip diameter 0.1 mm) and lay between 36°C and 37°C. Thus, no compensation of the tissue pO₂ readings for differences in temperature between the calibration chamber and the tissue measurement had to be performed. Following surgical opening of the chest cavity, removal of the pleura and exposure of the lung surface, the oxygen probe was inserted carefully into several different areas of the lung, where a distinct morphologically altered zone of fibrotic induration was macroscopically detectable (Fig. 22). Typically, three to four different regions of the lung were probed with an average penetration of 4-11 mm before the multiply damaged lung collapsed and cardiac function was compromised. Tumor-bearing mice were anaesthetized and the fur and superficial skin were surgically removed from the subcutaneous tumor before inserting the oxygen probe. Two measurements with the electrode placed at the center of the tumor were taken per mouse. After measuring the partial pressure of oxygen, the lung and the tumor were dissected and fixed in fresh 4% formalin in PBS, pH 7.4, for histological examination.

2. 3. 15. Statistics

Means, SDs, and statistics for quantifiable data, such as CFU counts, cytokine levels and pO₂ concentrations were calculated using Microsoft Office Excel 2003 for Windows and GraphPad Prism version 4.00 for Windows (GraphPad Software, San Diego, CA; www.graphpad.com).

Significance of the difference at a given time point was analyzed using one-way ANOVA, setting the confidence level at 99%. If not specifically indicated by an asterisk, the p-value is above 0.05 and there is no significant difference at a confidence level of 95% and 99%.

3. Results

3.1. Mouse model of mycobacteria-induced granuloma necrosis

In order to assess which mouse model best reflects the pathology of human TB, C57BL/6 mice were infected by aerosol with 100 CFU of *M. tuberculosis* H37Rv or with 10^5 CFU *M. avium* TMC724. *M. avium*-infected lungs were dissected 20 weeks post-infection, and *M. tuberculosis*-infected lungs were dissected at randomly chosen late stages of infection (e.g. day 345 post-infection).

In mice infected with *M. tuberculosis*, large lymphocytic aggregates were evident close to extensive areas of infiltrating cells composed in their majority of foamy macrophages and monocytes. A severe interstitial fibrosis was apparent resulting in a degenerative, “honeycomb” architecture of the lung. These degenerative changes and cellular infiltrations appeared to block or compress the alveolar spaces (Fig. 2A).

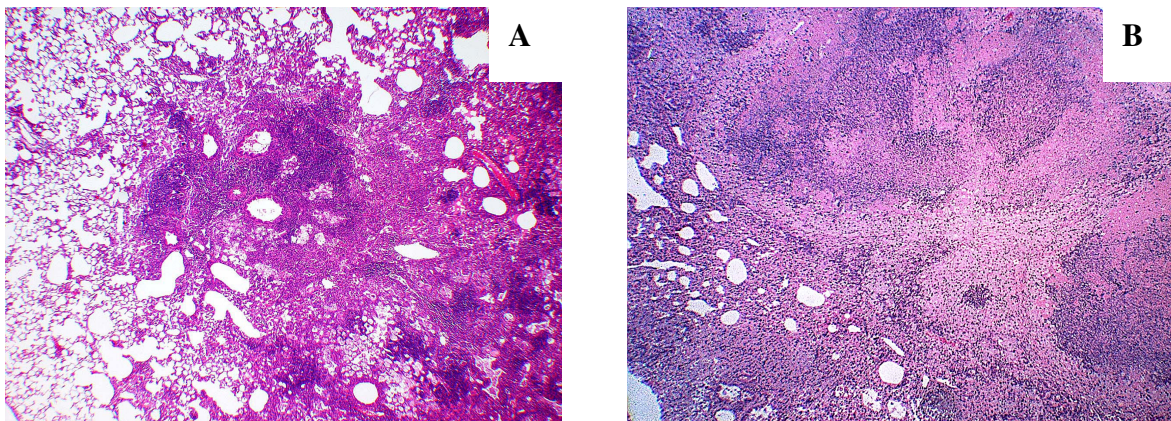


Figure 2: Mice infected with *M. avium* by aerosol develop granuloma necrosis. Histopathology of lungs from C57BL/6 mice, exposed to an aerosol containing *M. avium* TMC724 (panel B) or *M. tuberculosis* H37Rv (panel A) using an inhalation device calibrated to deposit 10^5 CFU *M. avium* or 100 CFU *M. tuberculosis* in the lungs of mice, respectively. *M. avium*-infected lungs were removed 20 weeks post-infection, while *M. tuberculosis*-infected lungs were dissected at day 345 post-infection. Lung sections were stained with HE (original magnification $\times 4$). Micrographs are representative of 5 mice examined.

Following *M. avium* infection in mice, central foci of an eosinophilic mass of acellular debris (presumably dead macrophages) were encircled by a granulocytic area. The granulocytes were packed within a surrounding belt of macrophages, at the border of which numerous lymphocytes could be discerned, often assembled in small aggregates.

Throughout the lung, dense accumulations of epithelioid cells co-existing with foamy cells were visible. In this highly organized solid structure alveolar spaces were effaced (Fig. 2B). The central necrosis within granulomatous lesions started to develop 16 weeks after infection. At later stages, peri-granulomatous fibrosis and pleural plaques were observed.

The *M. avium* infection in mice resembles the pathology following *M. tuberculosis* infection in humans [171], where mononuclear cells aggregate into a highly organized, centrally necrotizing granuloma, which is surrounded by a rim of lymphocytes.

M. avium-infected mice were therefore chosen as a suitable model to study the mechanisms of immunopathology of tuberculosis by further analysis.

3.2. Absence of granuloma necrosis in IFN- γ deficient mice

In order to confirm a previous report that IFN- γ was responsible for the granuloma necrosis evident in wild-type mice infected with *M. avium*, the course of aerosol infection with 10^5 CFU *M. avium* TMC724 was compared in IFN- γ -KO mice and C57BL/6 mice. The bacterial load in the lungs of IFN- γ -KO mice infected with *M. avium* was about 2 log/lung higher than in *M. avium*-infected C57BL/6 mice at 12, 14 and 16 weeks after infection (Fig. 3).

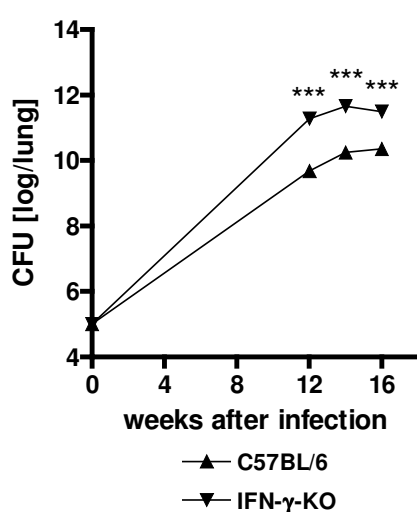


Figure 3: Bacterial load is increased in IFN- γ -KO mice infected with *M. avium* by aerosol. Mycobacterial growth pattern in C57BL/6 and IFN- γ -KO mice infected by aerosol with *M. avium* (TMC724, 10^5 CFU/mouse). *M. avium*-infected lungs were removed 12, 14 and 16 weeks post-infection. Mycobacterial colony enumeration in the lung was performed at indicated time points. Data represent the means of 4 mice \pm SD (error bars are too small to be seen). *** p < 0.001 at a confidence level of 99%.

16 weeks post-infection tissue sections of the lung were stained with Haematoxylin-Eosin to assess the degree and quality of granuloma formation. There was no granuloma necrosis in IFN- γ -KO mice. Instead, the pulmonary infiltrations were composed of a large number of granulocytic clusters varying in size. The clusters were interconnected via a dense network of “avenues”, formed by granulocytes, surrounding islands of giant and foamy macrophages that were occasionally interspersed by clusters of lymphocytes. Normal alveolar space was reduced in size, but blood vessels could be clearly seen (Fig. 4B).

On the other hand, granuloma necrosis was evident in the wild-type mice, where a necrotic core of dead cells was demarcated by a dense accumulation of epithelioid macrophages followed by a layer of fibroblasts and some small lymphocytic clusters. Alveolar spaces and larger blood vessels could only be seen outside this compact structure (Fig. 4A).

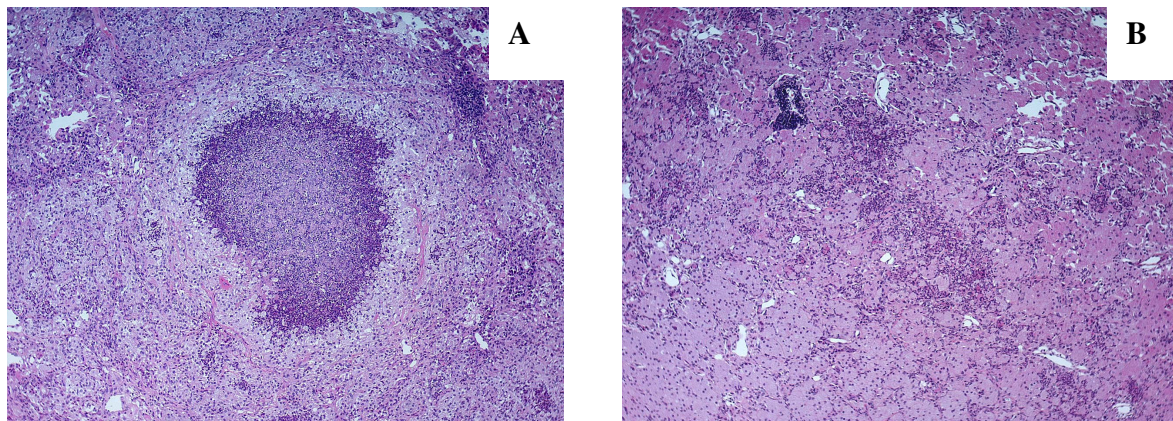


Figure 4: IFN- γ -KO mice infected with *M. avium* by aerosol do not develop granuloma necrosis. Histopathology of lungs from C57BL/6 (panel A) and IFN- γ -KO (panel B) mice infected by aerosol with *M. avium* (TMC724, 10^5 CFU/mouse). *M. avium*-infected lungs were removed 16 weeks post-infection. Lung sections were stained with HE (original magnification $\times 4$). Micrographs are representative of 4 mice examined.

This experiment confirmed previous data and revealed that deficiency in IFN- γ correlates with a lack of granuloma necrosis in response to *M. avium* infection [172].

3. 3. Granuloma necrosis in IL-18 deficient mice

Since IFN- γ proved to be essential for induction of granuloma necrosis, we next examined the role of the IFN- γ inducing cytokine, IL-18. Both IL-12 and IL-18 have been described to induce IFN- γ , thereby initiating a protective Th1-immune response [83, 190]. Mice deficient for IL-12 (p40, or both, p35 and p40 chains) are known not to develop granuloma

necrosis [172]. Thus, it was questioned whether only a minor reduction in IFN- γ levels caused by IL-18 deficiency might already suffice to prevent the development of granuloma necrosis.

Mice deficient for IL-18 were infected with *M. avium* TMC724 by aerosol, and the course of infection was compared to *M. avium*-infected wild-type mice. IFN- γ levels in infected lungs were significantly reduced to less than one-third at 14 weeks post-infection, but not completely suppressed in IL-18-KO mice compared to wild-type mice, while 20 weeks post-infection IFN- γ levels were similarly low in both IL-18-KO and wild-type mice (Fig. 5).

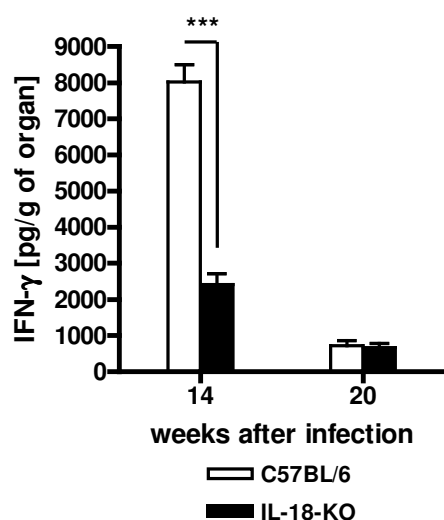


Figure 5: IFN- γ is reduced but not absent in IL-18-KO mice infected with *M. avium* by aerosol. C57BL/6 and IL-18-KO mice were infected by aerosol with *M. avium* (TMC724, 10^5 CFU/mouse). At 14 and 20 weeks post-infection, IFN- γ expression levels in lung homogenates were measured by ELISA. Data represent the means of 5 mice \pm SD. *** $p < 0.001$ at a confidence level of 99%, no significant difference $p > 0.05$ at a confidence level of 95% and 99%.

When examined at 14 weeks post-infection, the mycobacterial growth in the lungs of IL-18-KO mice was similar to that observed for the infected control mice, displaying bacterial loads of between 10^9 and 10^{10} CFU/lung, while 20 weeks post-infection, the mycobacterial growth in the lung of IL-18-KO mice was slightly higher than that observed for the infected control mice, displaying bacterial loads of between 10^{10} and 10^{11} CFU/lung (Fig. 6A). However, the mean survival times of IL-18-KO mice to mycobacterial infection were longer than of wild-type mice, as 50% of IL-18-KO mice succumbed to infection around day 170, while 50% of infected control mice succumbed to infection around day 130 (Fig. 6B).

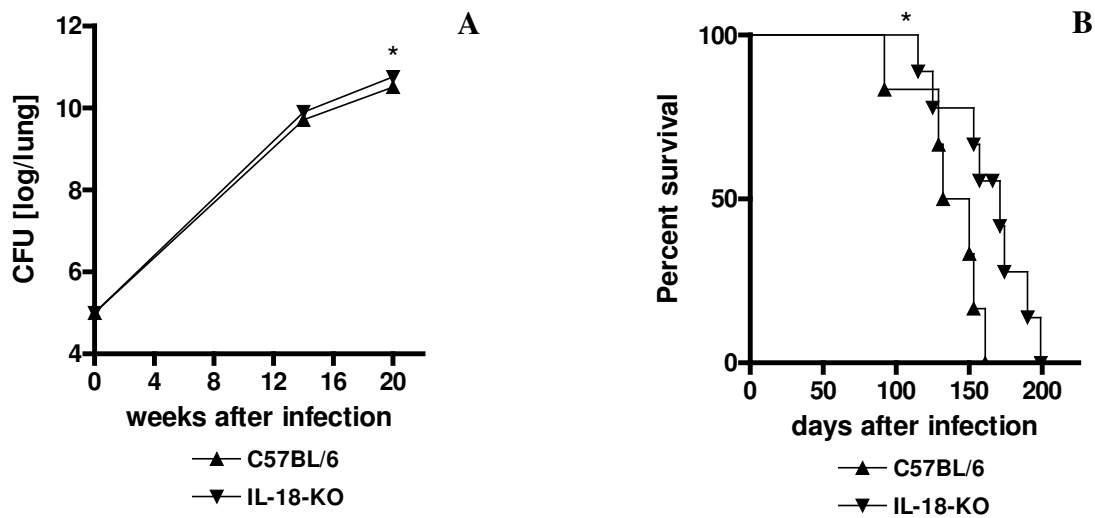


Figure 6: Bacterial load is slightly increased and survival time is prolonged in IL-18-KO mice infected with *M. avium* by aerosol. Mycobacterial growth pattern (panel A) and survival rate (panel B) in C57BL/6 and IL-18-KO mice infected by aerosol with *M. avium* (TMC724, 10^5 CFU/mouse). *M. avium*-infected lungs were removed 14 and 20 weeks post-infection. Mycobacterial colony enumeration in the lung was performed at indicated time points. Moribund mice were euthanized. Data represent the means of 5 mice \pm SD (error bars are too small to be seen). * $0.01 < p < 0.05$ at a confidence level of 99%, no significant difference $p > 0.05$ at a confidence level of 95% and 99%.

By 20 weeks post-infection several granulomas with necrotic centers had developed and there was no difference in the cellular composition of inflammatory infiltrations or the quantity of necrotizing granulomas between IL-18-KO and wild-type mice (Fig. 7).

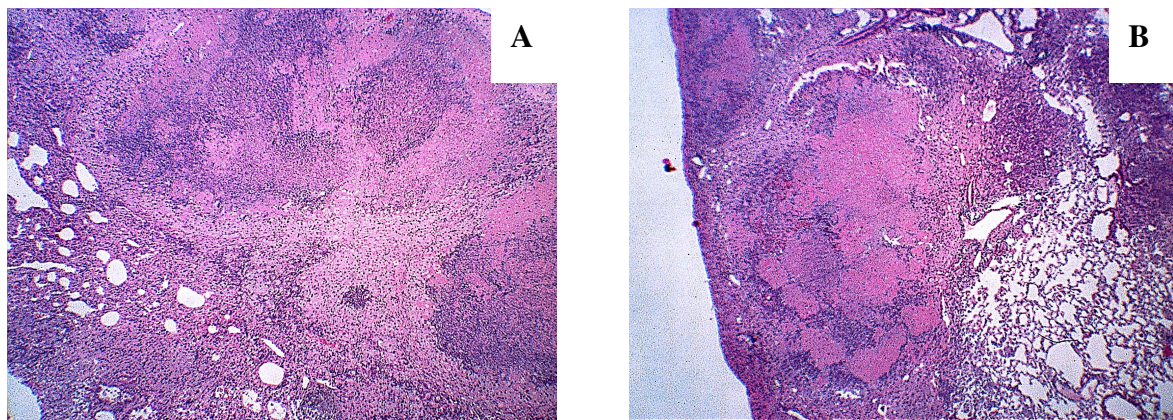


Figure 7: IL-18-KO mice infected with *M. avium* by aerosol resemble wild-type mice in terms of granuloma necrosis. Histopathology of lungs from C57BL/6 (panel A) and IL-18-KO (panel B) mice infected by aerosol with *M. avium* (TMC724, 10^5 CFU/mouse). *M. avium*-infected lungs were removed 20 weeks post-infection. Lung sections were stained with HE (original magnification $\times 4$). Micrographs are representative of 5 mice examined.

In conclusion, the reduction in IFN- γ levels evident in IL-18-KO mice is not sufficient to prevent the development of granuloma necrosis.

3.4. Absence of granuloma necrosis in mice deficient for the IFN- γ signaling molecules STAT-1 and IRF-1

IFN- γ is essential for granuloma necrosis, but a mere reduction in IFN- γ does not prevent necrosis. The signaling pathway of IFN- γ involves several key molecules. To determine whether key molecules involved either in early IFN- γ signaling events (STAT-1) or late IFN- γ signaling events (IRF-1) would be involved in granuloma necrosis, mice deficient for these molecules were infected with 10^5 CFU *M. avium* TMC724 and compared to C57BL/6 mice.

The bacterial load in the lungs of STAT-1-KO mice infected with *M. avium* was about 1 log/lung higher than in *M. avium*-infected C57BL/6 mice at 14 weeks after infection. 16 weeks after infection, lungs of wild-type mice reached the same CFU counts as STAT-1-KO mice (Fig. 8).

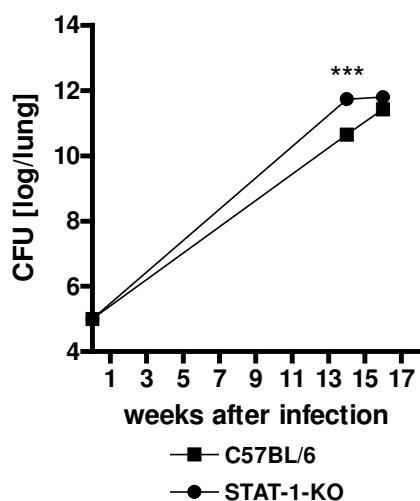


Figure 8: Bacterial load is higher in STAT-1-KO mice infected with *M. avium* by aerosol at 14 weeks post-infection. Mycobacterial growth in the lungs of C57BL/6 and STAT-1-KO mice infected by aerosol with *M. avium* (TMC724, 10^5 CFU/mouse). *M. avium*-infected lungs were removed 14 and 16 weeks post-infection. Mycobacterial colony enumeration in the lung was performed at indicated time points. Data represent the means of 4 mice \pm SD (error bars are too small to be seen). *** $p < 0.001$ at a confidence level of 99%, no significant difference $p > 0.05$ at a confidence level of 95% and 99%.

The IRF-1-KO mice infected with *M. avium* succumbed to infection after 24 weeks, while *M. avium*-infected C57BL/6 wild-type mice succumbed to infection after 20 weeks. The bacterial load at the last point examined in the lungs of IRF-1-KO mice infected with *M. avium* was 11.5 ± 0.10 and 11.2 ± 0.15 for *M. avium*-infected C57BL/6 control mice.

Results

Tissue sections from the lungs of STAT-1-KO and their control wild-type mice at 16 weeks post-infection, as well as from the lungs of IRF-1-KO at 24 weeks post-infection and their control wild-type mice at 20 weeks post-infection, were stained with Haematoxylin-Eosin to assess the degree and quality of granuloma formation. In STAT-1-KO mice (Fig. 9B) as well as in IRF-1-KO mice (Fig. 9D) granulocytes clustered inside large infiltrates. The clusters were mostly small in size, but they occasionally aggregated together. The clusters and aggregates were connected to each other by a granulocytic network that surrounded areas of giant and foamy macrophages. Small clusters of lymphocytes were sometimes seen. Alveolar spaces as well as blood vessels were also observed inside the infiltrates (Fig. 9B&D).

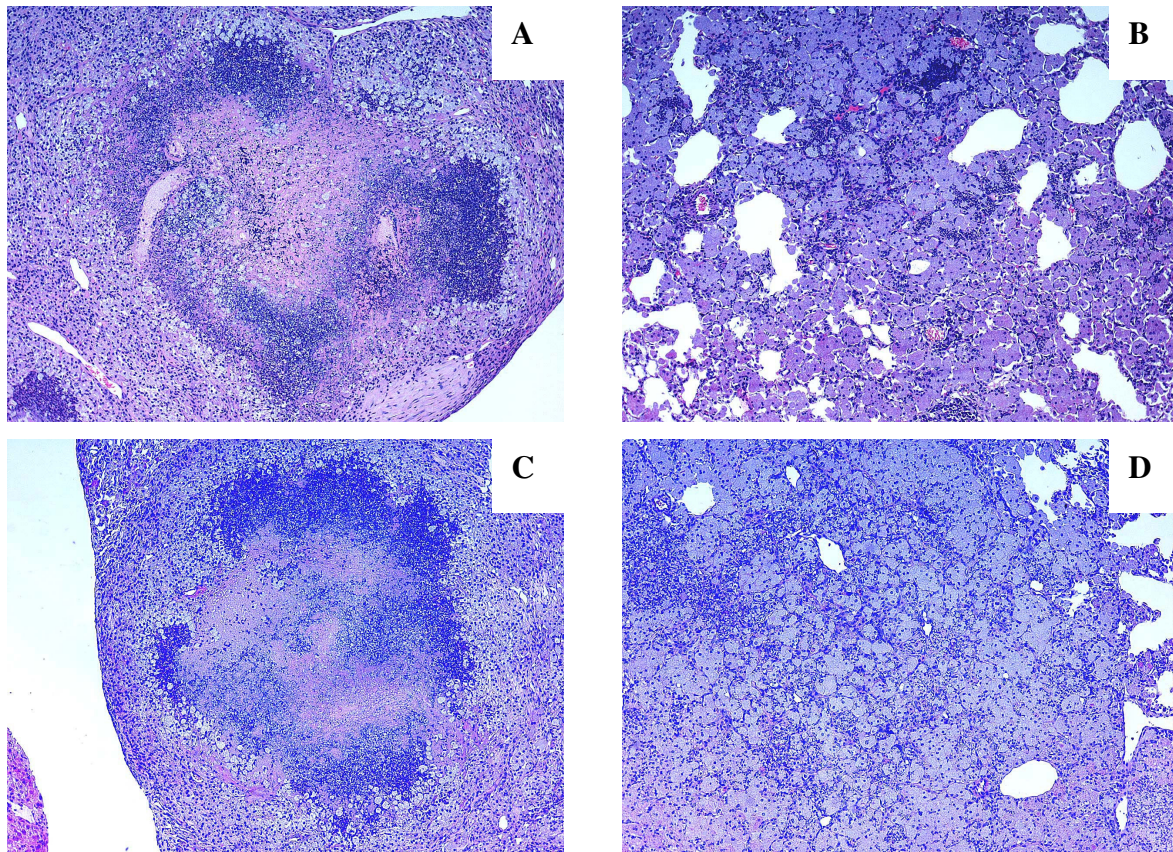


Figure 9: STAT-1-KO and IRF-1-KO mice infected with *M. avium* by aerosol do not develop granuloma necrosis. Histopathology of lungs from C57BL/6 (panel A&C), STAT-1-KO (panel B) and IRF-1-KO (panel D) mice infected by aerosol with *M. avium* (TMC724, 10^5 CFU/mouse). *M. avium*-infected lungs from STAT-1-KO and control wild-type mice were removed 16 weeks post-infection. *M. avium*-infected lungs from IRF-1-KO mice were removed 24 weeks post-infection and from control wild-type mice were removed 20 weeks post-infection. Lung sections were stained with HE (original magnification $\times 10$). Micrographs are representative of 4 mice examined.

In wild-type mice, a central necrosis of cell debris containing eosinophilic mass and basophilic remnants of nuclei was demarcated by granulocytes that were surrounded by a thick dense layer of epithelioid macrophages with interspersing fibroblasts. Some small clusters of lymphocytes were discerned at the outer border. Alveolar spaces and blood vessels were detected outside the necrotic granulomas (Fig. 9A&C).

Neither STAT-1-KO nor IRF-1-KO mice developed granuloma necrosis 16 nor 24 weeks after infection, respectively; instead, granulomatous lesions in these mice resembled very much those observed in IFN- γ -KO mice. Therefore, signaling events downstream of IRF-1 must be involved in driving granuloma necrosis.

3.5. Granuloma necrosis in IFN- α/β -receptor deficient mice

STAT-1 transduces signals from both the IFN type I as well as the IFN type II receptor. To determine whether IFN- α/β was also a critical inducer of STAT-1-mediated granuloma necrosis, IFN- α/β -R-KO and C57BL/6 mice were infected with 10^5 CFU *M. avium* TMC724. The mycobacterial growth in the lung of IFN- α/β -R-KO mice, 14 and 18 weeks post-infection, was identical to that observed for the control mice, displaying a bacterial load of about 10^{10} CFU/lung at 14 weeks and a bacterial load ranging between 10^{10} and 10^{11} CFU/lung at 18 weeks post-infection (Fig. 10).

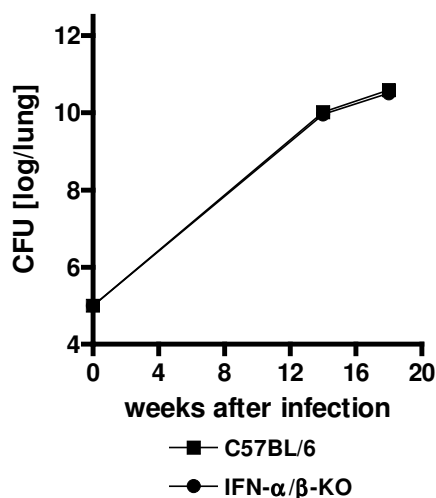


Figure 10: Bacterial load is identical in IFN- α/β -R-KO and wild-type mice infected with *M. avium* by aerosol. Mycobacterial growth pattern in C57BL/6 and IFN- α/β -R-KO mice infected by aerosol with *M. avium* (TMC724, 10^5 CFU/mouse). *M. avium*-infected lungs were removed 14 and 18 weeks post-infection. Mycobacterial colony enumeration in the lung was performed at indicated time points. Data represent the means of 4 mice \pm SD (error bars are too small to be seen). No significant difference $p > 0.05$ at a confidence level of 95% and 99%.

18 weeks post-infection tissue sections of the lung were stained with Haematoxylin-Eosin to assess the degree and quality of granuloma formation. A clear granuloma necrosis was evident in IFN- α/β -R-KO mice (Fig. 11B) as well as in wild-type mice (Fig. 11A). In both cases a central mass composed of acellular debris was contained in a rim of densely accumulating granulocytes surrounded by prominent layers of epithelioid macrophages and fibroblasts.

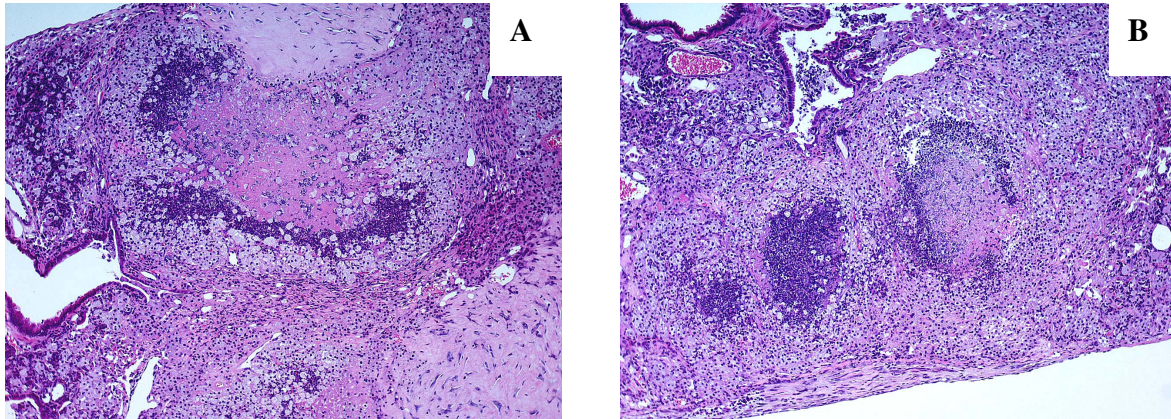


Figure 11: IFN- α/β -R-KO mice infected with *M. avium* by aerosol resemble wild-type mice in terms of granuloma necrosis. Histopathology of lungs from C57BL/6 (panel A) and IFN- α/β -R-KO (panel B) mice infected by aerosol with *M. avium* (TMC724, 10^5 CFU/mouse). *M. avium*-infected lungs were removed 18 weeks post-infection. Lung sections were stained with HE (original magnification $\times 10$). Micrographs are representative of 4 mice examined.

Thus, IFN type I signaling is not necessary for the development of granuloma necrosis in the lungs of mice infected with mycobacteria, while IFN- γ , STAT-1 and IRF-1 play a crucial role.

3. 6. Differential gene expression in wild-type versus IFN- γ deficient mice

IFN- γ , STAT-1 and IRF-1 are essential for granuloma necrosis, while a deficiency in IFN- α/β does not prevent necrosis. IFN- γ induces a variety of genes and the exhaustive analysis of individual mouse strains deficient for single molecules in IFN- γ -induced pathways of cell activation with respect to granuloma necrotization would be too time-consuming. We therefore resolved to undertake a comprehensive analysis of differentially expressed genes in wild-type and IFN- γ -KO mice to determine candidate genes highly regulated by IFN- γ

that might be critically involved in granuloma necrosis. IFN- γ -KO mice and C57BL/6 mice were infected with 10^5 CFU *M. avium* TMC724. Gene expression patterns were analyzed in the lungs of uninfected mice as well as of infected mice 14 weeks post-infection using Affymetrix micro-arrays (Fig. 12).

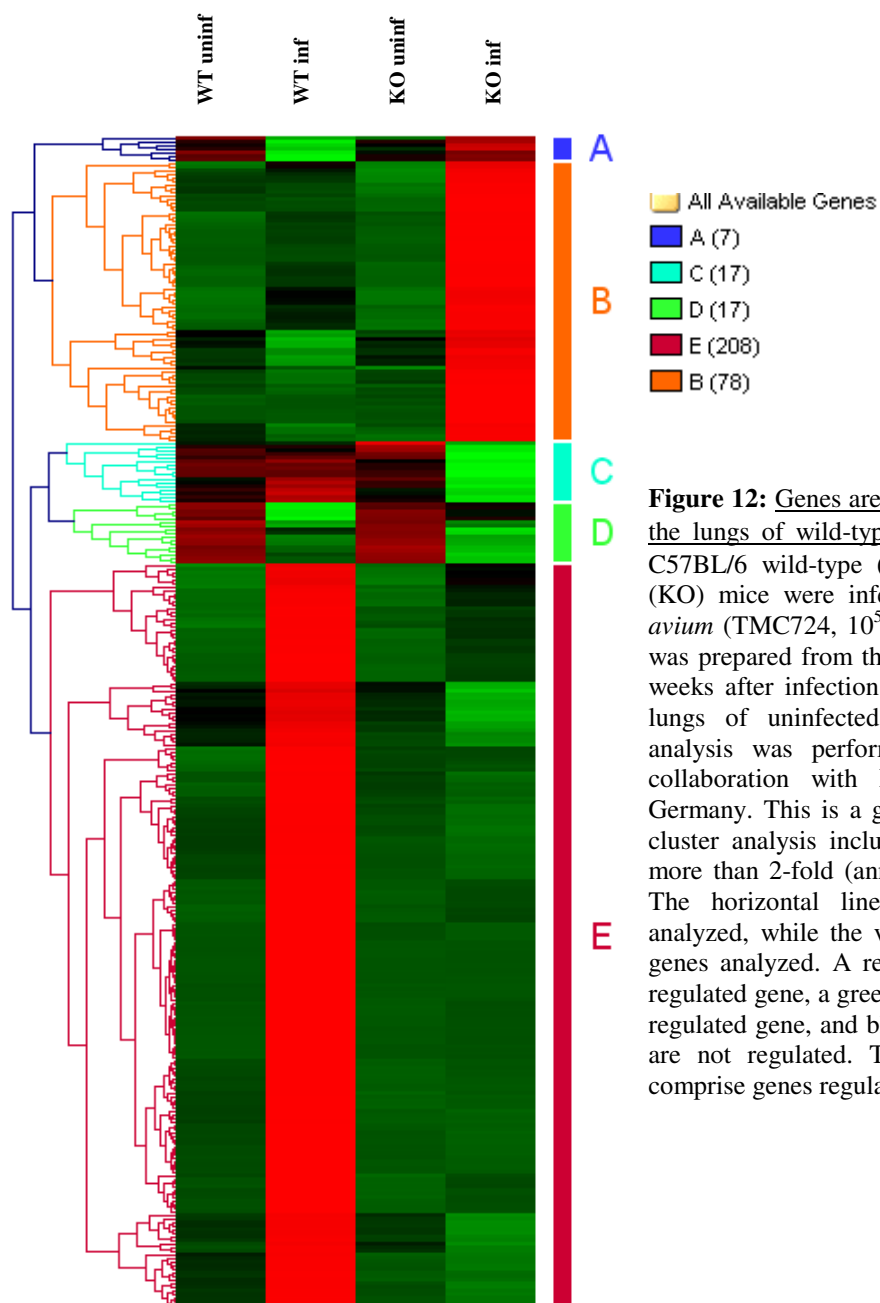


Figure 12: Genes are differentially expressed in the lungs of wild-type versus IFN- γ -KO mice. C57BL/6 wild-type (WT) and IFN- γ -deficient (KO) mice were infected by aerosol with *M. avium* (TMC724, 10^5 CFU/mouse). Total RNA was prepared from the right lungs harvested 14 weeks after infection as well as from the right lungs of uninfected mice. Gene expression analysis was performed via micro-arrays in collaboration with Roland Lang, München, Germany. This is a graphic representation of a cluster analysis including 327 genes regulated more than 2-fold (annotations see appendix 1). The horizontal lines represent the animals analyzed, while the vertical lines represent the genes analyzed. A red square indicates an up-regulated gene, a green square indicates a down-regulated gene, and black squares are genes that are not regulated. The different groups A-E comprise genes regulated in a similar manner.

As expected, many genes previously known to be regulated by IFN- γ (Tab. 1) were found to be differentially expressed in the two groups of mice. For example, STAT-1 and interferon-inducible small GTPases (like the interferon-gamma induced GTPase, the

Results

interferon inducible GTPase 1 and 2, as well as the T-cell specific GTPase) were almost exclusively regulated in C57BL/6 mice after infection, but not in IFN- γ -KO mice.

mRNA expression of genes increased in WT mice				
Gene Title	Gene Symbol	FC wt/ko	FC wt	FC ko
allograft inflammatory factor 1	Aif1	14.5	24.5	1.7
chemokine (C-X-C motif) ligand 10	Cxcl10	45.9	66.0	1.4
chemokine (C-X-C motif) ligand 11	Cxcl11	10.7	12.3	1.1
chemokine (C-X-C motif) ligand 9	Cxcl9	282.1	325.8	1.2
cystatin F (leukocystatin)	Cst7	12.9	52.7	4.1
expressed sequence AI132321	AI132321	10.4	6.1	-1.7
expressed sequence AI447904	AI447904	15.8	6.0	-2.7
fibrinogen-like protein 2	Fgl2	10.9	8.6	-1.3
guanylate nucleotide binding protein 1	Gbp1	26.4	29.7	1.1
guanylate nucleotide binding protein 2	Gbp2	17.5	9.7	-1.8
guanylate nucleotide binding protein 4	Gbp4	16.2	7.6	-2.1
histocompatibility 2, class II, locus Mb2	H2-DMb2	12.0	8.7	-1.4
histocompatibility 2, O region alpha locus	H2-Oa	18.0	18.1	1.0
HRAS like suppressor 3	Hrasls3	10.6	5.1	-2.1
immunoglobulin heavy chain 1a (serum IgG2a)	Igh-1a	57.4	304.9	5.3
indoleamine-pyrrole 2,3 dioxygenase	Indo	25.2	23.0	-1.1
interferon activated gene 205 /// myeloid cell nuclear differentiation antigen	Ifi205 /// Mnda	11.2	13.2	1.2
interferon inducible GTPase 1	Ilgp1	14.3	15.5	1.1
interferon, alpha-inducible protein 27	Ifi27	16.1	1.4	-11.1
interferon-induced protein 44	Ifi44	14.1	3.3	-4.2
interferon-induced protein with tetratricopeptide repeats 2	Ifit2	13.1	3.5	-3.7
interleukin 18 binding protein	Il18bp	13.4	22.0	1.6
macrophage activation 2 like	Mpa2l	25.9	26.0	1.0
membrane-spanning 4-domains, subfamily A, member 4C	Ms4a4c	12.7	10.6	-1.2
myeloid cell nuclear differentiation antigen	Mnda	12.0	8.3	-1.5
prostaglandin-endoperoxide synthase 2	Ptgs2	26.3	16.0	-1.6
radical S-adenosyl methionine domain containing 2	Rsad2	18.2	9.1	-2.0
RIKEN cDNA 2310016F22 gene /// hypothetical protein LOC223672	2310016F22Rik /// LOC223672	11.7	11.0	-1.1
RIKEN cDNA 5830443L24 gene	5830443L24Rik	24.3	36.3	1.5
signal transducer and activator of transcription 1	Stat1	13.1	6.4	-2.1
SLAM family member 8	Slamf8	47.2	100.0	2.1
ubiquitin D	Ubd	127.6	240.5	1.9
Z-DNA binding protein 1	Zbp1	11.0	19.8	1.8
mRNA expression of genes increased in KO mice				
Gene Title	Gene Symbol	FC ko/wt	FC wt	FC ko
cathepsin K	Ctsk	11.7	2.3	27.0
fibrinogen, alpha polypeptide	Fga	15.0	-1.2	13.5
fibrinogen, gamma polypeptide	Fgg	21.4	-1.4	15.0
immunoglobulin heavy chain 4 (serum IgG1)	Igh-4	17.4	21.9	380.8
neuropeptide Y	Npy	11.6	1.7	19.7
reduced expression 3	Rex3	66.0	-9.4	6.6

Table 1: Some genes are regulated higher than 10-fold in the lungs of wild-type versus IFN- γ -KO mice. A selection of 39 genes differentially expressed in the lungs of C57BL/6 wild-type (WT) and IFN- γ -deficient (KO) mice infected by aerosol with *M. avium* (TMC724, 10^5 CFU/mouse). Q value <0.01. The fold change (FC) is the gene expression in infected against uninfected mice, for wild-type mice FC wt and for IFN- γ -deficient mice FC ko. The cut-off set for differential expression is a gene expression difference above 10 between infected wild-type and infected IFN- γ -deficient mice FC wt/ko >10 and FC ko/wt >10, showing only highly regulated genes, where the fold change is higher than 10 comparing infected IFN- γ -deficient mice with infected wild-type mice.

Among the genes that were most differentially regulated between the two mouse strains, some chemokines stood out, in particular MIG, IP-10 and I-TAC. These chemokines were previously identified as having angiostatic potential [154].

3. 7. Differential expression of angiogenic and angiostatic factors in wild-type versus IFN- γ deficient mice

Since angiostatic chemokines were among the most differentially regulated genes in wild-type versus IFN- γ -KO mice, it appeared possible that a misbalance between angiogenic and anti-angiogenic factors might be associated with the development of granuloma necrosis.

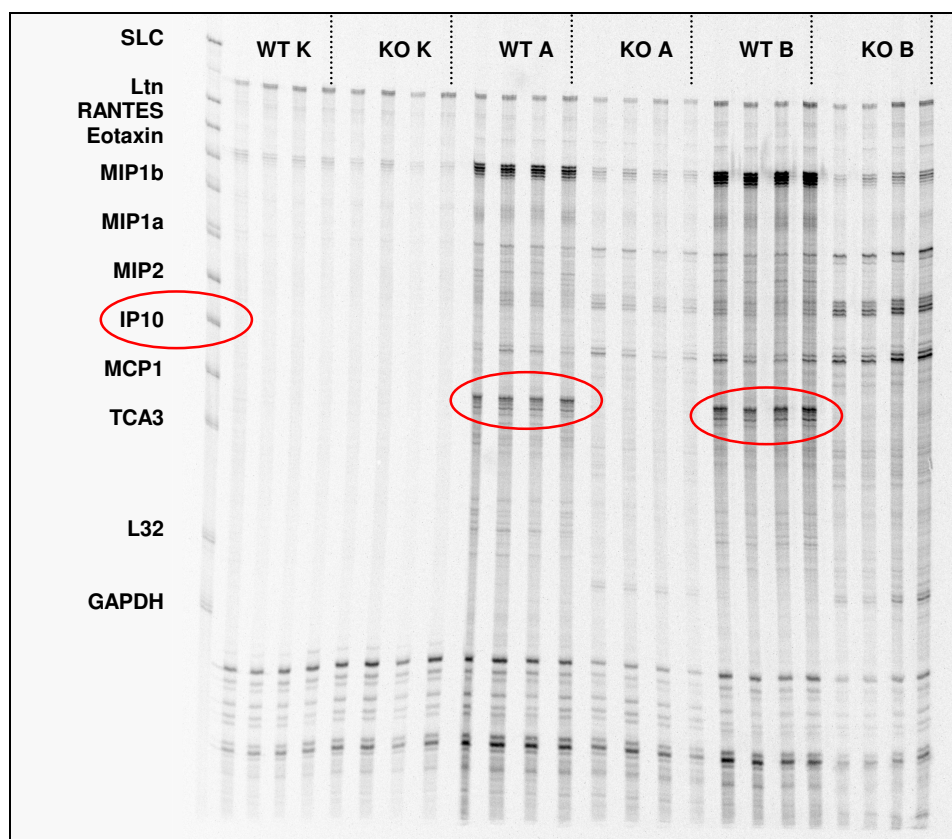


Figure 13: IP-10 is absent in the lungs of IFN- γ -KO compared to wild-type mice. A typical example of differential expression of several chemokines including IP-10 mRNA in the lungs of C57BL/6 wild-type (WT) and IFN- γ -deficient (KO) mice infected by aerosol with *M. avium* (TMC724, 10^5 CFU/mouse). Total RNA was prepared from the right lungs harvested 12 (A) and 14 (B) weeks after infection as well as from the right lungs of uninfected mice (K). 8 μ g samples of RNA from WT and KO mice were hybridized with the 33 P-labeled multi-probe template set and chemokine mRNA was analyzed by Ribonuclease Protection Assay (RPA). The differential expression of IP-10 is highlighted as an example of an angiostatic chemokine absent in IFN- γ -deficient mice, but present in C57BL/6 wild-type mice. The height difference on the gel is due to the difference in size between protected and unprotected probes. Protected probes are shorter, as residual single stranded RNA is digested and only the double stranded protected part runs on the gel. Thus, protected probes run further than unprotected single stranded markers that still contain some irrelevant plasmid sequences. WT: C57BL/6 wild-type mice, KO: IFN- γ -deficient mice, K: uninfected mice, A: infected mice after 12 weeks, B: infected mice after 14 weeks. IP-10 is highlighted by a red circle.

Results

Therefore, a number of chemokines and angiogenic mediators were closely examined by quantitative RPA to obtain proof of this concept by a quantitative method distinct from micro-array screening. IFN- γ -KO mice were compared to wild-type mice, and uninfected to infected mice at 12 and 14 weeks post-infection (Fig. 13).

A total of 25 factors was analyzed including CXC-chemokines, such as MIP-2, IP-10 and MIG; CC-chemokines, such as MIP-1 α , MIP-1 β , eotaxin, MCP-1 and TCA-3; as well as the XC-chemokine Ltn. Angiogenic factors like angiopoietin and its receptor TIE2, endoglin (which binds to TGF- β), VEGF and its receptor FLT1, as well as VEGFC and its receptor FLT4 were also included.

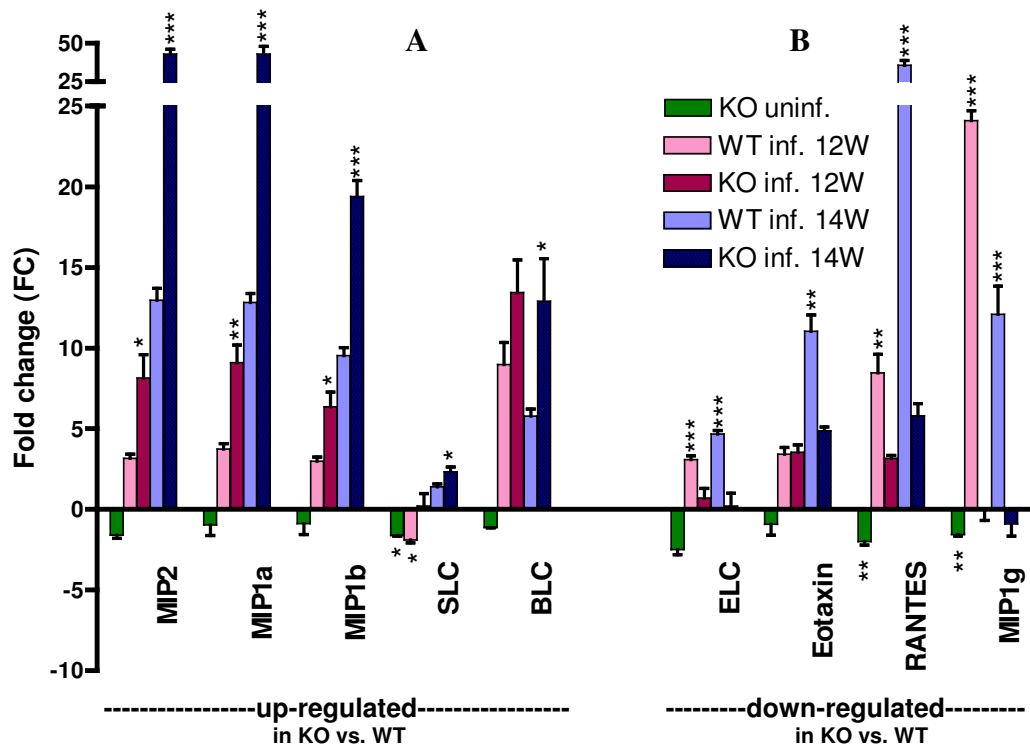


Figure 14: Chemokines are up-regulated in the lungs of infected compared to uninfected mice. Differential expression of chemokine mRNAs in the lungs of C57BL/6 wild-type (WT) and IFN- γ -deficient (KO) mice infected by aerosol with *M. avium* (TMC724, 10^5 CFU/mouse). Two subgroups of chemokines, up-regulated (A) and down-regulated (B), were identified in IFN- γ -KO compared to wild-type mice. Total RNA was prepared from the right lungs harvested 12 and 14 weeks (W) after infection (inf.) as well as from the right lungs of uninfected mice (uninf.). 8 μ g samples of RNA from WT and KO mice were hybridized with the 33 P-labeled multi-probe template set and mRNA was analyzed by Ribonuclease Protection Assay (RPA). The fold change (FC) is the gene expression in infected WT and KO, as well as uninfected KO against uninfected WT mice, *** $p < 0.001$, ** $0.001 < p < 0.01$, * $0.01 < p < 0.05$ at a confidence level of 99%, no significant difference $p > 0.05$ at a confidence level of 95% and 99%.

The chemokine expression pattern that governs cell migration into the infected areas differed in IFN- γ -KO mice from that present in wild-type mice. MIP-1 γ was absent and

RANTES, eotaxin, and ELC were down-regulated in IFN- γ -KO mice. On the other hand, SLC, BLC, and Ltn were up-regulated, while MIP-2, MIP-1 α and MIP-1 β were extremely high in IFN- γ -KO compared to wild-type mice. Therefore, the chemoattractants analyzed here could be categorized into two groups: one group contains genes up-regulated (Fig. 14A) and one group genes down-regulated (Fig. 14B) in infected IFN- γ -KO mice compared to wild-type mice; both groups being almost absent in uninfected mice.

The group of up-regulated chemokines is composed of MIP-2, MIP-1 α , MIP-1 β , SLC and BLC, while the group of down-regulated chemokines contains ELC, eotaxin, RANTES and MIP-1 γ , which is almost absent in infected IFN- γ -KO mice.

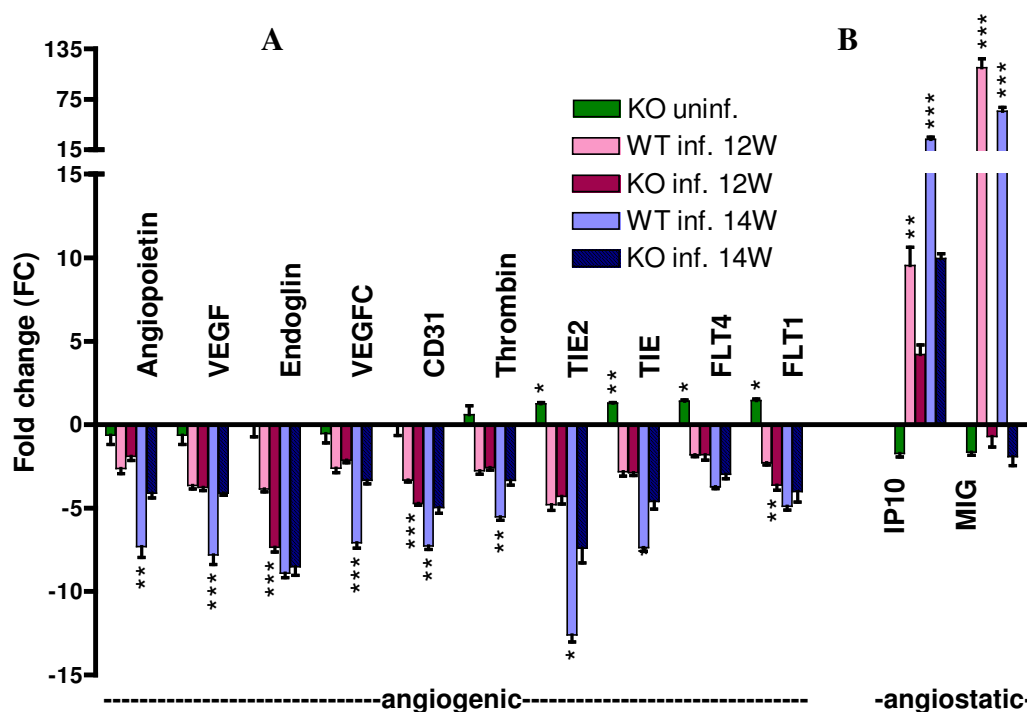


Figure 15: Angiogenic mediators are down-regulated in the lungs of infected compared to uninfected mice. Differential mRNA expression for angiogenic mediators (A) and angiostatic chemokines (B) in the lungs of C57BL/6 wild-type (WT) and IFN- γ -deficient (KO) mice infected by aerosol with *M. avium* (TMC724, 10^5 CFU/mouse). Total RNA was prepared from the right lungs harvested 12 and 14 weeks (W) after infection (inf.) as well as from the right lungs of uninfected mice (uninf.). 8 μ g samples of RNA from WT and KO mice were hybridized with the 33 P-labeled multi-probe template set and mRNA was analyzed by Ribonuclease Protection Assay (RPA). The fold change (FC) is the gene expression in infected WT and KO, as well as uninfected KO against uninfected WT mice, *** $p < 0.001$, ** $0.001 < p < 0.01$, * $0.01 < p < 0.05$ at a confidence level of 99%, no significant difference $p > 0.05$ at a confidence level of 95% and 99%.

In wild-type mice, the angiostatic chemokines MIG and IP-10 are extremely increased during infection especially at 14 weeks post-infection (Fig. 15), where MIG expression was almost undetectable in infected IFN- γ -KO mice. In comparison, IP-10 mRNA

expression was clearly detectable in infected IFN- γ -KO mice, but to a much lesser degree than in infected wild-type mice.

During infection, a strong and clear reduction of angiogenic mediators was observed in both wild-type and IFN- γ -KO mice. Except for endoglin and the two FLT receptors, the angiogenic factors examined showed a significantly reduced expression in the infected wild-type compared to the infected IFN- γ -KO mice at 14 weeks post-infection (Fig. 15), giving rise to a tendency for angiogenic factors to be expressed at higher levels in IFN- γ -KO mice compared to C57BL/6 mice.

In conclusion, there was a clear tendency towards a lower expression of angiogenic factors and a significantly higher expression of angiostatic chemokines in wild-type mice compared to IFN- γ -KO mice during infection. Therefore, the ratio of angiogenic to angiostatic factors was shifted towards angiostasis in wild-type mice.

3. 8. Granuloma vascularization in wild-type and IFN- γ deficient mice

It appeared possible that the increased expression of angiostatic chemokines in wild-type mice during infection might result in a lower level of vascularization in inflamed lungs.

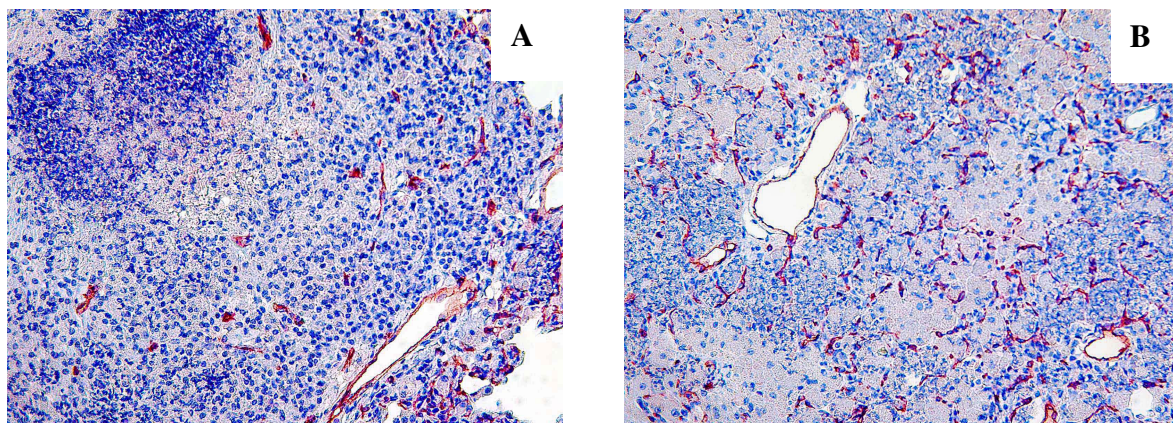


Figure 16: Capillary network is almost intact in IFN- γ -KO mice but rarefied in granulomatous lesions of wild-type mice. Histopathology of lungs of C57BL/6 (panel A) and IFN- γ -KO (panel B) mice, both infected by aerosol with *M. avium* (TMC724, 10^5 CFU/mouse). 16 weeks post-infection *M. avium*-infected mice were sacrificed and the lung was removed. Lung sections were stained with an anti-endomucin antibody (original magnification $\times 10$). Micrographs are representative of 4 mice examined. Red staining indicates blood vessels.

Therefore, 16 weeks post-infection with 10^5 CFU *M. avium* TMC724, lung sections of IFN- γ -KO mice and C57BL/6 mice were stained using an anti-endomucin antibody to compare the overall amount of vessels within granulomatous infiltrations. Endomucin is a sialomucin protein predominantly expressed in vascular endothelial cells [185].

The original lung architecture with its network of alveoli was intact in infected IFN- γ -KO mice, although there was severe myelomonocytic infiltration and plasma extravasation (Fig. 16B). The capillary network appeared equally distributed throughout the lung tissue. In contrast, the vascularization was irregular in wild-type mice (Fig. 16A), and alveolar septa containing capillaries could no longer be clearly discerned. Outside of the granulomas the vasculature was prominent, but capillary staining was reduced inside the granuloma and was least pronounced at the center of the granuloma close to the necrotic core. However, capillaries were not completely absent in any part of the granulomatous structure of wild-type mice, and even larger blood vessels could sometimes be detected in areas in close proximity to the necrotic center.

3.9. Vascularization and granuloma necrosis in CXC-receptor-3 deficient mice

The angiostatic chemokines MIG and IP-10 share one receptor, namely the CXC-receptor-3. It was hypothesized that, in the absence of CXCR3, angiostatic chemokines would be without effect and vascularization would be similar to that observed in IFN- γ -KO mice. If decreased vascularization was the cause for tissue necrotization, the absence of CXCR3 should be associated with the absence of granuloma necrosis.

Therefore, CXCR3-KO mice were infected with *M. avium* to determine the degree of vascularization and the development of granuloma necrosis in these mice. The mycobacterial growth in the lung of CXCR3-KO mice, 10, 14 and 20 weeks post-infection, was identical to that observed for wild-type mice. Both groups displayed a bacterial load of about 10^9 CFU/lung at 10 weeks and a bacterial load of about 10^{10} CFU/lung at 20 weeks post-infection (Fig. 17).

20 weeks post-infection with 10^5 CFU *M. avium* TMC724, lung sections of CXCR3-KO mice and C57BL/6 mice were stained using the anti-endomucin antibody to detect the intensity of vascularization throughout the tissue.

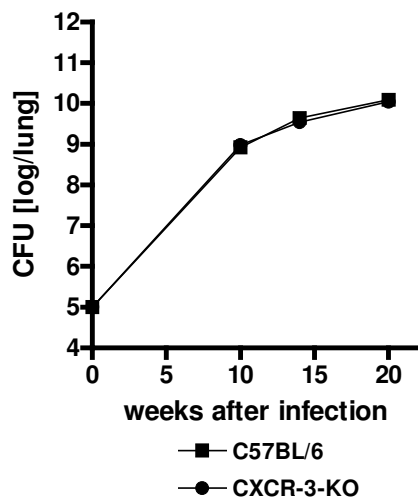


Figure 17: Bacterial load is identical in both CXCR3-KO and wild-type mice infected with *M. avium* by aerosol. Mycobacterial growth pattern in C57BL/6 and CXCR3-KO mice infected by aerosol with *M. avium* (TMC724, 10^5 CFU/mouse). *M. avium*-infected lungs were removed 10, 14 and 20 weeks post-infection. Mycobacterial colony enumeration in the lung was performed at indicated time points. Data represent the means of 4 mice \pm SD (error bars are too small to be seen). No significant difference $p > 0.05$ at a confidence level of 95% and 99%.

The vascularization in the lungs of CXCR3-KO mice (Fig. 18B) resembled that of C57BL/6 wild-type mice (Fig. 18A), with an irregular distribution pattern of blood vessels. Outside the granulomas the capillary network was prominent and often had a compressed appearance, while inside the granuloma, capillarization was more rarefied, particularly close to the center of the granuloma, where necrosis was apparent.

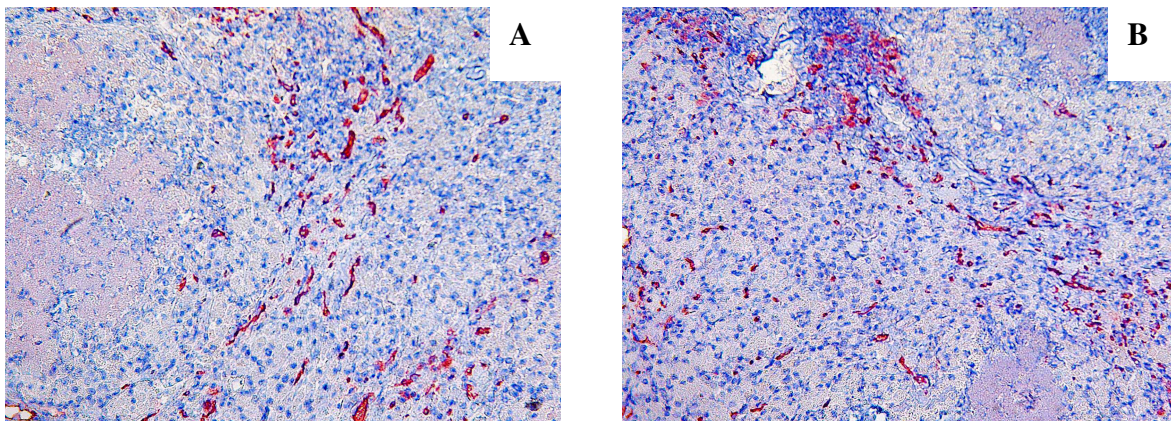


Figure 18: Capillary network is similarly rarefied in granulomatous lesions of CXCR3-KO and wild-type mice. Histopathology of lungs from C57BL/6 (panel A) and CXCR3-KO (panel B) mice, both infected by aerosol with *M. avium* (TMC724, 10^5 CFU/mouse). 20 weeks post-infection *M. avium*-infected mice were sacrificed and the lung was removed. Lung sections were stained with an anti-endomucin antibody (original magnification $\times 10$). Micrographs are representative of 5 mice examined. Red staining indicates blood vessels.

Lung sections of CXCR3-KO mice (Fig. 19B) and C57BL/6 mice (Fig. 19A) were stained with Haematoxylin-Eosin at the same time point to assess the degree of granuloma formation and necrosis. In CXCR3-KO mice, a large eosinophilic mass was visible at the

center of granulomatous lesions at 20 weeks after infection. This necrotic area contained acellular debris of dead macrophages, some foamy macrophages, some basophilic areas of presumably dead granulocytes, as well as interspersed granulocytes. This mass was well encapsulated with three distinct layers, a dense layer of accumulating granulocytes, a thick layer of epithelioid macrophages and a few aggregates of lymphocytes. At the outermost side, intact alveolar spaces and bronchial structures as well as blood vessels were observed.

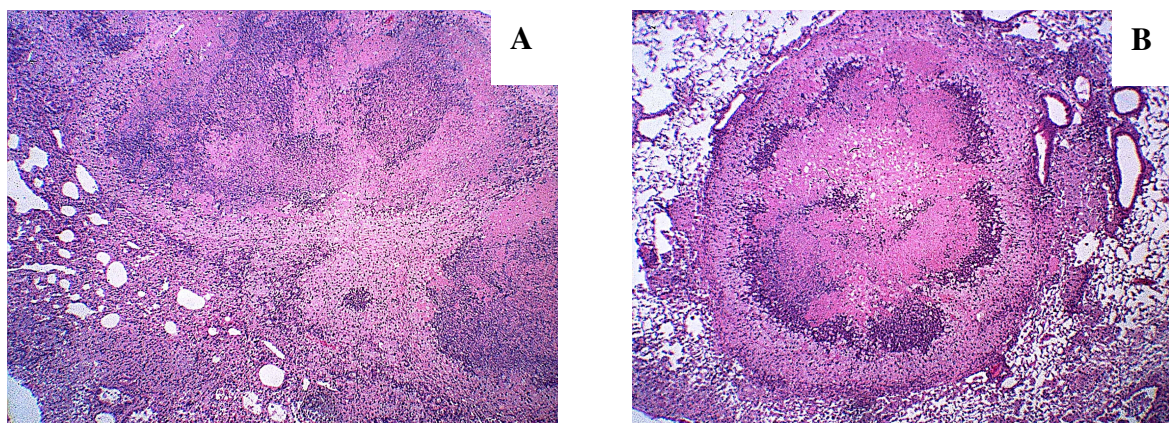


Figure 19: CXCR3-KO mice infected with *M. avium* by aerosol resemble wild-type mice in terms of granuloma necrosis. Histopathology of lungs from C57BL/6 (panel A) and CXCR3-KO (panel B) mice infected by aerosol with *M. avium* (TMC724, 10^5 CFU/mouse). *M. avium*-infected lungs were removed 20 weeks post-infection. Lung sections were stained with HE (original magnification $\times 4$). Micrographs are representative of 5 mice examined.

Granuloma necrosis was evident in CXCR3-KO mice to a similar extent as in wild-type mice. Thus, CXCR3 is not critically involved in reduced vascularization and granuloma necrotization in response to mycobacterial infections.

3. 10. Hypoxia in pulmonary granulomas of *M. avium*-infected mice

Due to reduced vascularization, a diminished blood supply might lead to nutrient deficiency and hypoxia within granulomatous lesions. An indication for the presence of hypoxia was initially sought by immunohistochemical staining for the hypoxia inducible factors (HIF)-1 and (HIF)-2. HIF-1 α (Fig. 20A) and HIF-2 α (Fig. 20B) were readily detectable in cells lining the ventricles of hypoxic mouse brains. In contrast, HIF-1 α and HIF-2 α could not be detected in uninfected lungs (Fig. 20C&D).

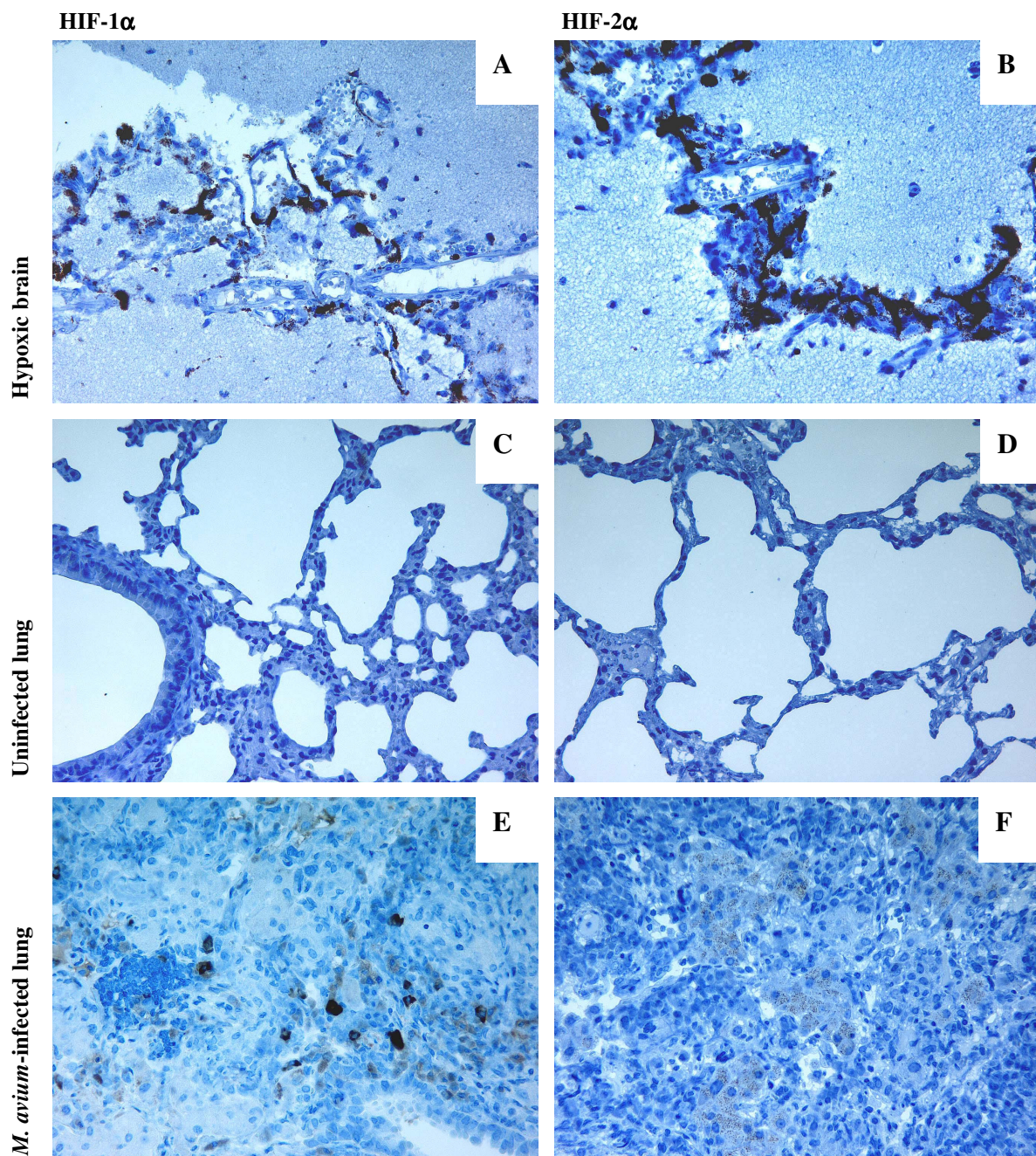


Figure 20: Marked staining for HIF-1 α and faint staining for HIF-2 α is evident in the lungs of C57BL/6 mice infected with *M. avium* by aerosol. Histopathology of lungs from C57BL/6 mice infected by aerosol with *M. avium* (TMC724, 10^5 CFU/mouse). *M. avium*-infected lungs (panel E&F) were removed 13 weeks post-infection. Lung sections were stained with an anti-HIF-1 α and an anti-HIF-2 α antibody. As a positive control, hypoxic brains (panel A&B) were used, while uninfected lungs (panel C&D) were used as a negative control (original magnification $\times 40$). Micrographs are representative of 4 mice examined.

Compared to uninfected lungs, *M. avium*-infected lungs, 13 weeks post-infection, were clearly positive for HIF-1 α (Fig. 20E). Staining was not prominent inside granulomas, but was confined to single infiltrating cells at the periphery of granulomas, especially those in

near proximity to bronchioli. HIF-2 α (Fig. 20F), however, showed only a very faint staining inside accumulating macrophages clustered adjacent to lymphocytic aggregates.

In order to determine whether hypoxia in lesions was severe, pimonidazole (PIM) was injected 1.5 or 3 hours prior to sacrifice of control tumor-bearing or *M. avium*-infected mice. In mice bearing subcutaneous MB49 tumor cells (Fig. 21A), there were clearly visible areas adjacent to necrotic zones that stained with a mAb reactive to a pimonidazole derivative known to develop under conditions of severe hypoxia (oxygen concentration <14 μ M).

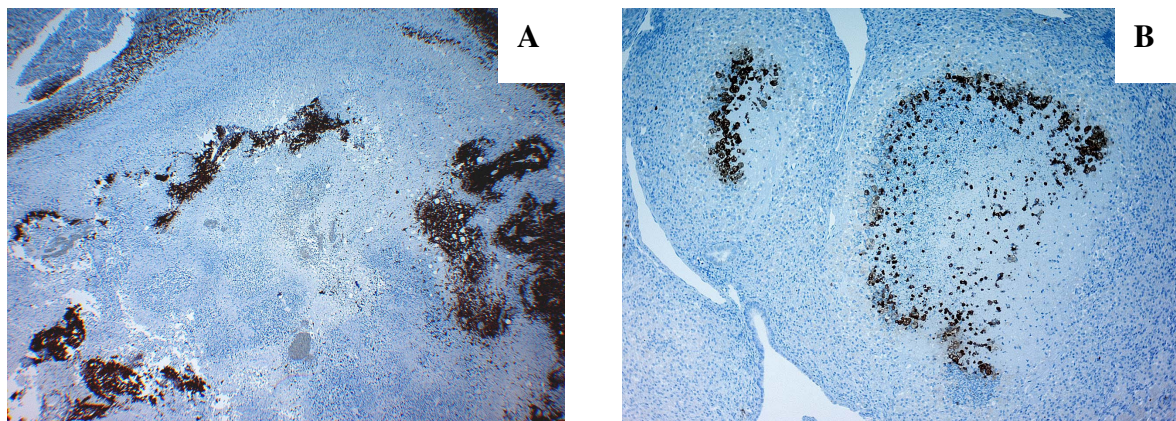


Figure 21: Marked staining for hypoxic cells is evident inside lung granulomas of C57BL/6 mice infected with *M. avium* by aerosol. One group of C57BL/6 mice was subcutaneously injected with 1×10^5 tumor cells (MB49). After becoming necrotic (5 weeks), the tumor (panel A) was removed from sacrificed mice. The other group of C57BL/6 mice was infected by aerosol with *M. avium* (TMC724, 10^5 CFU/mouse). 18 weeks post-infection *M. avium*-infected mice were sacrificed, and the lung (panel B) was removed. 3 hours prior to organ-harvesting the mice were intravenously injected with a hypoxia marker (pimonidazole-hydrochloride). Tumors and lungs were stained with an antibody against the marker derivative (reduced form, amino conjugate) arising under hypoxic conditions and binding to thiol-containing molecules (original magnification $\times 10$). Micrographs are representative of 4 mice examined.

In comparison, the PIM reagent did not indicate any areas of severe hypoxia at several consecutive early time points investigated (11-15 weeks) in mice infected with *M. avium* by aerosol, even in areas close to central caseation, while 18 weeks post aerosol infection, hypoxic cells were clearly detected inside the necrotic centers, as well as around the necrotic area. The cells staining for the hypoxia marker were much more numerous at the border of the necrosis than inside the necrotic areas (Fig. 21B).

3. 11. Hypoxia in pulmonary granulomas of *M. tuberculosis*-infected mice

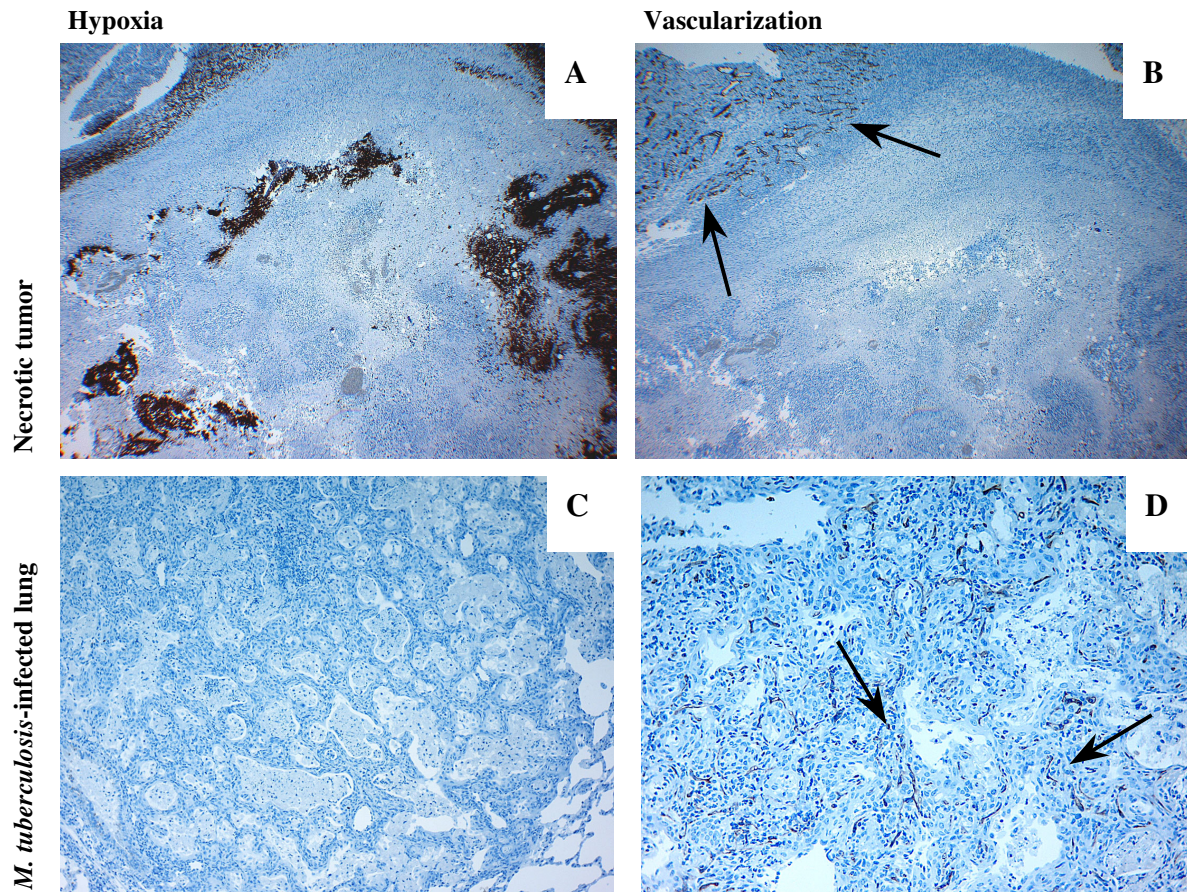


Figure 22: Hypoxia is absent and blood vessels are present in the lungs of C57BL/6 mice infected with *M. tuberculosis* by aerosol. Histopathology of lungs from 2 groups of C57BL/6 mice: both groups were infected by aerosol with *M. tuberculosis* (H37Rv, 100 CFU/mouse). At day 404 post-infection *M. tuberculosis*-infected mice were sacrificed, and the lung (panel C&D) was removed. In the first group, 3 hours prior to organ-harvesting the mice were intravenously injected with a hypoxia marker (pimonidazole-hydrochloride). Lungs were stained with an antibody against the marker derivative (reduced form, amino conjugate) arising under hypoxic conditions and binding to thiol-containing molecules (panel C). In the other group, lung sections were stained with an anti-endomucin antibody (panel D) (original magnification $\times 20$). As a positive control, a tumor model (panel A&B) was used. C57BL/6 mice were subcutaneously injected with 1×10^5 tumor cells (MB49). After becoming necrotic (5 weeks), the tumor was removed from sacrificed mice. As a control for hypoxia, 3 hours prior to organ-harvesting the mice were intravenously injected with a hypoxia marker (pimonidazole-hydrochloride). Tumors were stained with an antibody against the marker derivative (reduced form, amino conjugate) arising under hypoxic conditions and binding to thiol-containing molecules (panel A). As a control for vascularization, tumor sections were stained with an anti-endomucin antibody (panel B) (original magnification $\times 20$). Micrographs are representative of 4 mice examined. Black arrows point at stained blood vessels.

In mice infected with *M. avium* granuloma necrosis and hypoxia were observed in the lung. In order to determine whether hypoxia was also present in lung infiltrates of mice infected with *M. tuberculosis*, where no necrosis occurs, pimonidazole was injected 1.5 or 3 hours

prior to sacrifice of *M. tuberculosis*-infected mice. In contrast to tumor-bearing mice, even at day 404 post aerosol infection with *M. tuberculosis*, no staining for pimonidazole adducts was detectable in or around granulomatous lesions in infected organs (Fig. 22C).

To ascertain whether granulomas were sufficiently vascularized to allow transport of pimonidazole to lesion centers, immunohistochemical staining of capillaries was performed with an antibody specific for endomucin [185].

Both in tumors (Fig. 22A&B) and in granulomatous lesions (Fig. 22C&D) blood vessels (Fig. 22B&D) were clearly distinguishable throughout the tissue (see arrows), except for fully necrotic areas in the tumors (Fig. 22B). The tumor areas close to necrosis were free of blood vessels and showed a marked staining for hypoxia (Fig. 22A), particularly in the vicinity of necrotic bundles. In contrast, the lung infiltrates of *M. tuberculosis*-infected mice were completely devoid of staining for the hypoxia marker (Fig. 22C), and an intact uniformly distributed capillary network throughout the honey comb-like architecture of the chronically fibrotic lung was evident (Fig. 22D).

3. 12. Pulmonary oxygen concentrations in *M. tuberculosis*-infected mice

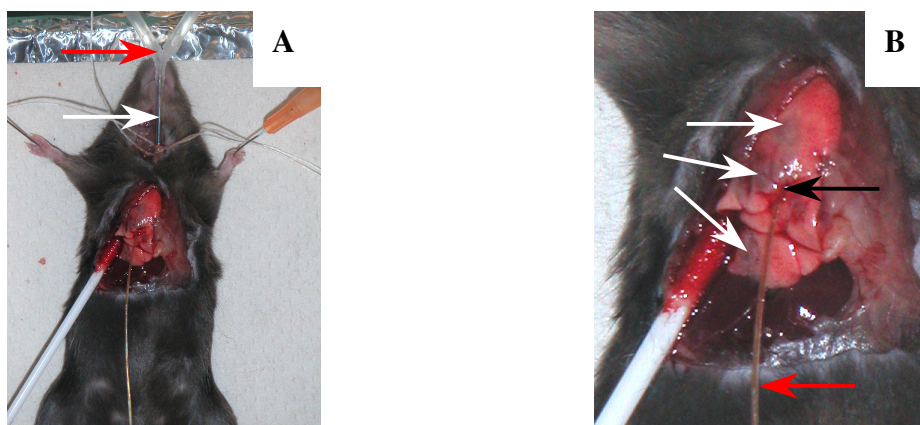


Figure 23: Experimental setup for direct oxygen measurement in infected mouse lungs *in vivo*. Mice were anaesthetized by intraperitoneal pentobarbital injection. Following tracheotomy a steel cannula was inserted into the trachea and the mice were artificially ventilated. A strictly median sternotomy was performed and the ribs dissected at the mid clavicular line (panel A). The lungs were exposed and the oxygen probe was inserted into indurated macroscopically visibly altered lesions (panel B). Panel A: red arrow points at tubing connected to respirator, white arrow points at steel cannula. Panel B: white arrows point at visibly altered lesions, black arrow points at entry point of oxygen micro-electrode, red arrow points at oxygen probe.

The hypoxia marker (pimonidazole-hydrochloride) binds only to cells with an oxygen concentration below 14 micromolar, which is equivalent to a partial oxygen pressure (pO₂) of 10 mmHg or less.

Therefore, we resolved to directly measure O₂ partial pressures in the lungs of infected mice by inserting a flexible Clarke-type catheter micro-electrode for oxygen (Fig. 23A) into the fibroid lung tissue (Fig. 23B) of artificially ventilated mice at various time points after infection. Subcutaneous MB49 tumors were used as a positive control. Those measurements were carried out in collaboration with Klaus Wagner, Lübeck, Germany.

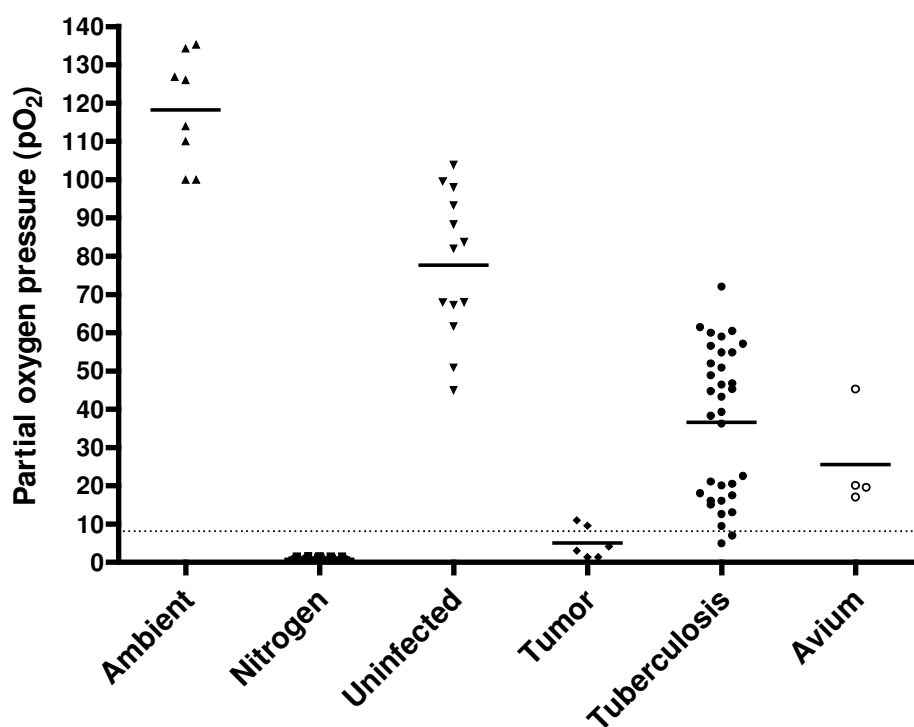


Figure 24: Partial oxygen pressure is reduced in the lungs of C57BL/6 mice infected with *M. tuberculosis* by aerosol. C57BL/6 wild-type mice were infected by aerosol with *M. tuberculosis* (H37Rv, 100 CFU/mouse) or *M. avium* (TMC724, 10⁵ CFU/mouse). At day 345 post-infection *M. tuberculosis*-infected mice were anaesthetized by intraperitoneal pentobarbital injection. A Clarke-type electrode was calibrated against oxygen in atmospheric air and against nitrogen, between individual measurements of oxygen saturation in the lungs of infected mice. The same procedure was performed in *M. avium*-infected mice, 16 weeks post-infection, as well as in uninfected mice and in MB49 skin tumors. Measurements and mean pO₂ values were derived from a total of 3 tumor-bearing mice (6 measurements), 10 *M. tuberculosis*-infected mice (34 measurements), 2 *M. avium*-infected mice (4 measurements) and 4 uninfected mice (13 measurements).

Severe hypoxia was present in subcutaneous tumors, with five out of six measurements of oxygen partial pressure clearly at or below 10 mmHg, one registering at 11 mmHg (Fig. 24). Compared to the mean pO₂ level for uninfected lungs, which was around 80 mmHg, *M. tuberculosis*-infected lungs showed reduced pO₂ levels that did not fall below

10 mmHg. The measurements for this group of mice can be subdivided into two separate clusters, one with a mean pO₂ level around 50 mmHg (indicating reduced oxygen tension), and the other around 15 mmHg (indicating hypoxia). Only two out of 34 measurements performed with a total of 10 *M. tuberculosis*-infected mice, recorded a level of oxygen below 10 mmHg.

It was difficult to insert the electrode through the hard structure of consolidated granulomas in *M. avium*-infected lungs into the center. Therefore, only few measurements were attempted. The mean pO₂ level measured in the lungs of *M. avium*-infected mice was around 25 mmHg (Fig. 24).

Thus, while pO₂ levels were clearly reduced in the lungs of *M. tuberculosis*-infected mice compared to uninfected mice, they did not reach the levels of severe hypoxia, let alone anoxia, consistently present in caseating tumors.

3. 13. Hypoxia in granulomas of guinea pig lungs infected with *M. tuberculosis*

Direct measurement of oxygen tension in *M. tuberculosis*-infected mouse lungs confirmed results using the hypoxia marker pimonidazole: granulomatous lesions in mice were not severely hypoxic. Mice are known not to develop the typical pathology of granuloma necrosis present in humans. Therefore, we resolved to perform immunohistochemical staining for hypoxia in an animal model of *M. tuberculosis* infection that mimics human pathology. The pimonidazole reagent was used to detect hypoxia in the guinea pig model of aerosol infection in collaboration with Ian Orme, Colorado, USA.

Compared to the mycobacteria-infected lungs of mice, the hypoxia staining inside and around the necrotic areas in the lungs and lymph nodes of *M. tuberculosis*-infected guinea pigs at day 30 and 60 was much more intensive resembling the staining in tumors.

In the lungs of guinea pigs, a marked staining for hypoxia was observed within the granuloma, but especially surrounding the necrotic center (Fig. 25A&C). In the lymph nodes of guinea pigs, a clear staining was detected with several rafts or aggregates of cells reacting with the antibody against pimonidazole adducts (Fig. 25B&D). Characteristically, cells staining positive for hypoxia were located immediately adjacent to the necrotic areas inside granulomas in both the lymph nodes and the lungs (Fig. 25). Similar results were also obtained at day 90 post-infection.

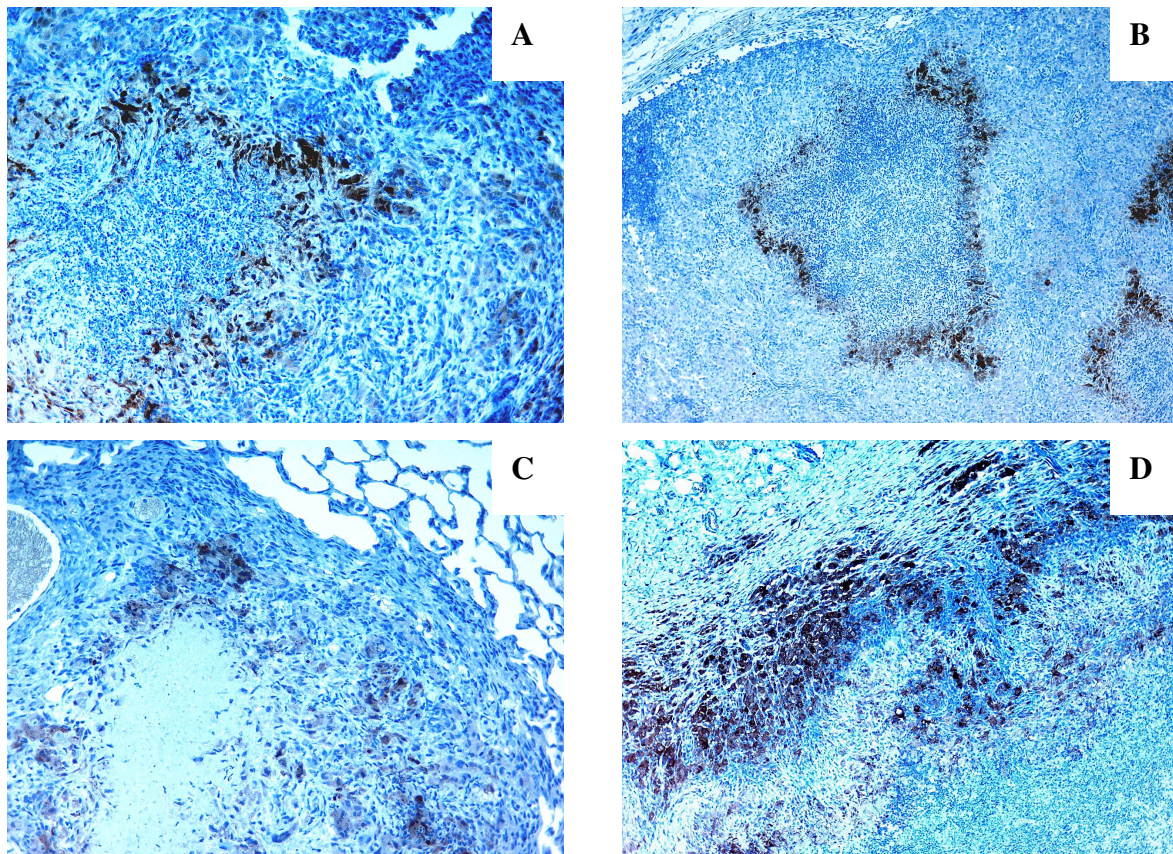


Figure 25: Hypoxia is evident in lung granulomas and lymph nodes of guinea pigs infected with *M. tuberculosis* by aerosol. Guinea pigs were infected by aerosol with *M. tuberculosis* (H37Rv, 20 CFU/ guinea pig) in collaboration with Ian Orme, Colorado, USA. At day 30 (panel A&B) and day 60 (panel C&D) post-infection *M. tuberculosis*-infected guinea pigs were sacrificed and the lung and mediastinal lymph node were removed. 2 hours prior to organ-harvesting the guinea pigs were intraperitoneally injected with a hypoxia marker (pimonidazole-hydrochloride). Lymph nodes (panel B&D) and lungs (panel A&C) were stained with an antibody against the marker derivative (reduced form, amino conjugate) arising under hypoxic conditions and binding to thiol-containing molecules (original magnification $\times 10$ for lymph nodes and $\times 20$ for lungs). Micrographs are representative of 4 mice examined.

In conclusion, guinea pigs develop granuloma necrosis in response to *M. tuberculosis* infection, and this is associated with a peri-necrotic rim of hypoxic cells, similar to that observed in mice infected with *M. avium*.

4. Discussion

Granuloma formation is a hallmark of mycobacterial infections. Granulomas are foci of mononuclear cell infiltration in which the interaction between T-cells and newly recruited macrophages leads to the activation of bacteriocidal programs aimed at the containment of the microbial invader.

However, granulomas are double-edged swords. While they may serve to encapsulate mycobacteria, arrest their growth and prevent further dissemination, they also displace parenchymal tissue, causing organ malfunction, as the resulting rigid lung tissue is unable to optimally perform respiratory functions. In addition, fully developed granulomas may centrally necrotize and destroy adjacent structures, a process that, in the lung, causes erosion of the granuloma into the bronchial system and spreading of granuloma contents into the environment.

In the context of tuberculosis, induction and maintenance of granulomatous lesions has long been thought of as primarily a protective response orchestrated by the immune system. However, since the times of Robert Koch, it has been well recognized that the specific response against mycobacterial antigens can aggravate pathology, cause tissue destruction, and may even lead to the premature death of the patient. Secretion of specific antigens to intensify the immune response [94] and to accelerate the onset of pathology is a mechanism harnessed by mycobacteria to ensure their survival inside the host as well as their consequent transmission to a naïve host. Without an adequate immune response leading to the development of a granuloma, the transmission of mycobacteria to other susceptible hosts is greatly reduced [191].

Controlling the pathological sequelae of immune-mediated granuloma formation without disrupting its anti-bacterial potential has been the driving force behind attempts to dissect, at the molecular level, the events governing granuloma development, persistence and necrosis. In addition, insight into the pathophysiological state of mycobacteria contained within the granuloma structure would undoubtedly further the identification of novel drug targets aimed at disrupting the metabolic adaptation of mycobacteria to the granulomatous environment and might therefore lead to novel therapeutic strategies.

The aim of the work presented in this thesis was to capitalize on a published model of *M. avium*-induced pulmonary immunopathology in the mouse in order to (i) identify molecular pathways involved in the development of granuloma necrosis, (ii) test whether

these pathways could be modulated to inhibit granuloma necrosis, and (iii) analyze whether the knowledge gained in this model could provide insight into the pathophysiological environment and the metabolic state of *M. tuberculosis* in lung granulomas.

The salient findings of the experiments conducted in this research program are:

1. Granuloma necrosis depends on the interferon-gamma signaling pathway, as mice deficient for IFN- γ , STAT-1 and IRF-1 did not develop granuloma necrosis.
2. IFN- γ -mediated granuloma necrosis is associated with a disbalance of angiostatic and angiogenic mediators which correlates with a decreased vascularization within mycobacteria-induced granulomas. However, attempts to block angiostasis by inhibiting the CXCR3-mediated pathway of chemokine induction did not prevent granuloma necrosis.
3. IFN- γ -mediated granuloma necrosis is associated with severe hypoxia in the model of *M. avium*-induced pathology in the mouse and in the guinea pig model of pulmonary tuberculosis, but not in the mouse model of *M. tuberculosis* infection. These findings have important implications for the use of the mouse model of *M. tuberculosis* infection in developing eradication chemotherapy and for evaluating putative mechanisms of chronic persistence and latency of *M. tuberculosis*.

4. 1. Signaling pathways downstream of IFN- γ

M. tuberculosis infection in mice does not cause granuloma necrosis, while *M. avium* infection results in granulomas with necrotic centers resembling the pathology of tuberculosis in humans [171, 172]. Thus, in order to examine individual elements of the IFN- γ -signaling pathway that was identified to be critically involved in the mechanism leading to granuloma necrosis, the mouse model of *M. avium*-induced immunopathology was employed.

4. 1. 1. Type I and II interferon systems

The signaling pathway of IFN- γ is interconnected with IFN- α/β signaling in multiple ways. A constitutive low spontaneous production of IFN- α/β is required for the activation of the type II IFN receptor (IFNGR). The IFN- γ signaling system is composed of a weak

association between the two subunits of the type I IFN receptor (IFNAR) with the two subunits of the IFNGR (Fig. 26). Upon stimulation by IFN- γ , which is known to function as a dimer, both Jak1 and Jak2, as well as Tyk2 are activated. STAT-1 is recruited and phosphorylated by Jak1 and Jak2 at the IFNGR, while STAT-2 is recruited and phosphorylated by Jak1 and Tyk2 at the IFNAR.

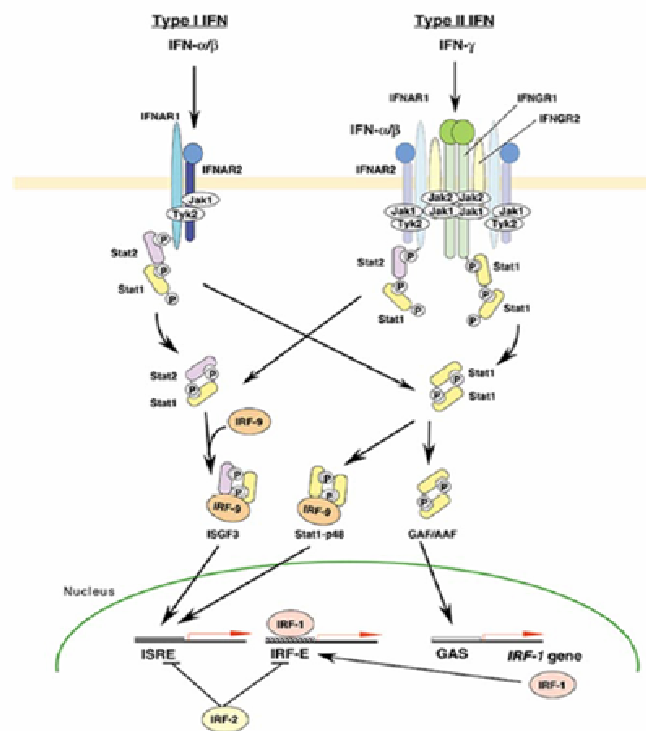


Figure 26: Both type I and type II interferon systems are involved in the IFN- γ -signaling pathway. The type I interferon system is activated by the binding of IFN- α/β to IFNAR subunit 1 and 2, while the type II interferon system is activated by the binding of the IFN- γ dimer to a quaternary receptor composed of the 2 subunits of IFNAR and the 2 subunits of IFNGR [173].

A double phosphorylated STAT-1/STAT-2 heterodimer binds to the IRF-9 to constitute the interferon-stimulated gene factor (ISGF)3 that translocates into the nucleus. There, it activates IFN-inducible genes by binding to the interferon-stimulated response element (ISRE) of those genes.

A homodimer of two phosphorylated STAT-1 molecules form the IFN- γ activated factor (GAF) / IFN- α activated factor (AAF) that activates another set of IFN-inducible genes by binding to the interferon-gamma activated site (GAS) on those genes. The GAF/AAF can also bind to the IRF-9 to constitute the STAT1-p48 trimeric complex (ISGF3 γ). The IRF-1 gene is induced via GAS which is found within the IRF-1 promoter [173].

This indicates that the following molecules play a key role in signaling: IFN- α/β and IFN- γ , STAT-1 and STAT-2, IRF-9 and IRF-1. In order to dissect which pathway critically contributes to granuloma necrosis, we first used IFN- α/β -R-KO and IFN- γ -KO mice and compared them with wild-type mice. Data from IFN- γ -KO mice confirmed the previous reports revealing no granuloma necrosis in IFN- γ -KO mice [171, 172]. In IFN- α/β -KO mice a clear necrosis was observed, excluding a critical involvement of IFN- α/β in the development of granuloma necrosis.

To further analyze the molecular pathway downstream of the IFN- γ receptor, we excluded STAT-2, as it is primarily implicated in the IFN- α/β signaling pathway, and used mice deficient for STAT-1 to compare with wild-type mice. STAT-1-KO mice did not develop granuloma necrosis and the pathology arising in the lungs of these mice was very similar to that observed in the lungs of IFN- γ -KO mice. The two KO strains agreed again in another point, the mice did not survive longer than 16 weeks after infection, compared to the wild-type mice that survived until 20 weeks post-infection. This was expected, as both molecules are very important for a protective immune response. This is reflected by the higher bacterial load in both KO strains compared to the wild-type mice at 16 weeks post-infection.

Concerning interferon regulatory factors (IRF), we focused on IRF-1. IRF-1-KO mice did not develop granuloma necrosis, although they survived 24 weeks after infection, in comparison with wild-type mice that succumbed to infection after 20 weeks. At 24 weeks after infection the bacterial load in IRF-1-KO mice was as high as the bacterial load in IFN- γ -KO mice 16 weeks post-infection. This clearly suggests that IRF-1 is responsible for granuloma necrosis and that in its absence the protective pathways are less disrupted than by the absence of IFN- γ or STAT-1.

4. 1. 2. IFN- γ -mediated mechanisms

As IFN- γ induces a variety of genes, it would be very time-consuming to analyze each gene reported to be IFN- γ -inducible. Thus, we preferred to further investigate IFN- γ -KO mice by gene expression analysis. This would give clues as to which IFN- γ -inducible genes are differentially regulated between IFN- γ -KO mice not developing granuloma necrosis and wild-type mice that develop granuloma necrosis. STAT-1 and STAT-2, as

well as IRF-1 and IRF-7 (involved in the constitutive induction of IFN- α/β) were significantly reduced in IFN- γ -KO mice. This shows that our gene expression arrays reproduced previous results reporting that those genes are downstream of IFN- γ [173].

As IRF-1 was shown to be involved in granuloma necrosis (Fig. 10), it was important to discern, which genes are IRF-1 dependent. After surveying published literature and comparing it with our data on IFN- γ -KO mice, we decided to identify novel candidate genes out of the intersection of IFN- γ - and IRF-1-dependent genes. The genes responsible for granuloma necrosis must be IFN- γ and as well IRF-1 dependent. Here, a comparison was carried out between published data on IRF-1 and our own data from IFN- γ gene expression arrays. Genes reported to be IRF-1 regulated [173] were selected from the genes found to be IFN- γ dependent in *M. avium* infection (Tab. 2).

mRNA expression of genes increased in WT mice				
Gene Title	Gene Symbol	FC wt/ko	FC wt	FC ko
2'-5' oligoadenylate synthetase 3	Oas3	3.4	9.4	2.7
2'-5' oligoadenylate synthetase-like 1	Oasl1	7.0	7.3	1.0
2'-5' oligoadenylate synthetase-like 2	Oasl2	9.6	5.0	-1.9
caspase 1	Casp1	2.9	10.6	3.7
class II transactivator	C2ta	6.8	8.6	1.3
histocompatibility 2, class II, locus DMA	H2-DMA	9.0	6.6	-1.4
histocompatibility 2, class II, locus Mb2	H2-DMb2	12.0	8.7	-1.4
histocompatibility 2, M region locus 3	H2-M3	4.6	4.3	-1.1
histocompatibility 2, O region alpha locus	H2-Oa	18.0	18.1	1.0
histocompatibility 2, T region locus 10, 17, 22, 9	H2-T10, 17, 22, 9	3.0	3.5	1.2
histocompatibility 2, T region locus 24	H2-T24	3.3	1.6	-2.0
interleukin 15	Il15	2.1	1.7	-1.3
interleukin 15 receptor, alpha chain	Il15ra	4.0	3.4	-1.2
interleukin 18	Il18	3.4	1.1	-3.1
interleukin 18 binding protein	Il18bp	13.4	22.0	1.6
nitric oxide synthase 2, inducible, macrophage	Nos2	8.3	15.9	1.9
promyelocytic leukemia	Pml	2.2	2.3	1.0
vascular cell adhesion molecule 1	Vcam1	4.4	2.6	-1.7

mRNA expression of genes increased in KO mice				
Gene Title	Gene Symbol	FC ko/wt	FC wt	FC ko
colony stimulating factor 3 (granulocyte)	Csf3	6.5	1.2	7.8

Table 2: Genes that are reported to be regulated by IRF-1 are also found to be regulated in IFN- γ -KO compared to wild-type mice as shown by micro-array analysis. A selection of IRF-1 induced genes found to be differentially expressed in the lungs of C57BL/6 wild-type (WT) and IFN- γ -deficient (KO) mice infected by aerosol with *M. avium* (TMC724, 10^5 CFU/mouse). Q value <0.01. The fold change (FC) is the gene expression in infected against uninfected mice, for wild-type mice FC wt and for IFN- γ -deficient mice FC ko. The cut-off set for differential expression is a gene expression difference above 2 between infected wild-type and infected IFN- γ -deficient mice FC wt/ko >2 and FC ko/wt >2.

The expression of all examined IRF-1 dependent genes, except one, were decreased in wild-type compared to IFN- γ -KO mice. It is difficult to subgroup related genes, as several are interconnected. 2'-5' oligoadenylate synthetase and caspase-1 could be related to a possible role of apoptosis in development of granuloma necrosis. IFN- γ induces the

enhanced transcription of the 2'-5' oligoadenylate synthetase genes that are known to result in the degradation of cellular and viral RNA, the inhibition of protein synthesis [192], and the induction of cellular apoptosis [193].

Some Gram-negative bacteria can induce apoptosis by directly activating caspase-1 [194-196]. In *M. tuberculosis*-infected alveolar epithelial cells, the induction of bcl-2 leads to the repression of caspase-1, while in *M. tuberculosis*-infected macrophages, bcl-2 is repressed [106, 197]. Bcl-2 inhibits the conversion of procaspase-1 into caspase-1 in human macrophages [198, 199]. This is consistent with our findings, as we could not detect a change in the mRNA expression of bcl-2, while caspase-1 was induced in wild-type mice to a higher extent than in IFN- γ -KO mice. Further investigations are needed to test if the caspase-1 expression is restricted to macrophages, and if macrophages undergoing apoptosis are responsible for the development of granuloma necrosis.

The increased expression of IL-15 and its receptor, as well as IL-18 and its binding protein could indicate the involvement of these IFN- γ -induced cytokines, or the cells stimulated by their production, in the development of a granuloma necrosis.

In response to IFN- α/β , APCs are stimulated and produce IL-15 [200] that enhances the activation of NK-cells [201, 202], is a key cytokine inducing the proliferation of memory CD8+ T-cell [200, 203, 204], and facilitates the attrition of existing memory CD8+ T-cell [205]. IL-15-deficient mice are more susceptible to mycobacterial infection [206], and exogenous administration of IL-15 increases the efficacy of BCG vaccination [207] and enhances the ability of mice to control *M. tuberculosis* infection [208].

In the context of mycobacteria-induced granuloma necrosis, the increase in IL-15 in wild-type mice might indicate an enhanced cytolytic function performed by NK-cells or CD8+ cells. Indeed, in another project performed in our group IL-15 deficient mice exhibited a delayed necrotization of granulomas in response to *M. avium* infection, while IL-15 transgenic mice displayed an accelerated granuloma necrosis [209]. In this context, it is noteworthy that the development of granuloma necrosis was neither influenced in β 2-microglobulin-KO mice (deficient for MHC class I and CD1) nor in CD8-KO mice [172]. However, the involvement of NK-cells in granuloma necrosis has not yet been elucidated, and the nature of the effector cell causing granuloma necrosis has not yet been definitively determined.

Recently, IL-18 was recognized as a potent cytokine promoting a Th1-response by inducing IFN- γ in a unique synergism with IL-12 [210, 211]. The interleukin-1 β

converting enzyme (ICE), known as caspase-1, cleaves the aspartic amino acid residue of proIL-18 converting it into an active IL-18 [212, 213]. As previously mentioned, the significantly up-regulated expression of both caspase-1 and IL-18 in wild-type compared IFN- γ -KO mice, suggests the involvement of IL-18 in the induction of granuloma necrosis. IFN- γ augments the production of IL-18 by up-regulating the caspase-1 activity [214]. This finding explains the decreased mRNA level of IL-18 in IFN- γ -KO mice. IL-18 contributes to the generation of CD8+ T-cells [215] and together with IL-12 induces the production of IFN- γ by T-cells and NK-cells [216-219]. A dysfunction in IL-18 has been postulated to result in the development of pulmonary TB [211].

Patients with pulmonary TB express more IL-18 than healthy individuals [220], and the levels of IL-18 decrease with the progress of TB therapy [221]. IL-18 was reported to be increased in chronic inflammatory diseases [222, 223]. Therefore, there is good evidence that IL-18 levels correlate with the extent of disease.

However, our data show for the first time that IL-18 is not critically required for the progression to granuloma necrosis. Although IL-18-KO mice infected with *M. avium* had lower levels of IFN- γ in their lungs than infected wild-type mice, they exhibited a similar bacterial load, as well as the same kinetics and magnitude of granuloma formation and necrosis as in wild-type mice. Thus, IL-18 may contribute to the pathogenesis of tuberculosis, but it is not essentially involved in immunopathology.

With regard to effector cells that might be involved in granuloma necrosis, our micro-array analysis revealed that the granulocyte colony-stimulating factor (G-CSF) in wild-type mice was markedly decreased compared to IFN- γ -KO mice. G-CSF is a growth factor supporting the survival, proliferation, differentiation and function of granulocytes and their precursors [224]. A marked induction of G-CSF in IFN- γ -KO mice correlates with our finding that granulocytes are much more prominent in the lesions of those mice, where they appear in aggregates interconnected by “avenues” of granulocytes (Fig. 4).

Transfer of normally functioning neutrophils to neutrophil-defective beige mice increased their resistance to *M. avium*, while neutrophil depletion in wild-type mice increased their susceptibility to *M. avium* [225]. During *M. avium* infection, G-CSF stimulated antimycobacterial activity in neutrophils decreasing the bacterial load [226], and it triggered neutrophils to produce cytokines like IL-1 [227], TNF- α [228] and IL-12 [229, 230] stimulating T-cells and the mycobacteriostatic activity of macrophages [228, 231, 232].

The recruitment of granulocytes cannot be solely attributed to G-CSF. There are chemokines known to be prominent attractants of neutrophil granulocytes. Our own findings show two groups of those chemokines, one was up-regulated to higher levels in IFN- γ -KO mice including MIP-2 and MIP-1 α/β , and the other up-regulated to higher levels in wild-type mice including MIP-1 γ and RANTES (Fig. 14).

This leads us to suggest that the granulocytes are differentially recruited depending on the chemokine expression pattern at the site of infection. Being almost absent (MIP-1 γ) or extremely reduced (RANTES) in IFN- γ -KO mice compared to wild-type mice (Fig. 14), this could indicate an involvement of MIP-1 γ and RANTES in the development of granuloma necrosis.

In order to elucidate the effect of those chemokines and the type of cells recruited by them that might be associated with granuloma necrosis, we would have to block MIP-1 γ and RANTES and find out if the infection with *M. avium* would still lead to granuloma necrosis or not. If not, it would be then possible to discover, which cells are missing and those cells would be most probably associated with granuloma necrosis. Unfortunately, it is difficult to elucidate the role of a specific cell type recruited by a chemokine, as the chemoattractant function of a chemokine is not restricted to a specific cell type and blocking those chemokines would not solely dismiss one cell type, but a variety of other cells that should remain active and present at the site of infection will be inhibited as well. Thus, it would not be possible to assign the overall effect to a single type of effector cell.

The overall number and distribution of granulocytes in the lung tissue of IFN- γ -KO mice seems to be higher than in wild-type mice, a finding also reported by others in *M. tuberculosis* infection [233]. On the other hand, the appearance of granulocytes in the necrotizing granulomas of wild-type mice is evident. In the course of *M. avium* infection, we observed the kinetics of developing granuloma necrosis. Starting at week 10 after infection, B- and T-lymphocytes started to accumulate in follicle-like structures, where B-lymphocytes tended to form dense well-organized aggregates that increased in size with the progress of the infection, with T-lymphocytes surrounding or spreading among the B-lymphocyte aggregates. As long as the granuloma did not start to necrotize, the B- and T-lymphocytes were markedly detectable. Upon granuloma necrosis approaching week 16 after infection, B- and T-lymphocytes appeared fewer in the granulomatous structure, until week 20, where we could hardly detect B- or T-lymphocytes, instead granulocytes appeared and became predominant (data not shown) [234].

Possibly the enhanced production and recruitment of granulocytes to the site of infection may be considered as a consequence of a defective anti-bacterial immunity and may represent a feed-back mechanism aiming to compensate the defunct activation status of macrophages or lymphocytes.

Inducible nitric oxide synthase (iNOS) was also up-regulated in wild-type mice compared to IFN- γ -KO mice (appendix 1). Hypoxic activation of iNOS transcription requires binding sites for IRF-1 and HIF-1 on the iNOS promoter region [235, 236]. HIF-1 α was also up-regulated in wild-type mice compared to IFN- γ -KO mice (appendix 1). Hypoxia alone cannot induce iNOS expression in macrophages, but together with IFN- γ , synergistically induced iNOS in macrophages [237-239]. Thus, the interconnection between oxygen-sensing and IFN- γ signaling might restrict production of NO by primed macrophages to hypoxic regions. This mechanism emphasizes the potential role of Th1-dependent killing of intracellular pathogens such as mycobacteria, which often reside in poorly vascularized, hypoxic granulomas [240]. In a previous report, nitric oxide synthase was examined for its involvement in granuloma necrosis, where iNOS-KO mice infected with *M. avium* developed granuloma necrosis, although to a lesser extent and in a delayed fashion than infected wild-type mice. This indicates that nitric oxide synthase is not critically necessary for the development of granuloma necrosis [172].

Integrins are essential for the lymphocyte-endothelial cell interaction as well as for the homing of activated memory lymphocytes to the site of infection [241-244]. Following an aerosol mycobacterial infection, the endothelial expression of the vascular cell adhesion molecule (VCAM)-1 is up-regulated, and the number of β integrin-expressing T-cells increases, thereby redirecting trafficking of specific lymphocytes to the lungs. Since $\alpha_4\beta_1^{\text{high}}$ T-cells are major IFN- γ -producing cells during pulmonary tuberculosis, the $\alpha_4\beta_1$:VCAM-1 interaction likely contributes to the control of mycobacterial infection [245].

The documented up-regulation of VCAM-1 in wild-type mice infected with *M. avium* correlates with the fact that activated T-cells are necessary to induce granuloma necrosis [172]. Decreased VCAM-1 mRNA levels in IFN- γ -KO mice correlate with the enhanced replication of *M. avium* in the lungs of these mice and the increased influx of granulocytes, described also for *M. tuberculosis* infection. Here, treatment of aerosol-infected mice with an antibody against α_4 integrin reduced the number of lymphocytes and increased the number of neutrophils in infected lungs *in vivo*. This resulted in the development of

disorganized infiltrates with a predominance of granulocytes. Ultimately, the exacerbation of *M. tuberculosis* replication resulted in wide-spread pulmonary necrosis [245].

The up-regulation of adhesion molecules for infiltrating cells is associated with an induced secretion of chemokines. The up-regulation of SLC and BLC confirms a previous report [246] revealing that an up-regulation of SLC promotes an increase in BLC.

SLC is the first chemokine demonstrated to have the characteristics required to mediate homing of T-lymphocytes to secondary lymphoid organs. BLC, on the other hand, is the only chemokine so far which is known to specifically chemoattract B-cells through the interaction with its receptor CXCR5. Not only B-cells, but also activated T-cells migrate towards BLC [247].

SLC and BLC were found to be induced in the lungs and within granulomatous lesions after infection with *M. tuberculosis*, indicating that mycobacterial infections might cause the formation of neolymphoid follicles in the lungs [248, 249]. This was also confirmed by our observations of B- and T-lymphoid follicles developing during the course of infection with *M. avium* (data not shown).

It is well-known that CXCR3-ligands (especially MIG and IP-10) are induced by IFN- α/β in response to *M. tuberculosis* infection [94, 250], but the main inducer of those chemokines is IFN- γ [251]. This is also confirmed by our data showing that the expression of CXCR3-ligands is strongly reduced in IFN- γ -KO mice infected with *M. avium*. Thus, the following hypothesis was proposed: IFN- γ induces angiostatic chemokines that cause a reduced vascularization leading to hypoxia. Cells under oxygen starvation die and result in a necrosis.

4. 2. Angiostasis and vascularization

4. 2. 1. Imbalanced angiogenesis in *M. avium*-infected mice

Angiostatic effects have been shown *in vivo* for both IP-10 and MIG. They share a common functional receptor CXCR3 together with I-TAC and bind it with high affinity. IP-10, MIG and I-TAC inhibited effectively the proliferation of endothelial cells. An antibody against the CXCR3 blocked this anti-proliferative effect. This explained the angiostatic activity of this receptor [252-254], as it is strictly associated to a cell-cycle phase and directly involved in the control of the endothelial cell proliferation [154].

In 1893 it was first reported that bacterial infection interferes with tumor growth [255]. Subsequent studies showed that protozoan pathogens like *Toxoplasma gondii* activate macrophages to kill tumor cells *in vitro* [256]. It was believed that cytotoxic mechanisms, cytolytic functions or immunomodulatory pathways are responsible for this effect. Upon infecting different mouse strains, in which the cytotoxic mechanisms are missing (such as knock-out mice deficient for inducible nitric oxide synthase, cytotoxic T-lymphocytes, natural killer cells); or mouse strains, in which the cytolytic functions are absent (such as perforin knock-out mice); or mouse strains, in which the immunomodulatory pathways are disrupted (such as knock-out mice lacking the p40 subunit of IL-12 or the type 1 TNF- α receptor); it became evident that the infection-induced resistance to tumors was not associated with any of the mentioned factors, because *T. gondii* infection was still able to suppress tumor growth in all of those mouse strains [257].

Examination of the tumor mass in *T. gondii*-infected compared to uninfected mice revealed the absence of blood vessels as well as the presence of necrotic areas surrounded with extensive areas of hypoxia. This correlation between inhibited angiogenesis that causes insufficient vascularization, hypoxia and necrosis being crucial for resistance to tumor [257] was reported as early as 1947, where treatment with LPS inhibited tumor vascularity [258].

In the mentioned mouse model of toxoplasmosis, the angiostatic activity of interferon-gamma induced chemokines was associated with tumor regression during infection [257]. Tumor growth and metastasis need the sprouting and formation of new blood vessels that supply the tumor with nutrients and oxygen. Based on this finding, it is conceivable that infection results in the increased expression of IFN- γ , which in turn induces angiostatic chemokines. When IFN- γ -KO mice were examined for angiostatic chemokine mRNA expression, MIG could not be detected on the mRNA level following *M. avium* infection, while it was clearly present in wild-type mice [186]. *M. avium*-infected mice deficient for IFN- γ show a loss of angiostatic chemokine expression, have a largely unaltered vascularization and do not develop granuloma necrosis [172].

The CXC-receptor-3 mediates an angiostatic effect. This receptor exists on activated T-lymphocytes [259], with a higher expression especially on Th1-cells [260, 261]. Based on this knowledge, it was worthwhile to prove the suggested correlation between inhibited angiogenesis and granuloma necrosis, which is also known to be associated with T-lymphocytes, especially CD4+ Th1-cells [172]. We examined the status of the angiostatic ligands MIG and IP-10 in IFN- γ -KO and wild-type mice during infection and compared

them with other chemoattractant chemokines as well as angiogenic factors by RPA analysis. The overall angiogenic or angiostatic tendency concluded from our findings is summarized in Tab. 3.

	Infection		Balance	WT	KO	Balance	
Angiogenic factors	↓	Angiopoietin	Angiostasis	↓	↑	Angiogenesis	
	↓	VEGF		↓	↑		
	↓	Endoglin		↔	↔		
	↓	VEGFC		↓	↑		
	↓	CD31		↓	↑		
	↓	Thrombin		↓	↑		
	↓	TIE2		↔	↔		
	↓	TIE		↓	↑		
	↓	FLT4		↔	↔		
	↓	FLT1		↔	↔		
Angiostatic chemokines	↑	IP-10		↑	↓		
	↑↑	MIG		↑↑	↓↓		

Table 3: Balance is shifted towards angiostasis in wild-type mice compared to IFN- γ -KO mice as shown by RPA. A summary of differential expression of angiostatic chemokines versus angiogenic factors mRNA in lungs of C57BL/6 wild-type (WT) and IFN- γ -deficient (KO) mice infected by aerosol with *M. avium* (TMC724, 10⁵ CFU/mouse). Total RNA was prepared from the right lungs harvested 12 and 14 weeks after infection as well as from the right lungs of uninfected mice. 8 μ g samples of RNA from WT and KO mice were hybridized with ³³P-labeled multi-probe template set and chemokine mRNA was analyzed by Ribonuclease Protection Assay (RPA). A double arrow means increased (↑↑) or decreased (↓↓), while a single arrow means higher (↑), lower (↓), or similar (↔).

Angiopoietin, VEGF, and their receptors TIE2, FLT1, respectively, as well as all angiogenic factors examined did not show a significant difference, while tending more to be increased in IFN- γ -KO mice compared to C57BL/6 mice, except for VEGFC, which was significantly higher in IFN- γ -KO compared to wild-type mice, while its receptor FLT4 was not significantly up-regulated. On the other hand, the angiostatic chemokines, like IP-10 and MIG, were either reduced or absent, which results in a shift towards angiogenesis in IFN- γ -KO mice.

During the course of infection, the angiogenic factors were markedly reduced in infected mice at week 12 and 14 post-infection, compared to control uninfected mice. Surprisingly, the angiostatic chemokines, as well as a diffuse pattern of chemokines including eotaxin, RANTES, ELC, MIP-1 γ , MIP-2, MIP-1 α , MIP-1 β , Ltn, BLC, TCA-3 and MCP-1 were highly increased in infected mice at week 12 and 14 post-infection, compared to control uninfected mice. This leads to the assumption that granuloma necrosis is associated with a

high influx of cells, a severe reduction in angiogenesis that might deprive the tissue of nutrients and oxygen.

4. 2. 2. CXCR3-mediated angiostasis in *M. avium*-infected mice

Concerning a reduced vascularization, the capillaries varied in their presence and intensity throughout the lung tissue of wild-type mice. Although the blood vessels were prominent outside the granuloma, they decreased at the borders of the granuloma and its outer layers, while capillaries lessened and rarefied more and more towards the center of the granuloma. The IFN- γ -KO mice maintained a uniformly distributed vascular structure throughout the tissue of the mouse lungs, suggesting the involvement of angiostasis in the development of granuloma necrosis.

Since CXCR3 is a common receptor of the most known angiostatic mediators found to be up-regulated in wild-type mice in this study, we hypothesized that the blocking of the CXCR3 might prevent this angiostatic function and granulomas would be more vascularized. CXCR3-KO mice would then resemble IFN- γ -KO mice that did not form necrosis, or at least necrosis would be reduced. However, 20 weeks after infection with *M. avium* TMC724, a clear-defined and far-developed granuloma necrosis arose in CXCR3-KO mice, as well as in C57BL/6 mice.

Considering the previous hypothesis, the CXCR3-mediated angiostasis could be a contributing factor but not the main cause precipitating granuloma necrosis in the lungs of mice infected with mycobacteria.

In conclusion, the reduction in vascularization in and around the granuloma could have two causes. It might result from the growing mass of the granuloma, where increasing numbers of cells continue to infiltrate at the site of infection, compressing thereby the adjacent tissue around the granuloma. The blood vessels existing in the tissue and suffering from the repulsive force of a growing granuloma might therefore become compact at the surrounding borders. The other cause could be the imbalance between angiogenic and angiostatic mediators. Our data have shown a clear down-regulation of angiogenic factors against a clear up-regulation of angiostatic chemokines during infection. The overall outcome would consequently be in favor of angiostasis, which might result in a reduced vascularization at the site of infection. This translates in our model to reduced blood vessels inside the granuloma.

4. 3. Oxygen concentration inside granulomas

4. 3. 1. Non-replicating persistence

Mycobacteria actively replicate at the beginning of an infection in the murine lung utilizing the high-energy cell membrane associated cytochrome c oxidases, as they require a high production of ATP for ATP synthesis. Cytochrome c oxidase reduces O₂ to H₂O acting thereby as a proton pump across the cell membrane, a process generating ATP [262].

The onset of a Th1-immune response induces nitric oxide synthase and IFN- γ activated macrophages produce reactive nitrogen intermediates (RNI) and nitric oxide that has bacteriostatic effects [33, 83]. Nitric oxide competes with oxygen for the binding sites on the cytochrome c oxidase [263, 264]. Even low concentrations cause poisoning of the cell-membrane associated cytochrome oxidases and loss of their respiratory function [262], thereby bacterial replication is arrested [265].

This chronic phase is referred to as the dormancy or non-replicating persistence (NRP) state [265]. Although mycobacteria in the late NRP state shut-down almost all gene expressions [266], bacterial replication cannot be completely absent at this state, however, a static equilibrium of a very low rate of intermittent cell division and replication must exist [267, 268]. Only this could explain the high increase of bacterial load at very late stages of the infection [269].

4. 3. 2. Anaerobic respiration

Granuloma formation is a process that is thought to result in oxygen depletion. *M. tuberculosis* was originally defined as an obligate aerobe that would not be expected to survive at a site of depleted oxygen. Recent studies showed that immunosuppression results in a reactivation of latent disease. The chronic phase of a mycobacterial infection is associated with granuloma formation involving the accumulation of large numbers of cells at the site of infection that could result in a low oxygen tension arresting mycobacterial growth [268, 270]. Hence, it remained unknown, how mycobacteria persist inside the host. This opened up the possibility that dormant mycobacteria might reside in the caseous lesion at the center of a granuloma [271, 272].

Several genes identified in *M. tuberculosis* were up-regulated upon oxygen depletion. Knocking out these mycobacterial genes in different models made the knock-out strain susceptible to the host immune defense during latent infection, where it lost its ability to persist and could be cleared by the immune system of the host.

The α -crystalline protein homologue or 16-kDa protein (Acr or HspX) is a major *M. tuberculosis* antigen induced under hypoxic [273] or anoxic [274] conditions, as well as upon exposure to nitric oxide [275]. Severe growth attenuation of a mutant of *M. tuberculosis* deficient for hspX was observed in a human macrophage-like THP-1 cell line, where this gene is induced, as well as in primary murine bone-marrow-derived macrophages. Activated macrophages consume more oxygen in a shorter time than do naïve macrophages, leading to a state of depleted oxygen at the site of activation that might inhibit the mycobacterial growth [276]. Thus, *acr* is rapidly induced upon mycobacterial entrance into macrophages [277].

Interestingly, the observations *in vitro* could not be confirmed by *in vivo* studies, where an increase of 1-2 log units in mycobacterial load was observed, when wild-type mice were infected with a mutant of *M. tuberculosis* H37Rv, where *acr* was deleted [278], indicating that there was no oxygen depletion. These results put the mouse model of *M. tuberculosis* infection in focus, questioning the hypoxic state of the granulomatous lung tissue.

During infection many pathogens starve for essential nutrients and cofactors like carbon sources, amino acids, purines, pyrimidines, magnesium and iron [166].

Bacterioferritin (BfrB) and mycobactin (MbtB) are iron storage and uptake proteins, respectively, that are induced during the chronic state. It is worth to mention, that the *bfrB* is co-induced with the *mbtB*, the iron mycobactin siderophore, which is important for the acquisition of iron from the environment. Although *bfrB* is down-regulated, when the mycobactin synthesis genes are up-regulated under iron deficiency, it seems that *M. tuberculosis* during the chronic state induces both uptake and storage functions to increase iron stores for the dormancy period [266]. It was reported that iron-responsive genes of *M. tuberculosis* were highly regulated especially at the late stages of aerosol-infected mice indicating the possibility of growth arrest due to iron limitation [279].

During the progress of infection, the blood support with nutrients decreases, reducing as a consequence the availability of carbohydrates. *M. tuberculosis* shifts from the utilization of carbohydrates to fatty acids [166, 280].

Isocitrate lyase (Icl) is an enzyme of the glyoxalate shunt. Converting isocitrate to succinate, it allows bacteria to grow on acetate or fatty acids as a sole carbon source [166,

280]. *In vitro*, isocitrate lyase activity in cells infected with *M. tuberculosis* increases dramatically at stationary phase [281]. mRNA levels of this enzyme increase in human macrophages upon *M. tuberculosis* infection [282, 283], as well as in the lungs of mice infected with *M. tuberculosis* with the progression of disease [284].

A mutant of *M. tuberculosis*, where *icl1* was inactivated, was shown to grow normally in wild-type mice at the beginning of the infection, but when cell-mediated immunity was activated, the mutant stopped growing in the lungs of wild-type mice and was cleared, while in IFN- γ -KO mice the mutant grew similarly to the wild-type mycobacterium [280]. In a subsequent report of the same group, the previous report was refined by showing that only the double mutant of *icl1* and *icl2* was significantly attenuated [267]. In the first report *icl1* seemed very important for the mycobacterial growth during late stages of infection, while the mycobacterial growth was not affected by the absence of *icl1* in the second report. These data suggest that severe hypoxia is not consistently present in *M. tuberculosis*-infected lungs of mice; they even question the presence of severe hypoxia at all in *M. tuberculosis*-induced pulmonary granulomas of mice.

The mycolic acid cyclopropane synthase (*PcaA*) is an enzyme coded in *M. tuberculosis*. A mutant of both *M. tuberculosis* and *M. bovis* BCG, where the *pcaA* was knocked-out, was able to replicate at the beginning of the infection, while losing the ability to persist in mice [285].

The attenuation of growth observed for the previously mentioned mutants during the chronic phase of infection in the mouse cannot be only attributed to hypoxia, as hypoxia-inducible genes could also be induced by nitric oxide, nutrient starvation or other stresses. These data could also indicate that severe hypoxia is not consistently present in tuberculous lesions of mice infected with *M. tuberculosis*.

The importance of enzymes allowing respiration under anaerobic conditions was recently realized. In a carbohydrate-deficient environment, where fatty acids are utilized as a carbon source, a reduced molecule of NADH and FADH₂ results for each produced acetyl-CoA. These reduced molecules must be reoxidized, so that a continuous metabolism can be assured. Only the function of glycine dehydrogenase (*GcvB*) reducing glyoxylate to glycine by amination would not maintain the redox balance, as it can only reoxidize one NADH molecule for each acetyl-CoA [286]. Fumarate reductase and nitrate reductase are important in decreasing the redox potential in this case [128]. Hypoxia induces the up-regulation of specific enzymes like nitrate reductase [175] and glycine dehydrogenase [281].

In order to prevent a disruption of the membrane potential, the less energy efficient cytochrome bd oxidase is up-regulated as well as the nitrate transporter narK2 that increases the nitrate reduction [182]. On restoring the membrane redox potential, the cytochrome bd oxidase is down-regulated and the respiratory nitrate reduction is responsible for maintaining an adequate redox balance. When the respiratory metabolism shifts to nitrate reduction to allow energy production from β -oxidation of fatty acids at the chronic phase of the infection in the absence of oxygen, the expression of genes required for ATP synthesis decreases [287].

Under anaerobic conditions *in vitro*, genes are induced in mycobacteria that allow the switch from aerobic to anaerobic respiration utilizing nitrates. Upon macrophage activation, nitric oxide synthase is induced and nitric oxide produced. Subsequently, nitric oxide is degraded into nitrate and nitrite [175]. Significant amounts of nitrate are detected in the urine of rodents, indicating that the substrate of nitrate reductases is available and distributed at different sites of the animal body, especially those suffering from inflammation [288, 289].

Nitrate reductase (NarG) is the key enzyme essential for anaerobic respiration in the presence of nitrates [274]. A gene cluster narGHJI encodes the anaerobic nitrate reductase proteins in *M. tuberculosis* [182, 290]. Under anaerobic conditions narG is responsible for the utilization of nitrates for energy production [291]. The absence of narG in a mycobacterium should not allow its survival under anaerobic conditions. Infecting mice with a narG mutant of *M. bovis* BCG resulted in less bacteria inside smaller granulomas compared with the wild-type strain [290].

A mycobacterial mutant of *M. tuberculosis* lacking narG survived in the lungs of mice infected with tuberculosis showing a growth pattern similar to wild-type mycobacteria [292]. This was consistent with previous data showing that the response regulator dosR, which contains the narK2-narX operon that encodes the nitrate reductase activity by narGHJI [182], if inactivated in a mutant, was not attenuated in the mouse model either [293].

These conflicting results seriously challenge the prevailing belief that anoxia or severe hypoxia exists inside granulomas in mouse lungs infected with *M. tuberculosis*.

4.3.3. Evidence for hypoxia

The high influx of macrophages and granulocytes to the site of infection is an oxygen-consuming process, resulting in a high consumption of oxygen, even though the infiltrates are well supported by the capillary system [294, 295]. A low blood supply could deprive the tissue from essential nutrients and oxygen.

Hypoxia inducible factors (HIF)-1 and (HIF)-2 are composed of two subunits α and β and are regulated in a similar manner [296, 297]. In contrast to HIF-1, the role of HIF-2 remains unclear [298]. The HIF-1 β protein is readily found in all cells, while HIF-1 α is almost undetectable under normal oxygen conditions. Reaching an oxygen concentration of 1%, the level of the HIF-1 α subunit is rapidly increased in the cell due to an inhibited degradation of HIF-1 α by the proteasome [299-304]. Under normoxic conditions, prolyl hydroxylation and acetylation of HIF-1 α allow proteasomal degradation [305]. Under hypoxic conditions, prolyl hydroxylation of HIF-1 α is blocked and acetylation is down-regulated, this stabilizes the HIF-1 α that binds with HIF-1 β forming the HIF-1 transcription complex. HIF-1 heterodimer binds to the hypoxic response elements (HRE) in its target genes including erythropoietin, glucose transporters, glycolytic enzymes, and vascular endothelial growth factor (VEGF) and increases their expression [306]. This contradicts with our findings, where the HIF-1 α mRNA was increased in wild-type mice, while the VEGF mRNA was decreased in wild-type mice.

In order to resolve this contradiction, we thought to detect the HIF-1 α and HIF-2 α proteins immunohistochemically in the lung tissue of our mouse model infected with *M. avium*. Our results showed a slight expression of HIF-1 α , especially at 13 weeks post-infection, while HIF-2 α was almost undetectable. This correlates to the reduced VEGF expression and suggests that the lesion is not severely hypoxic, while the increase in HIF-1 α could be related to a highly activated immune response of macrophages and neutrophils under normoxic conditions [307].

In order to support the previous finding, a hypoxia marker was used that could detect hypoxia in granulomas compared to tumors in mice [308]. The conditions for adduct formation have been systematically determined and prolonged oxygen tensions below 14 μ M, which is equivalent to 10 mmHg [309], are required for thiol bonds to be formed that can then be detected by specific antibodies [310]. This marker could not detect hypoxia in the lungs of mice infected with *M. tuberculosis*, even at late stages of the

infection, although the marker clearly detected hypoxia in the necrotic granulomas of mice 18 weeks after infection with *M. avium* as well as in necrotic tumors. On the other hand, guinea pigs showed a severe hypoxia already at day 30 after infection with *M. tuberculosis*. The staining for hypoxia was not restricted to the borders of the granuloma. Indeed, a marked staining was also observed inside the granuloma, at the center, where only acellular debris was expected to exist. Inside the necrotic region, the staining could only occur in a cell, where the NADPH redox state is active. Dead cells will not be able to perform a chemical reduction of the marker intermediate to enable the binding to thiol-containing proteins. Only viable cells can stain for hypoxia, which thereby indicates an estimate of viable and dead cells inside the necrotic region.

It was reported that in granulomas of mice infected with mycobacteria predominantly micro-aerobic regions could co-exist with limited anaerobic or hypoxic regions, both containing dormant mycobacteria [168]. Thus, we decided to directly measure the oxygen concentration in the lungs of mice infected with *M. tuberculosis* to determine the extent of oxygen depletion in the lung tissue of those animals.

The mean partial oxygen pressure (pO₂) level for *M. tuberculosis*-infected lungs was not below 10 mmHg (except two measurements out of 34). The measurements for those mice could be divided into two separate clusters, one with a mean pO₂ level around 50 mmHg, indicating reduced oxygen tension or micro-aerobiosis, and the other with a mean pO₂ level around 15 mmHg, indicating hypoxia or limited anaerobiosis. It appeared difficult to insert the electrode into the center of the necrotic granulomas of *M. avium*-infected lungs, because of their hard structure. Thus, we could not ascertain if the electrode entered the granuloma or was just adjacent to it. The mean pO₂ level that could be measured in the lungs of *M. avium*-infected mice was around 25 mmHg.

In summary, we could say that we could not detect anoxia or severe hypoxia in the lungs of mice infected with *M. tuberculosis*, even at late stages of the infection. Different degrees of hypoxia were indeed measured and observed. In the mouse model infected with *M. avium*, hypoxia was evident at late stages of the infection. If necrosis were to develop due to depletion of oxygen, hypoxia should be detected before the onset of necrosis. As hypoxia could only be detected at late stages of infection after the development of a granuloma necrosis, it is conceivable that hypoxia is not a cause, but rather a consequence resulting from granuloma necrosis in mice. On the other hand, guinea pigs showed a severe hypoxia already at day 30 after infection with *M. tuberculosis*, indicating that hypoxia indeed might

be a cause for the development of granuloma necrosis in guinea pigs and possibly in humans as well.

Our work explains the contradicting data obtained from *in vitro* and *in vivo* studies, as well as the contradiction observed upon infecting different animal models with mutant strains of *M. tuberculosis*. Data obtained herein, using immunohistochemical staining and biophysical measurement of the local oxygen concentration inside the lung tissue of mice infected with *M. tuberculosis* showed that those mice are neither anoxic nor severely hypoxic. Granulomas in the lungs of guinea pigs infected with *M. tuberculosis*, however, were severely hypoxic even at early stages of the infection. This correlates with previous results indicating that the response regulator *dosR* is required for virulence in guinea pigs that showed only minimal pathological lesions and a 3 log lower bacterial load, when infected with the mutant strain [311].

This indicated that the mouse model infected with *M. tuberculosis* cannot be used for virulence or strain testing, as granulomas in the lungs of mice infected with *M. tuberculosis* were not anoxic, genes required under anaerobic conditions did not play a role in the mouse model. Thus, several mutants tested and predicted to be of importance should be further studied in another animal model like guinea pigs as they could be promising drug target for tuberculosis therapy.

4.3.4. Consequences for TB treatment

Tuberculosis treatment is difficult, as it requires not only a long period of time (minimum 6-9 month), but also a combination of several drugs (multidrug therapy) to prevent a post-therapeutical relapse [312] as well as the emergence of multidrug resistant strains. Most of the conventional drugs in use target cellular mechanisms like cell replication, cell-wall biosynthesis and DNA synthesis, therefore these drugs are not effective against bacteria in NRP state [177, 313, 314].

Rifampin, which inhibits RNA polymerase during RNA synthesis [315], acts especially on extra-cellular bacteria [316]. It showed a diminished bactericidal action on mycobacteria in the NRP state [179, 265].

Isoniazid, which inhibits mycolate synthase during cell-wall mycolate biosynthesis [317], acts mainly on replicating bacteria. It failed to kill mycobacteria after entering the NRP state [265].

Nitroimidazoles, like metronidazole, are one exception: in spite of having no effect on aerobic or micro-aerobic bacteria even if exposed to high concentrations of the drug [265], anaerobic bacteria in the NRP state are susceptible to the bactericidal activity of those drugs [179, 265]. Metronidazole affects mycobacteria under latent anaerobic rather than under replicating aerobic conditions [179, 318]. Interestingly, in spite of having a strong bactericidal effect on anaerobic mycobacteria *in vitro*, *in vivo* metronidazole had only a minor bactericidal effect on mycobacteria in mice [319]. This is another observation that can be explained by our data showing that lesions in *M. tuberculosis*-infected mouse lungs are not anoxic.

The marked staining for hypoxia inside the granulomas of mouse lungs infected with *M. avium* indicated that the pimonidazole reagent was able to diffuse to the center of the granuloma into the necrotic areas in spite of the rarefied blood vessels around these areas in both granulomas of the lung as well as tumors in mice.

This makes antibiotics that are reactive under anaerobic conditions, targeting molecules involved in metabolic chains, of therapeutic importance. Imidazole derivatives, like metronidazole, are promising candidates for the therapy of latent infection and multidrug-resistant tuberculosis as they have bactericidal activity against static non-replicating *M. tuberculosis* persisting under anaerobic conditions [179, 265] unlike the conventional drugs that are active either against metabolically active mycobacteria [177, 320] or against actively replicating mycobacteria [321, 322].

5. References

- [1] Koch R. Die Aetiologie der Tuberkulose. *Berl.Klin.Wochenschr.* 1882;19:221-30.
- [2] Kaye K, Frieden TR. Tuberculosis control: the relevance of classic principles in an era of acquired immunodeficiency syndrome and multidrug resistance. *Epidemiol.Rev.* 1996;18(1):52-63.
- [3] Waaler HT. Tuberculosis and poverty. *Int.J.Tuberc.Lung Dis.* 2002;6(9):745-6.
- [4] WHO. Global tuberculosis control: surveillance, planning, financing, WHO Report 2005. Geneva: World Health Organization; 2005;Case notification and incidence. p. 22-6.
- [5] Bastian I, Stapledon R, Colebunders R. Current thinking on the management of tuberculosis. *Curr.Opin.Pulm.Med.* 2003;9(3):186-92.
- [6] Tuberculosis. Scientific blueprint for tuberculosis drug development. *Tuberculosis.(Edinb.)*. 2001;81 Suppl 1:1-52.:1-52.
- [7] Wiseman KC. Tuberculosis: an old disease with a new face. *ANNA.J.* 1995;22(6):541-54.
- [8] Onyebujoh P, Zumla A, Ribeiro I, et al. Treatment of tuberculosis: present status and future prospects. *Bull.World Health Organ.* 2005;83(11):857-65.
- [9] Frieden TR. Can tuberculosis be controlled? *Int.J.Epidemiol.* 2002;31(5):894-9.
- [10] Iseman MD. Evolution of drug-resistant tuberculosis: a tale of two species. *Proc.Natl.Acad.Sci.U.S.A.* 1994;91(7):2428-9.
- [11] O'Brien RJ, Pekar N, editors. Tuberculosis: scientific blueprint for tuberculosis drug development. New York: Global Alliance for TB Drug Development; 2001;The Need for New TB Drug Treatments. p. 3-4.
- [12] Andersen P. TB vaccines: progress and problems. *Trends Immunol.* 2001;22(3):160-8.
- [13] Behr MA, Wilson MA, Gill WP, et al. Comparative genomics of BCG vaccines by whole-genome DNA microarray. *Science.* 1999;284(5419):1520-3.
- [14] Brandt L, Feino CJ, Weinreich OA, et al. Failure of the Mycobacterium bovis BCG vaccine: some species of environmental mycobacteria block multiplication of BCG and induction of protective immunity to tuberculosis. *Infect.Immun.* 2002;70(2):672-8.
- [15] Kaufmann SH. Is the development of a new tuberculosis vaccine possible? *Nat.Med.* 2000;6(9):955-60.
- [16] Kaufmann SH. How can immunology contribute to the control of tuberculosis? *Nat.Rev.Immunol.* 2001;1(1):20-30.

-
- [17] WHO. Global tuberculosis control: surveillance, planning, financing, WHO Report 2002. Geneva: World Health Organization; 2002; Treatment results, 1994-1999 cohorts. p. 15-8.
- [18] WHO. Global tuberculosis control: surveillance, planning, financing, WHO Report 2004. Geneva: World Health Organization; 2004; Progress towards targets for case detection and treatment success. p. 29-31.
- [19] Chiang CY, Riley LW. Exogenous reinfection in tuberculosis. *Lancet Infect.Dis.* 2005;5(10):629-36.
- [20] Tufariello JM, Chan J, Flynn JL. Latent tuberculosis: mechanisms of host and bacillus that contribute to persistent infection. *Lancet Infect.Dis.* 2003;3(9):578-90.
- [21] Barreto AM, Araujo JB, Melo Medeiros RF, Souza Caldas PC. Evaluation of indirect susceptibility testing of *Mycobacterium tuberculosis* to the first- and second-line, and alternative drugs by the newer MB/BacT system. *Mem.Inst.Oswaldo Cruz.* 2003;98(6):827-30.
- [22] Fung-Tomec J, Minassian B, Kolek B, Washo T, Huczko E, Bonner D. In vitro antibacterial spectrum of a new broad-spectrum 8-methoxy fluoroquinolone, gatifloxacin. *J.Antimicrob.Chemother.* 2000;45(4):437-46.
- [23] Ji B, Lounis N, Truffot-Pernot C, Grosset J. In vitro and in vivo activities of levofloxacin against *Mycobacterium tuberculosis*. *Antimicrob.Agents Chemother.* 1995;39(6):1341-4.
- [24] Miyazaki E, Miyazaki M, Chen JM, Chaisson RE, Bishai WR. Moxifloxacin (BAY12-8039), a new 8-methoxyquinolone, is active in a mouse model of tuberculosis. *Antimicrob.Agents Chemother.* 1999;43(1):85-9.
- [25] Jarvis B, Lamb HM. Rifapentine. *Drugs.* 1998;56(4):607-16.
- [26] McGregor MM, Olliaro P, Wolmarans L, et al. Efficacy and safety of rifabutin in the treatment of patients with newly diagnosed pulmonary tuberculosis. *Am.J.Respir.Crit Care Med.* 1996;154(5):1462-7.
- [27] Shoen CM, DeStefano MS, Cynamon MH. Durable cure for tuberculosis: rifalazil in combination with isoniazid in a murine model of *Mycobacterium tuberculosis* infection. *Clin.Infect.Dis.* 2000;30 Suppl 3:S288-90.:S288-S290
- [28] Cynamon MH, Klemens SP, Sharpe CA, Chase S. Activities of several novel oxazolidinones against *Mycobacterium tuberculosis* in a murine model. *Antimicrob.Agents Chemother.* 1999;43(5):1189-91.
- [29] O'Brien RJ, Pekar N, editors. Tuberculosis: scientific blueprint for tuberculosis drug development. New York: Global Alliance for TB Drug Development; 2001; Objectives for TB Drug Development. p. 7-8.
- [30] Stover CK, Warrenner P, VanDevanter DR, et al. A small-molecule nitroimidazopyran drug candidate for the treatment of tuberculosis. *Nature.* 2000;405(6789):962-6.
-

References

- [31] Diekema DI, Jones RN. Oxazolidinones: a review. *Drugs*. 2000;59(1):7-16.
- [32] Cole ST, Brosch R, Parkhill J, et al. Deciphering the biology of *Mycobacterium tuberculosis* from the complete genome sequence. *Nature*. 1998;393(6685):537-44.
- [33] North RJ, Jung YJ. Immunity to tuberculosis. *Annu.Rev.Immunol*. 2004;22:599-623.:599-623.
- [34] Wayne LG. Kubica GP, Wayne LG, editors. *The Mycobacteria: a sourcebook*. New York: Marcel Dekker; 1984;Mycobacterial speciation. p. 25-65.
- [35] Timpe A, Runyon EH. The relationship of atypical acid-fast bacteria to human disease; a preliminary report. *J.Lab Clin.Med*. 1954;44(2):202-9.
- [36] Woods GL, Washington JA. Mycobacteria other than *Mycobacterium tuberculosis*: review of microbiologic and clinical aspects. *Rev.Infect.Dis*. 1987;9(2):275-94.
- [37] Greenwell-Wild T, Vazquez N, Sim D, et al. *Mycobacterium avium* infection and modulation of human macrophage gene expression. *J.Immunol*. 2002;169(11):6286-97.
- [38] Inderlied CB, Kemper CA, Bermudez LE. The *Mycobacterium avium* complex. *Clin.Microbiol.Rev*. 1993;6(3):266-310.
- [39] Iseman MD. *Mycobacterium avium* complex and the normal host: the other side of the coin. *N.Engl.J.Med*. 1989;321(13):896-8.
- [40] Schlesinger LS, Hull SR, Kaufman TM. Binding of the terminal mannosyl units of lipoarabinomannan from a virulent strain of *Mycobacterium tuberculosis* to human macrophages. *J.Immunol*. 1994;152(8):4070-9.
- [41] Schlesinger LS. Role of mononuclear phagocytes in *M tuberculosis* pathogenesis. *J.Investig.Med*. 1996;44(6):312-23.
- [42] Myones BL, Dalzell JG, Hogg N, Ross GD. Neutrophil and monocyte cell surface p150,95 has iC3b-receptor (CR4) activity resembling CR3. *J.Clin.Invest*. 1988;82(2):640-51.
- [43] van Crevel R, Ottenhoff TH, van der Meer JW. Innate immunity to *Mycobacterium tuberculosis*. *Clin.Microbiol.Rev*. 2002;15(2):294-309.
- [44] Schorey JS, Carroll MC, Brown EJ. A macrophage invasion mechanism of pathogenic mycobacteria. *Science*. 1997;277(5329):1091-3.
- [45] Stokes RW, Haidl ID, Jefferies WA, Speert DP. Mycobacteria-macrophage interactions. Macrophage phenotype determines the nonopsonic binding of *Mycobacterium tuberculosis* to murine macrophages. *J.Immunol*. 1993;151(12):7067-76.
- [46] Schlesinger LS, Bellinger-Kawahara CG, Payne NR, Horwitz MA. Phagocytosis of *Mycobacterium tuberculosis* is mediated by human monocyte complement receptors and complement component C3. *J.Immunol*. 1990;144(7):2771-80.

- [47] Schlesinger LS. Macrophage phagocytosis of virulent but not attenuated strains of *Mycobacterium tuberculosis* is mediated by mannose receptors in addition to complement receptors. *J.Immunol.* 1993;150(7):2920-30.
- [48] Schlesinger LS, Kaufman TM, Iyer S, Hull SR, Marchiando LK. Differences in mannose receptor-mediated uptake of lipoarabinomannan from virulent and attenuated strains of *Mycobacterium tuberculosis* by human macrophages. *J.Immunol.* 1996;157(10):4568-75.
- [49] Stahl PD, Ezekowitz RA. The mannose receptor is a pattern recognition receptor involved in host defense. *Curr.Opin.Immunol.* 1998;10(1):50-5.
- [50] Krieger M, Herz J. Structures and functions of multiligand lipoprotein receptors: macrophage scavenger receptors and LDL receptor-related protein (LRP). *Annu.Rev.Biochem.* 1994;63:601-37.:601-37.
- [51] Janeway CA, Jr., Travers P, Walport M, Shlomchik MJ. *Immunobiology: the immune system in health and disease.* 5th ed. New York: Garland Publishing; 2001;Innate Immunity. p. 35-91.
- [52] Platt N, Suzuki H, Kurihara Y, Kodama T, Gordon S. Role for the class A macrophage scavenger receptor in the phagocytosis of apoptotic thymocytes in vitro. *Proc.Natl.Acad.Sci.U.S.A.* 1996;93(22):12456-60.
- [53] Dunne DW, Resnick D, Greenberg J, Krieger M, Joiner KA. The type I macrophage scavenger receptor binds to gram-positive bacteria and recognizes lipoteichoic acid. *Proc.Natl.Acad.Sci.U.S.A.* 1994;91(5):1863-7.
- [54] Hampton RY, Golenbock DT, Penman M, Krieger M, Raetz CR. Recognition and plasma clearance of endotoxin by scavenger receptors. *Nature.* 1991;352(6333):342-4.
- [55] Pearson AM. Scavenger receptors in innate immunity. *Curr.Opin.Immunol.* 1996;8(1):20-8.
- [56] Zimmerli S, Edwards S, Ernst JD. Selective receptor blockade during phagocytosis does not alter the survival and growth of *Mycobacterium tuberculosis* in human macrophages. *Am.J.Respir.Cell Mol.Biol.* 1996;15(6):760-70.
- [57] Armstrong JA, Hart PD. Phagosome-lysosome interactions in cultured macrophages infected with virulent tubercle bacilli. Reversal of the usual nonfusion pattern and observations on bacterial survival. *J.Exp.Med.* 1975;142(1):1-16.
- [58] Aderem A, Underhill DM. Mechanisms of phagocytosis in macrophages. *Annu.Rev.Immunol.* 1999;17:593-623.:593-623.
- [59] Unkeless JC, Shen Z, Lin CW, DeBeus E. Function of human Fc gamma RIIA and Fc gamma RIIIB. *Semin.Immunol.* 1995;7(1):37-44.
- [60] Ravetch JV, Clynes RA. Divergent roles for Fc receptors and complement in vivo. *Annu.Rev.Immunol.* 1998;16:421-32.:421-32.
- [61] Ravetch JV. Fc receptors. *Curr.Opin.Immunol.* 1997;9(1):121-5.

References

- [62] Takeda K, Kaisho T, Akira S. Toll-like receptors. *Annu.Rev.Immunol.* 2003;21:335-76. Epub@2001 Dec@19.:335-76.
- [63] Medzhitov R, Preston-Hurlburt P, Kopp E, et al. MyD88 is an adaptor protein in the hToll/IL-1 receptor family signaling pathways. *Mol.Cell.* 1998;2(2):253-8.
- [64] Iwasaki A, Medzhitov R. Toll-like receptor control of the adaptive immune responses. *Nat.Immunol.* 2004;5(10):987-95.
- [65] Akira S, Takeda K, Kaisho T. Toll-like receptors: critical proteins linking innate and acquired immunity. *Nat.Immunol.* 2001;2(8):675-80.
- [66] Adachi O, Kawai T, Takeda K, et al. Targeted disruption of the MyD88 gene results in loss of IL-1- and IL-18-mediated function. *Immunity.* 1998;9(1):143-50.
- [67] Schnare M, Barton GM, Holt AC, Takeda K, Akira S, Medzhitov R. Toll-like receptors control activation of adaptive immune responses. *Nat.Immunol.* 2001;2(10):947-50.
- [68] Takeuchi O, Hoshino K, Akira S. Cutting edge: TLR2-deficient and MyD88-deficient mice are highly susceptible to *Staphylococcus aureus* infection. *J.Immunol.* 2000;165(10):5392-6.
- [69] Seki E, Tsutsui H, Tsuji NM, et al. Critical roles of myeloid differentiation factor 88-dependent proinflammatory cytokine release in early phase clearance of *Listeria monocytogenes* in mice. *J.Immunol.* 2002;169(7):3863-8.
- [70] Edelson BT, Unanue ER. MyD88-dependent but Toll-like receptor 2-independent innate immunity to *Listeria*: no role for either in macrophage listericidal activity. *J.Immunol.* 2002;169(7):3869-75.
- [71] Scanga CA, Aliberti J, Jankovic D, et al. Cutting edge: MyD88 is required for resistance to *Toxoplasma gondii* infection and regulates parasite-induced IL-12 production by dendritic cells. *J.Immunol.* 2002;168(12):5997-6001.
- [72] Shi S, Nathan C, Schnappinger D, et al. MyD88 primes macrophages for full-scale activation by interferon-gamma yet mediates few responses to *Mycobacterium tuberculosis*. *J.Exp.Med.* 2003;198(7):987-97.
- [73] Scanga CA, Bafica A, Feng CG, Cheever AW, Hieny S, Sher A. MyD88-deficient mice display a profound loss in resistance to *Mycobacterium tuberculosis* associated with partially impaired Th1 cytokine and nitric oxide synthase 2 expression. *Infect.Immun.* 2004;72(4):2400-4.
- [74] Brightbill HD, Libraty DH, Krutzik SR, et al. Host defense mechanisms triggered by microbial lipoproteins through toll-like receptors. *Science.* 1999;285(5428):732-6.
- [75] Underhill DM, Ozinsky A, Smith KD, Aderem A. Toll-like receptor-2 mediates mycobacteria-induced proinflammatory signaling in macrophages. *Proc.Natl.Acad.Sci.U.S.A.* 1999;96(25):14459-63.

- [76] Ehrt S, Schnappinger D, Bekiranov S, et al. Reprogramming of the macrophage transcriptome in response to interferon-gamma and Mycobacterium tuberculosis: signaling roles of nitric oxide synthase-2 and phagocyte oxidase. *J.Exp.Med.* 2001;194(8):1123-40.
- [77] Means TK, Wang S, Lien E, Yoshimura A, Golenbock DT, Fenton MJ. Human toll-like receptors mediate cellular activation by Mycobacterium tuberculosis. *J.Immunol.* 1999;163(7):3920-7.
- [78] Means TK, Jones BW, Schromm AB, et al. Differential effects of a Toll-like receptor antagonist on Mycobacterium tuberculosis-induced macrophage responses. *J.Immunol.* 2001;166(6):4074-82.
- [79] Ragno S, Romano M, Howell S, Pappin DJ, Jenner PJ, Colston MJ. Changes in gene expression in macrophages infected with Mycobacterium tuberculosis: a combined transcriptomic and proteomic approach. *Immunology.* 2001;104(1):99-108.
- [80] Janeway CA, Jr., Travers P, Walport M, Shlomchik MJ. *Immunobiology: the immune system in health and disease.* 5th ed. New York: Garland Publishing; 2001; Basic concepts of immunology. p. 1-34.
- [81] Bergeron A, Bonay M, Kambouchner M, et al. Cytokine patterns in tuberculous and sarcoid granulomas: correlations with histopathologic features of the granulomatous response. *J.Immunol.* 1997;159(6):3034-43.
- [82] Chensue SW, Warmington KS, Ruth JH, Lincoln P, Kunkel SL. Cytokine function during mycobacterial and schistosomal antigen-induced pulmonary granuloma formation. Local and regional participation of IFN-gamma, IL-10, and TNF. *J.Immunol.* 1995;154(11):5969-76.
- [83] Flynn JL, Chan J. Immunology of tuberculosis. *Annu.Rev.Immunol.* 2001;19:93-129.
- [84] Roach DR, Bean AG, Demangel C, France MP, Briscoe H, Britton WJ. TNF regulates chemokine induction essential for cell recruitment, granuloma formation, and clearance of mycobacterial infection. *J.Immunol.* 2002;168(9):4620-7.
- [85] Mazzaccaro RJ, Gedde M, Jensen ER, et al. Major histocompatibility class I presentation of soluble antigen facilitated by Mycobacterium tuberculosis infection. *Proc.Natl.Acad.Sci.U.S.A.* 1996;93(21):11786-91.
- [86] Jung YJ, LaCourse R, Ryan L, North RJ. Evidence inconsistent with a negative influence of T helper 2 cells on protection afforded by a dominant T helper 1 response against Mycobacterium tuberculosis lung infection in mice. *Infect.Immun.* 2002;70(11):6436-43.
- [87] Baggiolini M. Chemokines and leukocyte traffic. *Nature.* 1998;392(6676):565-8.
- [88] Chensue SW, Warmington K, Ruth J, Lincoln P, Kuo MC, Kunkel SL. Cytokine responses during mycobacterial and schistosomal antigen-induced pulmonary granuloma formation. Production of Th1 and Th2 cytokines and relative contribution of tumor necrosis factor. *Am.J.Pathol.* 1994;145(5):1105-13.

References

- [89] Chiu BC, Freeman CM, Stolberg VR, et al. Cytokine-chemokine networks in experimental mycobacterial and schistosomal pulmonary granuloma formation. *Am.J.Respir.Cell Mol.Biol.* 2003;29(1):106-16.
- [90] Qiu B, Frait KA, Reich F, Komuniecki E, Chensue SW. Chemokine expression dynamics in mycobacterial (type-1) and schistosomal (type-2) antigen-elicited pulmonary granuloma formation. *Am.J.Pathol.* 2001;158(4):1503-15.
- [91] Lazarevic V, Flynn J. CD8+ T cells in tuberculosis. *Am.J.Respir.Crit Care Med.* 2002;166(8):1116-21.
- [92] Schaible UE, Sturgill-Koszycki S, Schlesinger PH, Russell DG. Cytokine activation leads to acidification and increases maturation of *Mycobacterium avium*-containing phagosomes in murine macrophages. *J.Immunol.* 1998;160(3):1290-6.
- [93] Cooper AM, Magram J, Ferrante J, Orme IM. Interleukin 12 (IL-12) is crucial to the development of protective immunity in mice intravenously infected with mycobacterium tuberculosis. *J.Exp.Med.* 1997;186(1):39-45.
- [94] Lande R, Giacomini E, Grassi T, et al. IFN-alpha beta released by *Mycobacterium tuberculosis*-infected human dendritic cells induces the expression of CXCL10: selective recruitment of NK and activated T cells. *J.Immunol.* 2003;170(3):1174-82.
- [95] Sallusto F, Lenig D, Mackay CR, Lanzavecchia A. Flexible programs of chemokine receptor expression on human polarized T helper 1 and 2 lymphocytes. *J.Exp.Med.* 1998;187(6):875-83.
- [96] Gangur V, Simons FE, Hayglass KT. Human IP-10 selectively promotes dominance of polyclonally activated and environmental antigen-driven IFN-gamma over IL-4 responses. *FASEB J.* 1998;12(9):705-13.
- [97] Reinhart TA, Fallert BA, Pfeifer ME, et al. Increased expression of the inflammatory chemokine CXC chemokine ligand 9/monokine induced by interferon-gamma in lymphoid tissues of rhesus macaques during simian immunodeficiency virus infection and acquired immunodeficiency syndrome. *Blood.* 2002;99(9):3119-28.
- [98] Rhoades ER, Cooper AM, Orme IM. Chemokine response in mice infected with *Mycobacterium tuberculosis*. *Infect.Immun.* 1995;63(10):3871-7.
- [99] Cooper AM, Segal BH, Frank AA, Holland SM, Orme IM. Transient loss of resistance to pulmonary tuberculosis in p47(phox^{-/-}) mice. *Infect.Immun.* 2000;68(3):1231-4.
- [100] MacMicking JD, North RJ, LaCourse R, Mudgett JS, Shah SK, Nathan CF. Identification of nitric oxide synthase as a protective locus against tuberculosis. *Proc.Natl.Acad.Sci.U.S.A.* 1997;94(10):5243-8.
- [101] Nathan CF, Hibbs JB, Jr. Role of nitric oxide synthesis in macrophage antimicrobial activity. *Curr.Opin.Immunol.* 1991;3(1):65-70.

- [102] Nicholson S, Bonecini-Almeida MG, Lapa e Silva JR, et al. Inducible nitric oxide synthase in pulmonary alveolar macrophages from patients with tuberculosis. *J.Exp.Med.* 1996;183(5):2293-302.
- [103] Nozaki Y, Hasegawa Y, Ichiyama S, Nakashima I, Shimokata K. Mechanism of nitric oxide-dependent killing of *Mycobacterium bovis* BCG in human alveolar macrophages. *Infect.Immun.* 1997;65(9):3644-7.
- [104] Molloy A, Laochumroonvorapong P, Kaplan G. Apoptosis, but not necrosis, of infected monocytes is coupled with killing of intracellular bacillus Calmette-Guerin. *J.Exp.Med.* 1994;180(4):1499-509.
- [105] Ogawa T, Uchida H, Kusumoto Y, Mori Y, Yamamura Y, Hamada S. Increase in tumor necrosis factor alpha- and interleukin-6-secreting cells in peripheral blood mononuclear cells from subjects infected with *Mycobacterium tuberculosis*. *Infect.Immun.* 1991;59(9):3021-5.
- [106] Keane J, Balcewicz-Sablinska MK, Remold HG, et al. Infection by *Mycobacterium tuberculosis* promotes human alveolar macrophage apoptosis. *Infect.Immun.* 1997;65(1):298-304.
- [107] Balcewicz-Sablinska MK, Keane J, Kornfeld H, Remold HG. Pathogenic *Mycobacterium tuberculosis* evades apoptosis of host macrophages by release of TNF-R2, resulting in inactivation of TNF-alpha. *J.Immunol.* 1998;161(5):2636-41.
- [108] Glatman-Freedman A, Casadevall A. Serum therapy for tuberculosis revisited: reappraisal of the role of antibody-mediated immunity against *Mycobacterium tuberculosis*. *Clin.Microbiol.Rev.* 1998;11(3):514-32.
- [109] Reggiardo Z, Middlebrook G. Failure of passive serum transfer of immunity against aerogenic tuberculosis in rabbits. *Proc.Soc.Exp.Biol.Med.* 1974;145(1):173-5.
- [110] Laal S, Samanich KM, Sonnenberg MG, Zolla-Pazner S, Phadtare JM, Belisle JT. Human humoral responses to antigens of *Mycobacterium tuberculosis*: immunodominance of high-molecular-mass antigens. *Clin.Diagn.Lab Immunol.* 1997;4(1):49-56.
- [111] Samanich KM, Belisle JT, Sonnenberg MG, Keen MA, Zolla-Pazner S, Laal S. Delineation of human antibody responses to culture filtrate antigens of *Mycobacterium tuberculosis*. *J.Infect.Dis.* 1998;178(5):1534-8.
- [112] Converse PJ, Dannenberg AM, Jr., Estep JE, et al. Cavitory tuberculosis produced in rabbits by aerosolized virulent tubercle bacilli. *Infect.Immun.* 1996;64(11):4776-87.
- [113] Majno G, Joris I. *Cells, tissues, and disease: principles of general pathology.* Cambridge: Blackwell Science; 1996;p. 530-2.
- [114] Rich AR, Charles IL, Thomas C, editors. *The pathogenesis of tuberculosis, 2nd edition.* Springfield; 1951;Mechanisms of acquired resistance (continued); the role of antibodies, phagocytes, lymphoid cells and acquired tissue immunity. p. 570-613.

References

- [115] Cooper NR. Gallin JI, Snyderman R, Fearon DT, Haynes BF, Nathan C, editors. *Inflammation: basic principles and clinical correlates*, 3rd edition. Philadelphia: Lippincott Williams & Wilkins; 1999; *Biology of the complement system*. p. 281-315.
- [116] Czermak BJ, Lentsch AB, Bless NM, Schmal H, Friedl HP, Ward PA. Role of complement in in vitro and in vivo lung inflammatory reactions. *J.Leukoc.Biol.* 1998;64(1):40-8.
- [117] Gosset P, Tillie-Leblond I, Oudin S, et al. Production of chemokines and proinflammatory and antiinflammatory cytokines by human alveolar macrophages activated by IgE receptors. *J.Allergy Clin.Immunol.* 1999;103(2 Pt 1):289-97.
- [118] Ying S, Barata LT, Meng Q, et al. High-affinity immunoglobulin E receptor (Fc epsilon RI)-bearing eosinophils, mast cells, macrophages and Langerhans' cells in allergen-induced late-phase cutaneous reactions in atopic subjects. *Immunology.* 1998;93(2):281-8.
- [119] Nilsson G, Costa JJ, Metcalfe DD. Gallin JI, Snyderman R, Fearon DT, Haynes BF, Nathan C, editors. *Inflammation: basic principles and clinical correlates*, 3rd edition. Philadelphia: Lippincott Williams & Wilkins; 1999; *Mast cells and basophils*. p. 97-117.
- [120] Bradding P. Human mast cell cytokines. *Clin.Exp.Allergy.* 1996;26(1):13-9.
- [121] Rumsaeng V, Cruikshank WW, Foster B, et al. Human mast cells produce the CD4+ T lymphocyte chemoattractant factor, IL-16. *J.Immunol.* 1997;159(6):2904-10.
- [122] Shigenaga T, Dannenberg AM, Lowrie DB, et al. Immune responses in tuberculosis: antibodies and CD4-CD8 lymphocytes with vascular adhesion molecules and cytokines (chemokines) cause a rapid antigen-specific cell infiltration at sites of bacillus Calmette-Guerin reinfection. *Immunology.* 2001;102(4):466-79.
- [123] Johnson CM, Cooper AM, Frank AA, Bonorino CB, Wysoki LJ, Orme IM. *Mycobacterium tuberculosis* aerogenic rechallenge infections in B cell-deficient mice. *Tuber.Lung Dis.* 1997;78(5-6):257-61.
- [124] Turner J, Frank AA, Brooks JV, Gonzalez-Juarrero M, Orme IM. The progression of chronic tuberculosis in the mouse does not require the participation of B lymphocytes or interleukin-4. *Exp.Gerontol.* 2001;36(3):537-45.
- [125] Dannenberg AM, Jr. Cellular hypersensitivity and cellular immunity in the pathogenesis of tuberculosis: specificity, systemic and local nature, and associated macrophage enzymes. *Bacteriol.Rev.* 1968;32(2):85-102.
- [126] Russell DG. *Mycobacterium tuberculosis*: here today, and here tomorrow. *Nat.Rev.Mol.Cell Biol.* 2001;2(8):569-77.
- [127] Finlay BB, Falkow S. Common themes in microbial pathogenicity revisited. *Microbiol.Mol.Biol.Rev.* 1997;61(2):136-69.
- [128] Schnappinger D, Ehrt S, Voskuil MI, et al. Transcriptional Adaptation of *Mycobacterium tuberculosis* within Macrophages: Insights into the Phagosomal Environment. *J.Exp.Med.* 2003;198(5):693-704.

- [129] Mariano M. The experimental granuloma. A hypothesis to explain the persistence of the lesion. *Rev.Inst.Med.Trop.Sao Paulo.* 1995;37(2):161-76.
- [130] Orme IM, Collins FM, Bloom BR, editors. *Tuberculosis: pathogenesis, protection and control.* Washington: American Society for Microbiology Press; 1994; Mouse model of tuberculosis. p. 113-34.
- [131] Fuller CL, Flynn JL, Reinhart TA. In situ study of abundant expression of proinflammatory chemokines and cytokines in pulmonary granulomas that develop in cynomolgus macaques experimentally infected with *Mycobacterium tuberculosis*. *Infect.Immun.* 2003;71(12):7023-34.
- [132] Dannenberg AM, Jr. Delayed-type hypersensitivity and cell-mediated immunity in the pathogenesis of tuberculosis. *Immunol.Today.* 1991;12(7):228-33.
- [133] Dannenberg AM, Jr. Immunopathogenesis of pulmonary tuberculosis. *Hosp.Pract.(Off Ed).* 1993;28(1):51-8.
- [134] Dannenberg AM, Jr., Rook GAW, Bloom BR, editors. *Tuberculosis: pathogenesis, protection, and control.* Washington: American Society for Microbiology Press; 1994; Pathogenesis of pulmonary tuberculosis: an interplay of tissue-damaging and macrophage-activating immune response – dual mechanisms that control bacillary multiplication. p. 459-83.
- [135] Adams DO. The granulomatous inflammatory response. A review. *Am.J.Pathol.* 1976;84(1):164-91.
- [136] Orme IM, Cooper AM. Cytokine/chemokine cascades in immunity to tuberculosis. *Immunol.Today.* 1999;20(7):307-12.
- [137] Tsenova L, Bergtold A, Freedman VH, Young RA, Kaplan G. Tumor necrosis factor alpha is a determinant of pathogenesis and disease progression in mycobacterial infection in the central nervous system. *Proc.Natl.Acad.Sci.U.S.A.* 1999;96(10):5657-62.
- [138] Kindler V, Sappino AP, Grau GE, Piguet PF, Vassalli P. The inducing role of tumor necrosis factor in the development of bactericidal granulomas during BCG infection. *Cell.* 1989;56(5):731-40.
- [139] Senaldi G, Yin S, Shaklee CL, Piguet PF, Mak TW, Ulich TR. *Corynebacterium parvum*- and *Mycobacterium bovis* bacillus Calmette-Guerin-induced granuloma formation is inhibited in TNF receptor I (TNF-RI) knockout mice and by treatment with soluble TNF-RI. *J.Immunol.* 1996;157(11):5022-6.
- [140] Mohan VP, Scanga CA, Yu K, et al. Effects of tumor necrosis factor alpha on host immune response in chronic persistent tuberculosis: possible role for limiting pathology. *Infect.Immun.* 2001;69(3):1847-55.
- [141] Barnes PF, Fong SJ, Brennan PJ, Twomey PE, Mazumder A, Modlin RL. Local production of tumor necrosis factor and IFN-gamma in tuberculous pleuritis. *J.Immunol.* 1990;145(1):149-54.

References

- [142] Flynn JL, Chan J. Tuberculosis: latency and reactivation. *Infect.Immun.* 2001;69(7):4195-201.
- [143] Keane J, Gershon S, Wise RP, et al. Tuberculosis associated with infliximab, a tumor necrosis factor alpha-neutralizing agent. *N.Engl.J.Med.* 2001;345(15):1098-104.
- [144] Turner J, Frank AA, Brooks JV, Marietta PM, Orme IM. Pentoxifylline treatment of mice with chronic pulmonary tuberculosis accelerates the development of destructive pathology. *Immunology.* 2001;102(2):248-53.
- [145] Dinarello CA, Novick D, Puren AJ, et al. Overview of interleukin-18: more than an interferon-gamma inducing factor. *J.Leukoc.Biol.* 1998;63(6):658-64.
- [146] O'Neill LA, Greene C. Signal transduction pathways activated by the IL-1 receptor family: ancient signaling machinery in mammals, insects, and plants. *J.Leukoc.Biol.* 1998;63(6):650-7.
- [147] Sugawara I, Yamada H, Kaneko H, Mizuno S, Takeda K, Akira S. Role of interleukin-18 (IL-18) in mycobacterial infection in IL-18-gene-disrupted mice. *Infect.Immun.* 1999;67(5):2585-9.
- [148] Abbas AK, Murphy KM, Sher A. Functional diversity of helper T lymphocytes. *Nature.* 1996;383(6603):787-93.
- [149] Fulton SA, Johnsen JM, Wolf SF, Sieburth DS, Boom WH. Interleukin-12 production by human monocytes infected with *Mycobacterium tuberculosis*: role of phagocytosis. *Infect.Immun.* 1996;64(7):2523-31.
- [150] Ladel CH, Szalay G, Riedel D, Kaufmann SH. Interleukin-12 secretion by *Mycobacterium tuberculosis*-infected macrophages. *Infect.Immun.* 1997;65(5):1936-8.
- [151] Wakeham J, Wang J, Magram J, et al. Lack of both types 1 and 2 cytokines, tissue inflammatory responses, and immune protection during pulmonary infection by *Mycobacterium bovis* bacille Calmette-Guerin in IL-12-deficient mice. *J.Immunol.* 1998;160(12):6101-11.
- [152] Wang J, Wakeham J, Harkness R, Xing Z. Macrophages are a significant source of type 1 cytokines during mycobacterial infection. *J.Clin.Invest.* 1999;103(7):1023-9.
- [153] Algood HM, Chan J, Flynn JL. Chemokines and tuberculosis. *Cytokine Growth Factor Rev.* 2003;14(6):467-77.
- [154] Romagnani P, Annunziato F, Lasagni L, et al. Cell cycle-dependent expression of CXC chemokine receptor 3 by endothelial cells mediates angiostatic activity. *J.Clin.Invest* 2001;107(1):53-63.
- [155] Canetti G. The tubercle bacillus in the pulmonary lesion of man: histobacteriology and its bearing on the therapy of pulmonary tuberculosis. New York: Springer Publishing Co.; 1955;Tuberculous lesions and immunity: nature of the tuberculous lesion. p. 145-50.
- [156] Koch R. Weitere Mitteilungen über ein Heilmittel gegen Tuberkulose. *Dtsche.Med.Wochenschr.* 1890;16:1029-32.

- [157] Ehlers S, Hölscher C. Kaufmann SH, Steward MW, editors. *Topley & Wilson's microbiology and microbial infections: immunology*. 10th ed. London: Hodder Arnold; 2005; DTH-associated pathology. p. 705-29.
- [158] Grosset J. *Mycobacterium tuberculosis* in the extracellular compartment: an underestimated adversary. *Antimicrob. Agents Chemother.* 2003;47(3):833-6.
- [159] Cosma CL, Sherman DR, Ramakrishnan L. The secret lives of the pathogenic mycobacteria. *Annu. Rev. Microbiol.* 2003;57:641-76.:641-76.
- [160] Dannenberg AM, Jr., Sugimoto M. Liquefaction of caseous foci in tuberculosis. *Am. Rev. Respir. Dis.* 1976;113(3):257-9.
- [161] Long ER. *The chemistry and chemotherapy of tuberculosis*. 3rd ed. Baltimore: Williams & Wilkins; 1958.
- [162] Long ER. From pathology to epidemiology in tuberculosis: softening of the caseous tubercle and its results. *J. Am. Med. Assoc.* 1935;104:1883-8.
- [163] Capuano SV, III, Croix DA, Pawar S, et al. Experimental *Mycobacterium tuberculosis* infection of cynomolgus macaques closely resembles the various manifestations of human *M. tuberculosis* infection. *Infect. Immun.* 2003;71(10):5831-44.
- [164] Langermans JA, Andersen P, van Soolingen D, et al. Divergent effect of bacillus Calmette-Guerin (BCG) vaccination on *Mycobacterium tuberculosis* infection in highly related macaque species: implications for primate models in tuberculosis vaccine research. *Proc. Natl. Acad. Sci. U.S.A.* 2001;98(20):11497-502.
- [165] Walsh GP, Tan EV, dela Cruz EC, et al. The Philippine cynomolgus monkey (*Macaca fascicularis*) provides a new nonhuman primate model of tuberculosis that resembles human disease. *Nat. Med.* 1996;2(4):430-6.
- [166] Smith I. *Mycobacterium tuberculosis* pathogenesis and molecular determinants of virulence. *Clin. Microbiol. Rev.* 2003;16(3):463-96.
- [167] Orme IM, McMurray DN, Rom WN, Garay S, editors. *Tuberculosis*. Boston: Little, Brown and Co.; 1996; The immune response to tuberculosis in animal models. p. 269-80.
- [168] Smith DW, Kubica GP, Wayne LG, editors. *The mycobacteria: a sourcebook*. New York: Marcel Dekker; 1984; Diseases in guinea pigs. p. 925-46.
- [169] North RJ. *Mycobacterium tuberculosis* is strikingly more virulent for mice when given via the respiratory than via the intravenous route. *J. Infect. Dis.* 1995;172(6):1550-3.
- [170] Rhoades ER, Frank AA, Orme IM. Progression of chronic pulmonary tuberculosis in mice aerogenically infected with virulent *Mycobacterium tuberculosis*. *Tuber. Lung Dis.* 1997;78(1):57-66.
- [171] Benini J, Ehlers EM, Ehlers S. Different types of pulmonary granuloma necrosis in immunocompetent vs. TNFRp55-gene-deficient mice aerogenically infected with highly virulent *Mycobacterium avium*. *J. Pathol.* 1999;189(1):127-37.

References

- [172] Ehlers S, Benini J, Held HD, Roeck C, Alber G, Uhlig S. Alphabeta T cell receptor-positive cells and interferon-gamma, but not inducible nitric oxide synthase, are critical for granuloma necrosis in a mouse model of mycobacteria-induced pulmonary immunopathology. *J.Exp.Med.* 2001;194(12):1847-59.
- [173] Taniguchi T, Ogasawara K, Takaoka A, Tanaka N. IRF family of transcription factors as regulators of host defense. *Annu.Rev.Immunol.* 2001;19:623-55.:623-55.
- [174] Remoli ME, Giacomini E, Lutfalla G, et al. Selective expression of type I IFN genes in human dendritic cells infected with *Mycobacterium tuberculosis*. *J.Immunol.* 2002;169(1):366-74.
- [175] Wayne LG, Hayes LG. Nitrate reduction as a marker for hypoxic shutdown of *Mycobacterium tuberculosis*. *Tuber.Lung Dis.* 1998;79(2):127-32.
- [176] Wayne LG, Sohaskey CD. Nonreplicating persistence of mycobacterium tuberculosis. *Annu.Rev.Microbiol.* 2001;55:139-63.:139-63.
- [177] Mitchison DA. The search for new sterilizing anti-tuberculosis drugs. *Front Biosci.* 2004;9:1059-72.:1059-72.
- [178] Hopewell PC. Using conventional and molecular epidemiological analyses to target tuberculosis control interventions in a low incidence area. *Novartis.Found.Symp.* 1998;217:42-54; discussion 54-6.:42-54.
- [179] Wayne LG, Sramek HA. Metronidazole is bactericidal to dormant cells of *Mycobacterium tuberculosis*. *Antimicrob.Agents Chemother.* 1994;38(9):2054-8.
- [180] Park HD, Guinn KM, Harrell MI, et al. Rv3133c/dosR is a transcription factor that mediates the hypoxic response of *Mycobacterium tuberculosis*. *Mol.Microbiol.* 2003;48(3):833-43.
- [181] Saini DK, Malhotra V, Dey D, Pant N, Das TK, Tyagi JS. DevR-DevS is a bona fide two-component system of *Mycobacterium tuberculosis* that is hypoxia-responsive in the absence of the DNA-binding domain of DevR. *Microbiology* 2004;150(Pt 4):865-75.
- [182] Sohaskey CD, Wayne LG. Role of narK2X and narGHJI in hypoxic upregulation of nitrate reduction by *Mycobacterium tuberculosis*. *J.Bacteriol.* 2003;185(24):7247-56.
- [183] Johnson CM, Pandey R, Sharma S, et al. Oral therapy using nanoparticle-encapsulated antituberculosis drugs in guinea pigs infected with *Mycobacterium tuberculosis*. *Antimicrob.Agents Chemother.* 2005;49(10):4335-8.
- [184] Bohle A, Brandau S. Immune mechanisms in bacillus Calmette-Guerin immunotherapy for superficial bladder cancer. *J.Urol.* 2003;170(3):964-9.
- [185] Kuhn A, Brachtendorf G, Kurth F, et al. Expression of endomucin, a novel endothelial sialomucin, in normal and diseased human skin. *J.Invest Dermatol.* 2002;119(6):1388-93.

- [186] Muller K, Ehlers S, Solbach W, Laskay T. Novel multi-probe RNase protection assay (RPA) sets for the detection of murine chemokine gene expression. *J.Immunol.Methods* 2001;249(1-2):155-65.
- [187] Irizarry RA; Gautier L; Bolstad BM. *affy: Methods for Affymetrix Oligonucleotide Arrays*, R package version 1.6.7. 2005.
- [188] Benjamini Y, Hochberg Y. Controlling the false discovery rate: a practical and powerful approach to multiple testing. *Journal of the Royal Statistical Society B* 1995;57:289-300.
- [189] R Development Core Team. *R: A language and environment for statistical computing*. Vienna: R Foundation for Statistical Computing; 2005.
- [190] Losana G, Rigamonti L, Borghi I, et al. Requirement for both IL-12 and IFN-gamma signaling pathways in optimal IFN-gamma production by human T cells. *Eur.J.Immunol.* 2002;32(3):693-700.
- [191] Flynn JL, Chan J. What's good for the host is good for the bug. *Trends Microbiol.* 2005;13(3):98-102.
- [192] Silverman RH, Cirino NM. Morris DR, Hartford JB, editors. *Gene regulation*. New York: John Wiley & Sons; 1997;p. 295-309.
- [193] Ghosh A, Sarkar SN, Rowe TM, Sen GC. A specific isozyme of 2'-5' oligoadenylate synthetase is a dual function proapoptotic protein of the Bcl-2 family. *J.Biol.Chem.* 2001;276(27):25447-55.
- [194] Hersh D, Monack DM, Smith MR, Ghori N, Falkow S, Zychlinsky A. The Salmonella invasin SipB induces macrophage apoptosis by binding to caspase-1. *Proc.Natl.Acad.Sci.U.S.A.* 1999;96(5):2396-401.
- [195] Chen Y, Smith MR, Thirumalai K, Zychlinsky A. A bacterial invasin induces macrophage apoptosis by binding directly to ICE. *EMBO J.* 1996;15(15):3853-60.
- [196] Hilbi H, Moss JE, Hersh D, et al. Shigella-induced apoptosis is dependent on caspase-1 which binds to IpaB. *J.Biol.Chem.* 1998;273(49):32895-900.
- [197] Danelishvili L, McGarvey J, Li YJ, Bermudez LE. Mycobacterium tuberculosis infection causes different levels of apoptosis and necrosis in human macrophages and alveolar epithelial cells. *Cell Microbiol.* 2003;5(9):649-60.
- [198] Shimizu S, Eguchi Y, Kamiike W, Matsuda H, Tsujimoto Y. Bcl-2 expression prevents activation of the ICE protease cascade. *Oncogene.* 1996;12(11):2251-7.
- [199] Renvoize C, Roger R, Moulian N, Bertoglio J, Breard J. Bcl-2 expression in target cells leads to functional inhibition of caspase-3 protease family in human NK and lymphokine-activated killer cell granule-mediated apoptosis. *J.Immunol.* 1997;159(1):126-34.
- [200] Zhang X, Sun S, Hwang I, Tough DF, Sprent J. Potent and selective stimulation of memory-phenotype CD8+ T cells in vivo by IL-15. *Immunity.* 1998;8(5):591-9.

References

- [201] Liu CC, Perussia B, Young JD. The emerging role of IL-15 in NK-cell development. *Immunol.Today.* 2000;21(3):113-6.
- [202] Fehniger TA, Suzuki K, Ponnappan A, et al. Fatal leukemia in interleukin 15 transgenic mice follows early expansions in natural killer and memory phenotype CD8+ T cells. *J.Exp.Med.* 2001;193(2):219-31.
- [203] Li XC, Demirci G, Ferrari-Lacraz S, et al. IL-15 and IL-2: a matter of life and death for T cells in vivo. *Nat.Med.* 2001;7(1):114-8.
- [204] Sprent J, Surh CD. Generation and maintenance of memory T cells. *Curr.Opin.Immunol.* 2001;13(2):248-54.
- [205] Chapdelaine Y, Smith DK, Pedras-Vasconcelos JA, Krishnan L, Sad S. Increased CD8+ T cell memory to concurrent infection at the expense of increased erosion of pre-existing memory: the paradoxical role of IL-15. *J.Immunol.* 2003;171(10):5454-60.
- [206] Saito K, Yajima T, Kumabe S, et al. Impaired Protection against *Mycobacterium bovis* Bacillus Calmette-Guerin Infection in IL-15-Deficient Mice. *J.Immunol.* 2006;176(4):2496-504.
- [207] Umemura M, Nishimura H, Saito K, et al. Interleukin-15 as an immune adjuvant to increase the efficacy of *Mycobacterium bovis* bacillus Calmette-Guerin vaccination. *Infect.Immun.* 2003;71(10):6045-8.
- [208] Maeurer MJ, Trinder P, Hommel G, et al. Interleukin-7 or interleukin-15 enhances survival of *Mycobacterium tuberculosis*-infected mice. *Infect.Immun.* 2000;68(5):2962-70.
- [209] Rausch,A. Die Bedeutung von Interleukin-15 für die zellvermittelte Immunantwort nach der Infektion mit *Mycobacterium tuberculosis* 2004; Universität zu Lübeck.
- [210] Munder M, Mallo M, Eichmann K, Modolell M. Murine macrophages secrete interferon gamma upon combined stimulation with interleukin (IL)-12 and IL-18: A novel pathway of autocrine macrophage activation. *J.Exp.Med.* 1998;187(12):2103-8.
- [211] Okamura H, Tsutsi H, Komatsu T, et al. Cloning of a new cytokine that induces IFN-gamma production by T cells. *Nature.* 1995;378(6552):88-91.
- [212] Ghayur T, Banerjee S, Hugunin M, et al. Caspase-1 processes IFN-gamma-inducing factor and regulates LPS-induced IFN-gamma production. *Nature.* 1997;386(6625):619-23.
- [213] Gu Y, Kuida K, Tsutsui H, et al. Activation of interferon-gamma inducing factor mediated by interleukin-1beta converting enzyme. *Science.* 1997;275(5297):206-9.
- [214] Vankayalapati R, Wizel B, Lakey DL, et al. T cells enhance production of IL-18 by monocytes in response to an intracellular pathogen. *J.Immunol.* 2001;166(11):6749-53.
- [215] Okamoto I, Kohno K, Tanimoto T, Ikegami H, Kurimoto M. Development of CD8+ effector T cells is differentially regulated by IL-18 and IL-12. *J.Immunol.* 1999;162(6):3202-11.

- [216] Fehniger TA, Shah MH, Turner MJ, et al. Differential cytokine and chemokine gene expression by human NK cells following activation with IL-18 or IL-15 in combination with IL-12: implications for the innate immune response. *J.Immunol.* 1999;162(8):4511-20.
- [217] Fantuzzi G, Reed DA, Dinarello CA. IL-12-induced IFN-gamma is dependent on caspase-1 processing of the IL-18 precursor. *J.Clin.Invest.* 1999;104(6):761-7.
- [218] Takeda K, Tsutsui H, Yoshimoto T, et al. Defective NK cell activity and Th1 response in IL-18-deficient mice. *Immunity.* 1998;8(3):383-90.
- [219] Yoshimoto T, Takeda K, Tanaka T, et al. IL-12 up-regulates IL-18 receptor expression on T cells, Th1 cells, and B cells: synergism with IL-18 for IFN-gamma production. *J.Immunol.* 1998;161(7):3400-7.
- [220] Yamada G, Shijubo N, Shigehara K, Okamura H, Kurimoto M, Abe S. Increased levels of circulating interleukin-18 in patients with advanced tuberculosis. *Am.J.Respir.Crit Care Med.* 2000;161(6):1786-9.
- [221] Fujiuchi S, Matsumoto H, Yamazaki Y, et al. Impaired interleukin-1beta converting enzyme (ICE) activity in patients with pulmonary tuberculosis. *Int.J.Tuberc.Lung Dis.* 2003;7(11):1109-12.
- [222] Shigehara K, Shijubo N, Ohmichi M, et al. IL-12 and IL-18 are increased and stimulate IFN-gamma production in sarcoid lungs. *J.Immunol.* 2001;166(1):642-9.
- [223] Pizarro TT, Michie MH, Bentz M, et al. IL-18, a novel immunoregulatory cytokine, is up-regulated in Crohn's disease: expression and localization in intestinal mucosal cells. *J.Immunol.* 1999;162(11):6829-35.
- [224] Demetri GD, Griffin JD. Granulocyte colony-stimulating factor and its receptor. *Blood.* 1991;78(11):2791-808.
- [225] Appelberg R, Castro AG, Gomes S, Pedrosa J, Silva MT. Susceptibility of beige mice to *Mycobacterium avium*: role of neutrophils. *Infect.Immun.* 1995;63(9):3381-7.
- [226] Bermudez LE, Petrofsky M, Stevens P. Treatment with recombinant granulocyte colony-stimulating factor (Filgrastin) stimulates neutrophils and tissue macrophages and induces an effective non-specific response against *Mycobacterium avium* in mice. *Immunology.* 1998;94(3):297-303.
- [227] Denis M, Ghadirian E. IL-10 neutralization augments mouse resistance to systemic *Mycobacterium avium* infections. *J.Immunol.* 1993;151(10):5425-30.
- [228] Bermudez LE, Young LS. Tumor necrosis factor, alone or in combination with IL-2, but not IFN-gamma, is associated with macrophage killing of *Mycobacterium avium* complex. *J.Immunol.* 1988;140(9):3006-13.
- [229] Kobayashi K, Yamazaki J, Kasama T, et al. Interleukin (IL)-12 deficiency in susceptible mice infected with *Mycobacterium avium* and amelioration of established infection by IL-12 replacement therapy. *J.Infect.Dis.* 1996;174(3):564-73.

References

- [230] Bermudez LE, Wu M, Young LS. Interleukin-12-stimulated natural killer cells can activate human macrophages to inhibit growth of *Mycobacterium avium*. *Infect.Immun.* 1995;63(10):4099-104.
- [231] Denis M, Ghadirian E. Interleukin-1 is involved in mouse resistance to *Mycobacterium avium*. *Infect.Immun.* 1994;62(2):457-61.
- [232] Bermudez LE, Stevens P, Kolonoski P, Wu M, Young LS. Treatment of experimental disseminated *Mycobacterium avium* complex infection in mice with recombinant IL-2 and tumor necrosis factor. *J.Immunol.* 1989;143(9):2996-3000.
- [233] Cooper AM, Dalton DK, Stewart TA, Griffin JP, Russell DG, Orme IM. Disseminated tuberculosis in interferon gamma gene-disrupted mice. *J.Exp.Med.* 1993;178(6):2243-7.
- [234] Florido M, Pearl JE, Solache A, et al. Gamma interferon-induced T-cell loss in virulent *Mycobacterium avium* infection. *Infect.Immun.* 2005;73(6):3577-86.
- [235] Kamijo R, Harada H, Matsuyama T, et al. Requirement for transcription factor IRF-1 in NO synthase induction in macrophages. *Science.* 1994;263(5153):1612-5.
- [236] Martin E, Nathan C, Xie QW. Role of interferon regulatory factor 1 in induction of nitric oxide synthase. *J.Exp.Med.* 1994;180(3):977-84.
- [237] Melillo G, Musso T, Sica A, Taylor LS, Cox GW, Varesio L. A hypoxia-responsive element mediates a novel pathway of activation of the inducible nitric oxide synthase promoter. *J.Exp.Med.* 1995;182(6):1683-93.
- [238] Melillo G, Taylor LS, Brooks A, Musso T, Cox GW, Varesio L. Functional requirement of the hypoxia-responsive element in the activation of the inducible nitric oxide synthase promoter by the iron chelator desferrioxamine. *J.Biol.Chem.* 1997;272(18):12236-43.
- [239] Melillo G, Taylor LS, Brooks A, Cox GW, Varesio L. Regulation of inducible nitric oxide synthase expression in IFN-gamma-treated murine macrophages cultured under hypoxic conditions. *J.Immunol.* 1996;157(6):2638-44.
- [240] Tandler DS, Bao C, Wang T, et al. Intersection of interferon and hypoxia signal transduction pathways in nitric oxide-induced tumor apoptosis. *Cancer Res.* 2001;61(9):3682-8.
- [241] Perry LL, Feilzer K, Portis JL, Caldwell HD. Distinct homing pathways direct T lymphocytes to the genital and intestinal mucosae in *Chlamydia*-infected mice. *J.Immunol.* 1998;160(6):2905-14.
- [242] Picker LJ, Martin RJ, Trumble A, et al. Differential expression of lymphocyte homing receptors by human memory/effector T cells in pulmonary versus cutaneous immune effector sites. *Eur.J.Immunol.* 1994;24(6):1269-77.
- [243] Engelhardt B, Conley FK, Kilshaw PJ, Butcher EC. Lymphocytes infiltrating the CNS during inflammation display a distinctive phenotype and bind to VCAM-1 but not to MAdCAM-1. *Int.Immunol.* 1995;7(3):481-91.

- [244] Salmi M, Jalkanen S. How do lymphocytes know where to go: current concepts and enigmas of lymphocyte homing. *Adv.Immunol.* 1997;64:139-218.:139-218.
- [245] Feng CG, Britton WJ, Palendira U, Groat NL, Briscoe H, Bean AG. Up-regulation of VCAM-1 and differential expansion of beta integrin-expressing T lymphocytes are associated with immunity to pulmonary *Mycobacterium tuberculosis* infection. *J.Immunol.* 2000;164(9):4853-60.
- [246] Fan L, Reilly CR, Luo Y, Dorf ME, Lo D. Cutting edge: ectopic expression of the chemokine TCA4/SLC is sufficient to trigger lymphoid neogenesis. *J.Immunol.* 2000;164(8):3955-9.
- [247] Ebert LM, Schaerli P, Moser B. Chemokine-mediated control of T cell traffic in lymphoid and peripheral tissues. *Mol.Immunol.* 2005;42(7):799-809.
- [248] Schreiber T, Ehlers S, Aly S, et al. Selectin ligand-independent priming and maintenance of T cell immunity during airborne tuberculosis. *J.Immunol.* 2006;176(2):1131-40.
- [249] Ulrichs T, Kosmiadi GA, Trusov V, et al. Human tuberculous granulomas induce peripheral lymphoid follicle-like structures to orchestrate local host defence in the lung. *J.Pathol.* 2004;204(2):217-28.
- [250] Ogasawara K, Hida S, Weng Y, et al. Requirement of the IFN-alpha/beta-induced CXCR3 chemokine signalling for CD8+ T cell activation. *Genes Cells.* 2002;7(3):309-20.
- [251] Sallusto F, Mackay CR, Lanzavecchia A. The role of chemokine receptors in primary, effector, and memory immune responses. *Annu.Rev.Immunol.* 2000;18:593-620.:593-620.
- [252] Luster AD, Greenberg SM, Leder P. The IP-10 chemokine binds to a specific cell surface heparan sulfate site shared with platelet factor 4 and inhibits endothelial cell proliferation. *J.Exp.Med.* 1995;182(1):219-31.
- [253] Strieter RM, Polverini PJ, Kunkel SL, et al. The functional role of the ELR motif in CXC chemokine-mediated angiogenesis. *J.Biol.Chem.* 1995;270(45):27348-57.
- [254] Arenberg DA, Polverini PJ, Kunkel SL, et al. The role of CXC chemokines in the regulation of angiogenesis in non-small cell lung cancer. *J.Leukoc.Biol.* 1997;62(5):554-62.
- [255] Coley WB. A Preliminary Note on the Treatment of Inoperable Sarcoma by the Toxic Product of Erysipelas. *Post-graduate* 1893;8:278-86.
- [256] Hibbs JB, Jr. Role of activated macrophages in nonspecific resistance to neoplasia. *J.Reticuloendothel.Soc.* 1976;20(3):223-31.
- [257] Hunter CA, Yu D, Gee M, et al. Cutting edge: systemic inhibition of angiogenesis underlies resistance to tumors during acute toxoplasmosis. *J.Immunol.* 2001;166(10):5878-81.

References

- [258] Algire GH, Legallais FY, Park HD. Vascular reactions of normal and malignant tissues in vivo. II. The vascular reaction of normal and neoplastic tissues of mice to a bacterial polysaccharide from *Serratia marcescens* (*Bacillus prodigiosus*) culture filtrates. *J.Natl.Cancer Inst.* 1947;8:53-62.
- [259] Loetscher M, Gerber B, Loetscher P, et al. Chemokine receptor specific for IP10 and mig: structure, function, and expression in activated T-lymphocytes. *J.Exp.Med.* 1996;184(3):963-9.
- [260] Bonecchi R, Bianchi G, Bordignon PP, et al. Differential expression of chemokine receptors and chemotactic responsiveness of type 1 T helper cells (Th1s) and Th2s. *J.Exp.Med.* 1998;187(1):129-34.
- [261] Qin S, Rottman JB, Myers P, et al. The chemokine receptors CXCR3 and CCR5 mark subsets of T cells associated with certain inflammatory reactions. *J.Clin.Invest.* 1998;101(4):746-54.
- [262] Voskuil MI, Schnappinger D, Visconti KC, et al. Inhibition of respiration by nitric oxide induces a *Mycobacterium tuberculosis* dormancy program. *J.Exp.Med.* 2003;198(5):705-13.
- [263] Brunori M, Giuffre A, Forte E, Mastronicola D, Barone MC, Sarti P. Control of cytochrome c oxidase activity by nitric oxide. *Biochim.Biophys.Acta.* 2004;1655(1-3):365-71.
- [264] Shiva S, Darley-Usmar VM. Control of the nitric oxide-cytochrome c oxidase signaling pathway under pathological and physiological conditions. *IUBMB.Life.* 2003;55(10-11):585-90.
- [265] Wayne LG, Hayes LG. An in vitro model for sequential study of shutdown of *Mycobacterium tuberculosis* through two stages of nonreplicating persistence. *Infect.Immun.* 1996;64(6):2062-9.
- [266] Voskuil MI, Visconti KC, Schoolnik GK. *Mycobacterium tuberculosis* gene expression during adaptation to stationary phase and low-oxygen dormancy. *Tuberculosis.(Edinb.).* 2004;84(3-4):218-27.
- [267] Munoz-Elias EJ, Timm J, Botha T, Chan WT, Gomez JE, McKinney JD. Replication dynamics of *Mycobacterium tuberculosis* in chronically infected mice. *Infect.Immun.* 2005;73(1):546-51.
- [268] Sever JL, Youmans GP. Enumeration of viable tubercle bacilli from the organs of nonimmunized and immunized mice. *Am.Rev.Tuberc.* 1957;76(4):616-35.
- [269] Orme IM. A mouse model of the recrudescence of latent tuberculosis in the elderly. *Am.Rev.Respir.Dis.* 1988;137(3):716-8.
- [270] Sever JL, Youmans GP. The relation of oxygen tension to virulence of tubercle bacilli and to acquired resistance in tuberculosis. *J.Infect.Dis.* 1957;101(2):193-202.
- [271] Condos R, Rom WN. Rom WN, Garay SM, editors. *Tuberculosis*. Philadelphia: Lippincott Williams & Wilkins; 2004;p. 285-99.

- [272] Daley CL, Rom WN, Garay SM, editors. *Tuberculosis*. Philadelphia: Lippincott Williams & Wilkins; 2004;p. 85-99.
- [273] Yuan Y, Crane DD, Barry CE, III. Stationary phase-associated protein expression in *Mycobacterium tuberculosis*: function of the mycobacterial alpha-crystallin homolog. *J.Bacteriol.* 1996;178(15):4484-92.
- [274] Wayne LG. Dormancy of *Mycobacterium tuberculosis* and latency of disease. *Eur.J.Clin.Microbiol.Infect.Dis.* 1994;13(11):908-14.
- [275] Garbe TR, Hibler NS, Deretic V. Response to reactive nitrogen intermediates in *Mycobacterium tuberculosis*: induction of the 16-kilodalton alpha-crystallin homolog by exposure to nitric oxide donors. *Infect.Immun.* 1999;67(1):460-5.
- [276] Raffel S, Wolstenholme GEW, Cameron MP, O'Connor CM, editors. *Ciba Foundation Symposium on Experimental Tuberculosis: bacillus and host*. Boston: Little Brown and Co.; 1955;The mechanism involved in acquired immunity to tuberculosis. p. 261-78.
- [277] Yuan Y, Crane DD, Simpson RM, et al. The 16-kDa alpha-crystallin (Acr) protein of *Mycobacterium tuberculosis* is required for growth in macrophages. *Proc.Natl.Acad.Sci.U.S.A.* 1998;95(16):9578-83.
- [278] Stewart JN, Rivera HN, Karls R, Quinn FD, Roman J, Rivera-Marrero CA. Increased pathology in lungs of mice after infection with an alpha-crystallin mutant of *Mycobacterium tuberculosis*: changes in cathepsin proteases and certain cytokines. *Microbiology.* 2006;152(Pt 1):233-44.
- [279] Timm J, Post FA, Bekker LG, et al. Differential expression of iron-, carbon-, and oxygen-responsive mycobacterial genes in the lungs of chronically infected mice and tuberculosis patients. *Proc.Natl.Acad.Sci.U.S.A.* 2003;100(24):14321-6.
- [280] McKinney JD, Honer zu BK, Munoz-Elias EJ, et al. Persistence of *Mycobacterium tuberculosis* in macrophages and mice requires the glyoxylate shunt enzyme isocitrate lyase. *Nature.* 2000;406(6797):735-8.
- [281] Wayne LG, Lin KY. Glyoxylate metabolism and adaptation of *Mycobacterium tuberculosis* to survival under anaerobic conditions. *Infect.Immun.* 1982;37(3):1042-9.
- [282] Dubnau E, Fontan P, Manganelli R, Soares-Appel S, Smith I. *Mycobacterium tuberculosis* genes induced during infection of human macrophages. *Infect.Immun.* 2002;70(6):2787-95.
- [283] Graham JE, Clark-Curtiss JE. Identification of *Mycobacterium tuberculosis* RNAs synthesized in response to phagocytosis by human macrophages by selective capture of transcribed sequences (SCOTS). *Proc.Natl.Acad.Sci.U.S.A.* 1999;96(20):11554-9.
- [284] Shi L, Jung YJ, Tyagi S, Gennaro ML, North RJ. Expression of Th1-mediated immunity in mouse lungs induces a *Mycobacterium tuberculosis* transcription pattern characteristic of nonreplicating persistence. *Proc.Natl.Acad.Sci.U.S.A.* 2003;100(1):241-6.

References

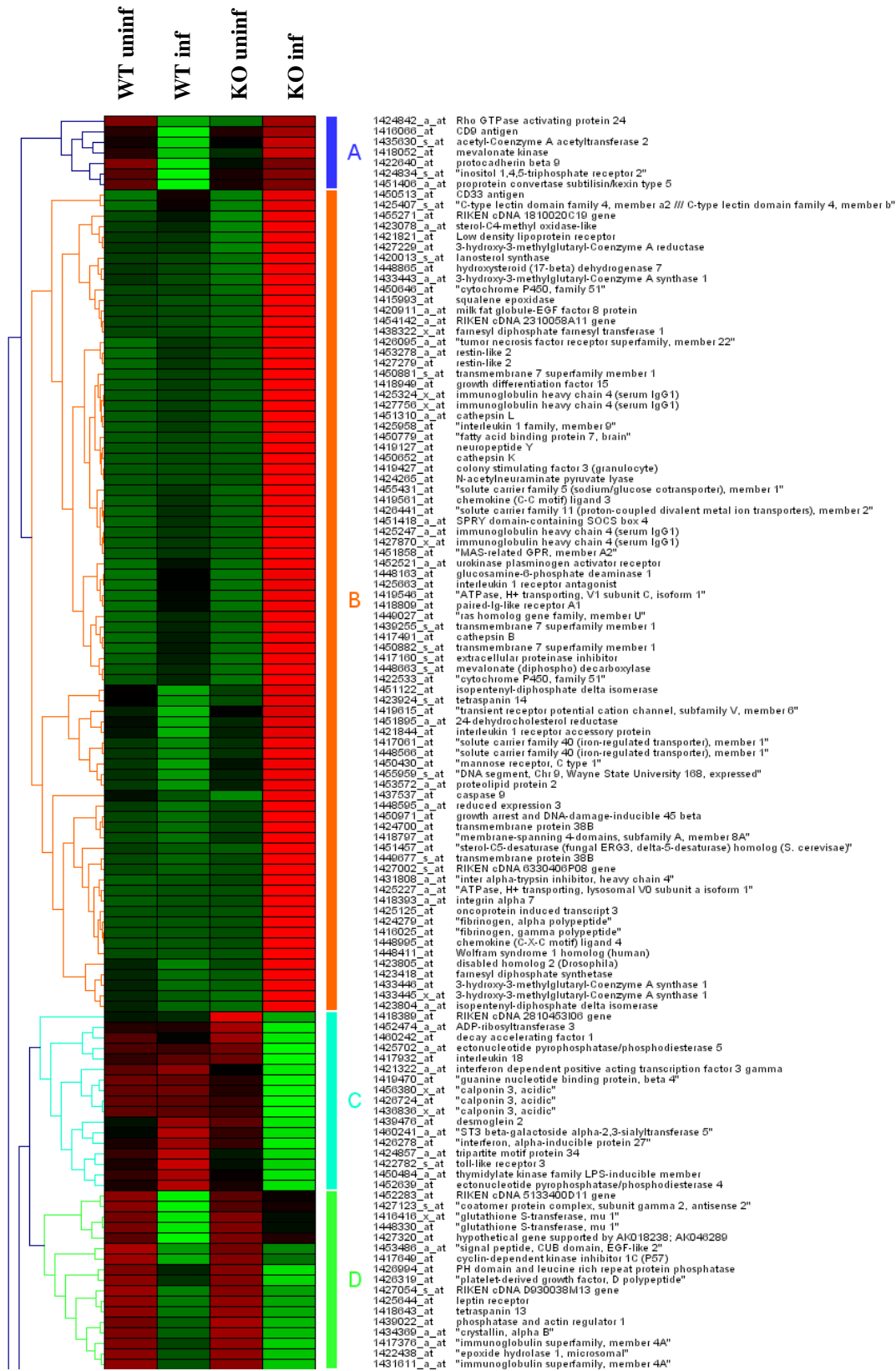
- [285] Glickman MS, Cox JS, Jacobs WR, Jr. A novel mycolic acid cyclopropane synthetase is required for cording, persistence, and virulence of *Mycobacterium tuberculosis*. *Mol.Cell.* 2000;5(4):717-27.
- [286] Goldman DS, Wagner MJ. Enzyme systems in the mycobacteria. XIII. Glycine dehydrogenase and the glyoxylic acid cycle. *Biochim.Biophys.Acta.* 1962;65:297-306.:297-306.
- [287] Shi L, Sohaskey CD, Kana BD, et al. Changes in energy metabolism of *Mycobacterium tuberculosis* in mouse lung and under in vitro conditions affecting aerobic respiration. *Proc.Natl.Acad.Sci.U.S.A.* 2005;102(43):15629-34.
- [288] Boockvar KS, Granger DL, Poston RM, et al. Nitric oxide produced during murine listeriosis is protective. *Infect.Immun.* 1994;62(3):1089-100.
- [289] Flesch IE, Kaufmann SH. Mechanisms involved in mycobacterial growth inhibition by gamma interferon-activated bone marrow macrophages: role of reactive nitrogen intermediates. *Infect.Immun.* 1991;59(9):3213-8.
- [290] Weber I, Fritz C, Ruttkowski S, Kreft A, Bange FC. Anaerobic nitrate reductase (narGHJI) activity of *Mycobacterium bovis* BCG in vitro and its contribution to virulence in immunodeficient mice. *Mol.Microbiol.* 2000;35(5):1017-25.
- [291] Boshoff HI, Barry CE, III. Tuberculosis - metabolism and respiration in the absence of growth. *Nat.Rev.Microbiol.* 2005;3(1):70-80.
- [292] Aly S, Wagner K, Keller C, et al. Granulomatous lesions in the lungs of mice chronically infected with *Mycobacterium tuberculosis* are not severely hypoxic. submitted for publication 2006.
- [293] Parish T, Smith DA, Kendall S, Casali N, Bancroft GJ, Stoker NG. Deletion of two-component regulatory systems increases the virulence of *Mycobacterium tuberculosis*. *Infect.Immun.* 2003;71(3):1134-40.
- [294] Knighton DR, Halliday B, Hunt TK. Oxygen as an antibiotic. The effect of inspired oxygen on infection. *Arch.Surg.* 1984;119(2):199-204.
- [295] Knighton DR, Halliday B, Hunt TK. Oxygen as an antibiotic. A comparison of the effects of inspired oxygen concentration and antibiotic administration on in vivo bacterial clearance. *Arch.Surg.* 1986;121(2):191-5.
- [296] Ema M, Taya S, Yokotani N, Sogawa K, Matsuda Y, Fujii-Kuriyama Y. A novel bHLH-PAS factor with close sequence similarity to hypoxia-inducible factor 1alpha regulates the VEGF expression and is potentially involved in lung and vascular development. *Proc.Natl.Acad.Sci.U.S.A.* 1997;94(9):4273-8.
- [297] Tian H, McKnight SL, Russell DW. Endothelial PAS domain protein 1 (EPAS1), a transcription factor selectively expressed in endothelial cells. *Genes Dev.* 1997;11(1):72-82.
- [298] Karhausen J, Haase VH, Colgan SP. Inflammatory hypoxia: role of hypoxia-inducible factor. *Cell Cycle.* 2005;4(2):256-8.

- [299] Maxwell PH, Wiesener MS, Chang GW, et al. The tumour suppressor protein VHL targets hypoxia-inducible factors for oxygen-dependent proteolysis. *Nature*. 1999;399(6733):271-5.
- [300] Jaakkola P, Mole DR, Tian YM, et al. Targeting of HIF-alpha to the von Hippel-Lindau ubiquitylation complex by O₂-regulated prolyl hydroxylation. *Science*. 2001;292(5516):468-72.
- [301] Ivan M, Kondo K, Yang H, et al. HIFalpha targeted for VHL-mediated destruction by proline hydroxylation: implications for O₂ sensing. *Science*. 2001;292(5516):464-8.
- [302] Cockman ME, Masson N, Mole DR, et al. Hypoxia inducible factor-alpha binding and ubiquitylation by the von Hippel-Lindau tumor suppressor protein. *J.Biol.Chem*. 2000;275(33):25733-41.
- [303] Bruick RK, McKnight SL. A conserved family of prolyl-4-hydroxylases that modify HIF. *Science*. 2001;294(5545):1337-40.
- [304] Epstein AC, Gleadle JM, McNeill LA, et al. *C. elegans* EGL-9 and mammalian homologs define a family of dioxygenases that regulate HIF by prolyl hydroxylation. *Cell*. 2001;107(1):43-54.
- [305] Jeong JW, Bae MK, Ahn MY, et al. Regulation and destabilization of HIF-1alpha by ARD1-mediated acetylation. *Cell*. 2002;111(5):709-20.
- [306] Wang GL, Jiang BH, Rue EA, Semenza GL. Hypoxia-inducible factor 1 is a basic-helix-loop-helix-PAS heterodimer regulated by cellular O₂ tension. *Proc.Natl.Acad.Sci.U.S.A.* 1995;92(12):5510-4.
- [307] Madjdpour C, Jewell UR, Kneller S, et al. Decreased alveolar oxygen induces lung inflammation. *Am.J.Physiol Lung Cell Mol.Physiol*. 2003;284(2):L360-L367
- [308] Arteel GE, Thurman RG, Raleigh JA. Reductive metabolism of the hypoxia marker pimonidazole is regulated by oxygen tension independent of the pyridine nucleotide redox state. *Eur.J.Biochem*. 1998;253(3):743-50.
- [309] Arteel GE, Thurman RG, Yates JM, Raleigh JA. Evidence that hypoxia markers detect oxygen gradients in liver: pimonidazole and retrograde perfusion of rat liver. *Br.J.Cancer*. 1995;72(4):889-95.
- [310] Raleigh JA, La Dine JK, Cline JM, Thrall DE. An enzyme-linked immunosorbent assay for hypoxia marker binding in tumours. *Br.J.Cancer*. 1994;69(1):66-71.
- [311] Malhotra V, Sharma D, Ramanathan VD, et al. Disruption of response regulator gene, devR, leads to attenuation in virulence of *Mycobacterium tuberculosis*. *FEMS Microbiol.Lett*. 2004;231(2):237-45.
- [312] El Sadr WM, Perlman DC, Denning E, Matts JP, Cohn DL. A review of efficacy studies of 6-month short-course therapy for tuberculosis among patients infected with human immunodeficiency virus: differences in study outcomes. *Clin.Infect.Dis*. 2001;32(4):623-32.

References

- [313] McKinney JD. In vivo veritas: the search for TB drug targets goes live. *Nat.Med.* 2000;6(12):1330-3.
- [314] Stewart GR, Robertson BD, Young DB. Tuberculosis: a problem with persistence. *Nat.Rev.Microbiol.* 2003;1(2):97-105.
- [315] Harshey RM, Ramakrishnan T. Purification and properties of DNA-dependent RNA polymerase from *Mycobacterium tuberculosis* H37RV. *Biochim.Biophys.Acta.* 1976;432(1):49-59.
- [316] Grosset J, Truffot C, Fermanian J, Lecoer H. [Sterilizing activity of the main drugs on the mouse experimental tuberculosis (author's transl)]. *Pathol.Biol.(Paris).* 1982;30(6):444-8.
- [317] Takayama K, Armstrong EL, David HL. Restoration of mycolate synthetase activity in *Mycobacterium tuberculosis* exposed to isoniazid. *Am.Rev.Respir.Dis.* 1974;110(1):43-8.
- [318] Lenaerts AJ, Gruppo V, Marietta KS, et al. Preclinical testing of the nitroimidazopyran PA-824 for activity against *Mycobacterium tuberculosis* in a series of in vitro and in vivo models. *Antimicrob.Agents Chemother.* 2005;49(6):2294-301.
- [319] Brooks JV, Furney SK, Orme IM. Metronidazole therapy in mice infected with tuberculosis. *Antimicrob.Agents Chemother.* 1999;43(5):1285-8.
- [320] Mitchison DA, Coates AR. Predictive in vitro models of the sterilizing activity of anti-tuberculosis drugs. *Curr.Pharm.Des.* 2004;10(26):3285-95.
- [321] Schroeder EK, de Souza N, Santos DS, Blanchard JS, Basso LA. Drugs that inhibit mycolic acid biosynthesis in *Mycobacterium tuberculosis*. *Curr.Pharm.Biotechnol.* 2002;3(3):197-225.
- [322] Scior T, Meneses M, I, Garces Eisele SJ, Domeyer D, Laufer S. Antitubercular isoniazid and drug resistance of *Mycobacterium tuberculosis*--a review. *Arch.Pharm.(Weinheim).* 2002;335(11-12):511-25.

Appendix 1





Appendices

Gene Title	Gene Symbol	FC wt/ko	FC wt	FC ko
---	---	2.5	2.6	1.0
---	---	5.5	6.8	1.2
---	---	4.3	8.6	2.0
---	---	2.3	2.5	1.0
2'-5' oligoadenylate synthetase 3	Oas3	3.4	9.4	2.7
2'-5' oligoadenylate synthetase-like 1	Oas1	7.0	7.3	1.0
2'-5' oligoadenylate synthetase-like 2	Oas2	9.6	5.0	-1.9
24-dehydrocholesterol reductase	Dhcr24	0.3	-2.1	1.9
3-hydroxy-3-methylglutaryl-Coenzyme A reductase	Hmgcr	0.3	-1.0	3.1
3-hydroxy-3-methylglutaryl-Coenzyme A synthase 1	Hmgcs1	0.3	-1.3	2.4
3-hydroxy-3-methylglutaryl-Coenzyme A synthase 1	Hmgcs1	0.4	-1.2	2.2
3-hydroxy-3-methylglutaryl-Coenzyme A synthase 1	Hmgcs1	0.4	-1.1	2.5
acetyl-Coenzyme A acetyltransferase 2	Acat2	0.4	-1.9	1.4
Acyl-CoA synthetase long-chain family member 1	Acs1	4.7	4.5	-1.0
acyl-CoA synthetase long-chain family member 1	Acs1	9.0	8.7	-1.0
acyl-CoA synthetase long-chain family member 1	Acs1	7.3	6.9	-1.1
ADP-ribosyltransferase 3	Art3	6.2	-1.0	-6.3
allograft inflammatory factor 1	Aif1	14.5	24.5	1.7
ankyrin repeat and SOCS box-containing protein 11	Asb11	7.2	6.3	-1.1
ATPase, H+ transporting, lysosomal V0 subunit a isoform 1	Atp6v0a1	0.3	1.0	3.0
ATPase, H+ transporting, V1 subunit C, isoform 1	Atp6v1c1	0.5	1.7	3.5
AXL receptor tyrosine kinase	Axl	3.1	1.7	-1.8
calponin 3, acidic	Cnn3	2.6	-1.0	-2.6
calponin 3, acidic	Cnn3	2.3	1.0	-2.3
calponin 3, acidic	Cnn3	2.2	-1.0	-2.2
caspase 1	Casp1	2.9	10.6	3.7
caspase 12	Casp12	3.0	2.1	-1.5
caspase 12	Casp12	3.4	2.2	-1.6
caspase 7	Casp7	3.3	2.6	-1.2
caspase 9	Casp9	0.5	-1.1	1.8
cathepsin B	Ctsb	0.4	1.7	4.0
cathepsin K	Ctsk	0.1	2.3	27.0
cathepsin L	Ctsl	0.5	1.1	2.4
CD1d1 antigen	Cd1d1	6.9	8.1	1.2
CD1d1 antigen	Cd1d1	6.0	6.3	1.0
CD33 antigen	Cd33	0.3	5.5	16.4
CD72 antigen	Cd72	4.3	7.6	1.8
CD86 antigen	Cd86	4.2	8.5	2.0
CD9 antigen	Cd9	0.5	-1.8	1.2
CDNA clone MGC:6071 IMAGE:3492410, complete cds	---	2.8	3.0	1.1
cDNA sequence BC010462	BC010462	4.2	5.6	1.3
cDNA sequence BC023105	BC023105	5.5	6.5	1.2
chemokine (C-C motif) ligand 19	Ccl19	8.5	8.9	1.0
chemokine (C-C motif) ligand 3	Ccl3	0.1	22.8	207.5
chemokine (C-X3-C) receptor 1	Cx3cr1	2.5	3.0	1.2
chemokine (C-X-C motif) ligand 10	Cxcl10	45.9	66.0	1.4
chemokine (C-X-C motif) ligand 11	Cxcl11	10.7	12.3	1.1
chemokine (C-X-C motif) ligand 4	Cxcl4	0.2	-1.1	5.1
chemokine (C-X-C motif) ligand 9	Cxcl9	282.1	325.8	1.2
class II transactivator	C2ta	6.8	8.6	1.3
coatamer protein complex, subunit gamma 2, antisense 2	Copg2as2	0.1	-10.3	-1.2
colony stimulating factor 3 (granulocyte)	Csf3	0.2	1.2	7.8
complement component 1, q subcomponent, alpha polypeptide	C1qa	2.3	10.2	4.5
complement component 1, q subcomponent, beta polypeptide	C1qb	2.8	12.9	4.5
complement component 1, r subcomponent	C1r	3.4	4.1	1.2
complement component 1, r subcomponent	C1r	2.8	3.6	1.3
complement component 1, s subcomponent	C1s	3.8	2.8	-1.3
complement component 2 (within H-2S)	C2	4.7	3.1	-1.5
component of Sp100-rs	Csprs	4.4	5.3	1.2
component of Sp100-rs	Csprs	9.0	18.6	2.1
crystallin, alpha B	Cryab	2.0	-2.1	-4.3
C-type lectin domain family 4, member a2 /// C-type lectin domain family 4, member b	Clec4a2 /// Clec4b	0.5	2.0	4.4
cyclin B1	Ccnb1	2.3	2.3	1.0
cyclin G1	Ccng1	3.0	2.2	-1.4
cyclin G1	Ccng1	2.7	2.6	-1.1
cyclin G1	Ccng1	3.0	2.8	-1.1
cyclin-dependent kinase inhibitor 1C (P57)	Cdkn1c	0.3	-12.7	-3.9
cystatin F (leukocystatin)	Cst7	12.9	52.7	4.1

cytochrome P450, family 4, subfamily v, polypeptide 3	Cyp4v3	2.0	3.1	1.5
cytochrome P450, family 51	Cyp51	0.2	1.0	5.5
cytochrome P450, family 51	Cyp51	0.3	1.4	5.3
decay accelerating factor 1	Daf1	3.1	-1.2	-3.8
deoxyribonuclease 1-like 3	DNase113	9.4	10.8	1.1
desmoglein 2	Dsg2	4.3	1.5	-2.9
Diabetic nephropathy-like protein (Dnr12) mRNA, partial sequence	---	6.9	3.5	-2.0
dihydropyrimidinase	Dpys	2.4	3.0	1.2
disabled homolog 2 (Drosophila)	Dab2	0.4	-1.3	1.9
DNA segment, Chr 11, Lothar Hennighausen 2, expressed	D11Lgp2e	3.3	3.7	1.1
DNA segment, Chr 9, Wayne State University 168, expressed	D9Wsu168e	0.5	-1.3	1.6
ectodermal-neural cortex 1	Enc1	2.8	3.3	1.2
ectodermal-neural cortex 1	Enc1	2.8	4.4	1.6
ectonucleotide pyrophosphatase/phosphodiesterase 4	Enpp4	2.4	1.3	-1.9
ectonucleotide pyrophosphatase/phosphodiesterase 5	Enpp5	3.7	-1.0	-3.9
epoxide hydrolase 1, microsomal	Ephx1	2.4	-2.2	-5.3
expressed sequence AI132321	AI132321	10.4	6.1	-1.7
expressed sequence AI447904	AI447904	15.8	6.0	-2.7
expressed sequence AI447904	AI447904	7.8	4.3	-1.8
extracellular proteinase inhibitor	Expi	0.2	2.0	8.0
farnesyl diphosphate farnesyl transferase 1	Fdft1	0.3	-1.0	3.5
farnesyl diphosphate synthetase	Fdps	0.2	-1.4	2.9
fatty acid binding protein 7, brain	Fabp7	0.1	1.8	15.3
Fc receptor, IgG, high affinity I	Fcgr1	5.6	13.0	2.3
fibrinogen, alpha polypeptide	Fga	0.1	-1.2	13.5
fibrinogen, gamma polypeptide	Fgg	0.0	-1.4	15.0
fibrinogen-like protein 2	Fgl2	8.7	7.1	-1.2
fibrinogen-like protein 2	Fgl2	10.9	8.6	-1.3
glucosamine-6-phosphate deaminase 1	Gnpdal	0.5	2.1	4.6
glutathione S-transferase, mu 1	Gstm1	0.5	-3.0	-1.4
glutathione S-transferase, mu 1	Gstm1	0.4	-3.2	-1.4
G-protein coupled receptor 65	Gpr65	4.4	12.3	2.8
growth arrest and DNA-damage-inducible 45 beta	Gadd45b	0.4	-1.2	2.3
growth differentiation factor 15	Gdf15	0.2	2.0	10.3
guanine nucleotide binding protein, beta 4	Gnb4	2.3	-1.0	-2.3
guanylate nucleotide binding protein 1	Gbp1	26.4	29.7	1.1
guanylate nucleotide binding protein 2	Gbp2	17.5	9.7	-1.8
guanylate nucleotide binding protein 2	Gbp2	13.1	8.3	-1.6
guanylate nucleotide binding protein 4	Gbp4	16.2	7.6	-2.1
histocompatibility 2, class II, locus DMa	H2-DMa	9.0	6.6	-1.4
histocompatibility 2, class II, locus Mb2	H2-DMb2	12.0	8.7	-1.4
histocompatibility 2, M region locus 3	H2-M3	4.6	4.3	-1.1
histocompatibility 2, O region alpha locus	H2-Oa	18.0	18.1	1.0
histocompatibility 2, T region locus 10 /// histocompatibility 2, T region locus 17 /// histocompatibility 2, T region locus 22 /// histocompatibility 2, T region locus 9	H2-T10 /// H2-T17 /// H2-T22 /// H2-T9	3.0	3.5	1.2
histocompatibility 2, T region locus 24	H2-T24	3.3	1.6	-2.0
HRAS like suppressor 3	Hrasls3	10.6	5.1	-2.1
hydroxysteroid (17-beta) dehydrogenase 7	Hsd17b7	0.3	-1.1	3.0
hypothetical gene supported by AK018238; AK046289	LOC434002	0.2	-6.5	-1.3
hypoxia inducible factor 1, alpha subunit	Hif1a	2.8	4.2	1.5
immunoglobulin heavy chain 1a (serum IgG2a)	Igh-1a	57.4	304.9	5.3
immunoglobulin heavy chain 4 (serum IgG1)	Igh-4	0.1	21.9	380.8
immunoglobulin heavy chain 4 (serum IgG1)	Igh-4	0.1	8.9	120.0
immunoglobulin heavy chain 4 (serum IgG1)	Igh-4	0.1	18.5	187.6
immunoglobulin heavy chain 4 (serum IgG1)	Igh-4	0.1	9.4	82.7
immunoglobulin superfamily, member 4A	Igsf4a	2.3	-1.8	-4.2
immunoglobulin superfamily, member 4A	Igsf4a	2.2	-2.1	-4.7
indoleamine-pyrrole 2,3 dioxygenase	Indo	25.2	23.0	-1.1
inositol 1,4,5-triphosphate receptor 2	Itpr2	0.4	-1.9	1.2
integrin alpha 7	Itga7	0.3	1.1	3.6
integrin beta 7	Itgb7	3.6	5.1	1.4
inter alpha-trypsin inhibitor, heavy chain 4	Itih4	0.3	1.1	4.0
interferon activated gene 203	Ifi203	6.9	3.6	-1.9
interferon activated gene 203	Ifi203	5.3	2.8	-1.9
interferon activated gene 203	Ifi203	4.7	3.2	-1.5
interferon activated gene 204	Ifi204	10.7	11.4	1.1
interferon activated gene 205 /// myeloid cell nuclear differentiation antigen	Ifi205 /// Mnda	11.2	13.2	1.2
interferon consensus sequence binding protein 1	Icsbp1	3.7	4.8	1.3
interferon dependent positive acting transcription factor 3 gamma	Isgf3g	2.2	1.1	-2.1
interferon gamma induced GTPase	Igtp	9.2	9.6	1.0

Appendices

interferon gamma inducible protein 47	Ifi47	5.6	7.3	1.3
interferon induced with helicase C domain 1	Ifih1	3.2	1.8	-1.8
interferon inducible GTPase 1	Iigp1	14.3	15.5	1.1
interferon inducible GTPase 1	Iigp1	10.8	8.2	-1.3
interferon inducible GTPase 2	Iigp2	6.9	3.6	-1.9
interferon inducible protein 1	Ifi1	9.5	8.0	-1.2
interferon regulatory factor 1	Irf1	3.7	3.3	-1.1
interferon regulatory factor 7	Irf7	6.7	5.4	-1.2
interferon, alpha-inducible protein	G1p2	6.1	4.7	-1.3
interferon, alpha-inducible protein 27	Ifi27	16.1	1.4	-11.1
interferon-induced protein 44	Ifi44	14.1	3.3	-4.2
interferon-induced protein with tetratricopeptide repeats 1	Ifit1	6.2	2.8	-2.2
interferon-induced protein with tetratricopeptide repeats 2	Ifit2	13.1	3.5	-3.7
interferon-induced protein with tetratricopeptide repeats 3	Ifit3	5.5	2.2	-2.5
interleukin 1 family, member 9	Il1f9	0.1	2.8	22.8
interleukin 1 receptor accessory protein	Il1rap	0.4	-1.5	1.6
interleukin 1 receptor antagonist	Il1rn	0.3	8.2	25.6
interleukin 12 receptor, beta 1	Il12rb1	5.2	6.9	1.3
interleukin 15	Il15	2.1	1.7	-1.3
interleukin 15 receptor, alpha chain	Il15ra	4.0	3.4	-1.2
interleukin 15 receptor, alpha chain	Il15ra	3.6	2.9	-1.2
interleukin 18	Il18	3.4	1.1	-3.1
interleukin 18 binding protein	Il18bp	13.4	22.0	1.6
isopentenyl-diphosphate delta isomerase	Idi1	0.2	-2.1	2.2
isopentenyl-diphosphate delta isomerase	Idi1	0.2	-1.4	3.2
killer cell lectin-like receptor subfamily B member 1B	Klrb1b	9.8	5.3	-1.9
killer cell lectin-like receptor subfamily B member 1D	Klrb1d	6.8	5.0	-1.4
killer cell lectin-like receptor subfamily K, member 1	Klrk1	3.3	2.5	-1.3
killer cell lectin-like receptor, subfamily A, member 2	Klra2	9.8	9.5	-1.0
lanosterol synthase	Lss	0.3	-1.0	2.9
leptin receptor	Lepr	3.8	-5.5	-20.7
leukocyte-associated Ig-like receptor 1	Lair1	5.5	11.5	2.1
Low density lipoprotein receptor	Ldlr	0.3	1.0	3.1
lymphocyte antigen 6 complex, locus I	Ly6i	8.9	49.8	5.6
macrophage activation 2 like	Mpa2l	25.9	26.0	1.0
mannose receptor, C type 1	Mrc1	0.2	-2.7	2.3
MAS-related GPR, member A2	Mrgpra2	0.1	3.8	25.8
membrane-spanning 4-domains, subfamily A, member 4C	Ms4a4c	12.7	10.6	-1.2
membrane-spanning 4-domains, subfamily A, member 4C	Ms4a4c	4.7	3.9	-1.2
membrane-spanning 4-domains, subfamily A, member 8A	Ms4a8a	0.2	-1.6	3.7
mevalonate (diphospho) decarboxylase	Mvd	0.2	1.7	8.2
mevalonate kinase	Mvk	0.5	-1.5	1.4
milk fat globule-EGF factor 8 protein	Mfge8	0.3	-1.0	3.9
myeloid cell nuclear differentiation antigen	Mnda	12.0	8.3	-1.5
myxovirus (influenza virus) resistance 1	Mx1	5.1	5.3	1.1
N-acetylneuraminidase	Npl	0.2	1.1	4.5
neuropeptide Y	Npy	0.1	1.7	19.7
nitric oxide synthase 2, inducible, macrophage	Nos2	8.3	15.9	1.9
N-myc (and STAT) interactor	Nmi	2.6	1.6	-1.6
nucleolar and spindle associated protein 1	Nusap1	3.0	2.2	-1.4
oncoprotein induced transcript 3	Oit3	0.2	1.0	4.6
paired-Ig-like receptor A1	Pira1	0.3	6.0	22.2
palmitoyl-protein thioesterase 1	Ppt1	2.8	2.1	-1.4
PH domain and leucine rich repeat protein phosphatase	Phlpp	2.1	-1.4	-3.0
phosphatase and actin regulator 1	Phactr1	2.3	-2.2	-5.1
phospholipase A1 member A	Pla1a	4.1	23.1	5.6
phospholipase A2, group IVA (cytosolic, calcium-dependent)	Pla2g4a	5.1	6.4	1.2
phospholipase A2, group V	Pla2g5	4.2	4.0	-1.0
platelet-derived growth factor, D polypeptide	Pdgfd	2.4	-1.7	-4.0
plectin 1	Plec1	3.7	4.3	1.1
poly (ADP-ribose) polymerase family, member 14	---	3.5	3.0	-1.2
poly (ADP-ribose) polymerase family, member 8	Parp8	2.6	3.0	1.2
poly (ADP-ribose) polymerase family, member 9	Parp9	3.8	3.3	-1.1
promyelocytic leukemia	Pml	2.2	2.3	1.0
proprotein convertase subtilisin/kexin type 5	Pcsk5	0.2	-4.4	1.3
prostaglandin E receptor 3 (subtype EP3)	Ptger3	3.3	4.0	1.2
prostaglandin-endoperoxide synthase 2	Ptgs2	26.3	16.0	-1.6
prostaglandin-endoperoxide synthase 2	Ptgs2	20.1	20.1	-1.0
protease, serine, 11 (Igf binding)	Prss11	2.3	1.7	-1.3
protease, serine, 11 (Igf binding)	Prss11	2.2	1.5	-1.4
proteasome (prosome, macropain) 28 subunit, alpha	Psme1	2.3	2.1	-1.1
proteasome (prosome, macropain) 28 subunit, beta	Psme2	2.9	2.9	1.0

proteasome (prosome, macropain) subunit, beta type 10	Psmb10	3.9	3.3	-1.2
protein C receptor, endothelial	Procr	3.5	54.5	15.5
protein tyrosine phosphatase, receptor type, f polypeptide (PTPRF), interacting protein (liprin), alpha 4	Ppfia4	2.9	2.4	-1.2
proteolipid protein 2	Plp2	0.5	-1.3	1.6
proteosome (prosome, macropain) subunit, beta type 8 (large multifunctional protease 7)	Psmb8	4.2	5.5	1.3
proteosome (prosome, macropain) subunit, beta type 9 (large multifunctional protease 2)	Psmb9	4.8	5.4	1.1
protocadherin beta 9	Pcdhb9	0.3	-2.7	1.3
purine-nucleoside phosphorylase	Pnp	2.1	2.2	1.1
pyrophosphatase	Pyp	2.7	2.9	1.1
radical S-adenosyl methionine domain containing 2	Rsad2	18.2	9.1	-2.0
radical S-adenosyl methionine domain containing 2	Rsad2	11.1	7.2	-1.5
radical S-adenosyl methionine domain containing 2	Rsad2	8.1	5.9	-1.4
ras homolog gene family, member U	Rhou	0.4	2.0	5.6
reduced expression 3	Rex3	0.0	-9.4	6.6
restin-like 2	Rsnl2	0.5	1.4	2.9
restin-like 2	Rsnl2	0.4	1.4	3.7
Rho GTPase activating protein 24	Arhgap24	0.4	-1.6	1.5
RIKEN cDNA 0610025L06 gene	0610025L06Rik	2.2	1.9	-1.1
RIKEN cDNA 1110007F12 gene	1110007F12Rik	3.0	1.8	-1.7
RIKEN cDNA 1300010A20 gene	1300010A20Rik	3.3	3.0	-1.1
RIKEN cDNA 1700013H19 gene	1700013H19Rik	2.0	2.9	1.4
RIKEN cDNA 1810020C19 gene	1810020C19Rik	0.5	1.2	2.4
RIKEN cDNA 2310016F22 gene /// hypothetical protein LOC223672	2310016F22Rik /// LOC223672	11.7	11.0	-1.1
RIKEN cDNA 2310056P07 gene	2310056P07Rik	2.4	2.1	-1.1
RIKEN cDNA 2310058A11 gene	2310058A11Rik	0.5	-1.0	2.0
RIKEN cDNA 2700019D07 gene	2700019D07Rik	2.5	1.9	-1.3
RIKEN cDNA 2810453I06 gene	2810453I06Rik	2.3	-1.0	-2.4
RIKEN cDNA 4933430F08 gene	4933430F08Rik	5.4	7.7	1.4
RIKEN cDNA 4933430F08 gene	4933430F08Rik	9.3	11.5	1.2
RIKEN cDNA 5133400D11 gene	5133400D11Rik	0.3	-3.4	-1.2
RIKEN cDNA 5133401N09 gene	5133401N09Rik	2.1	2.2	1.1
RIKEN cDNA 5430413I02 gene	5430413I02Rik	3.8	7.1	1.8
RIKEN cDNA 5730507H05 gene	5730507H05Rik	2.1	2.3	1.1
RIKEN cDNA 5830443L24 gene	5830443L24Rik	24.3	36.3	1.5
RIKEN cDNA 5830458K16 gene	5830458K16Rik	10.0	2.1	-4.7
RIKEN cDNA 5830484A20 gene	5830484A20Rik	2.6	3.4	1.3
RIKEN cDNA 6330406P08 gene	6330406P08Rik	0.5	-1.1	2.0
RIKEN cDNA 6330442E10 gene	6330442E10Rik	2.5	2.3	-1.1
RIKEN cDNA 9430083G14 gene	9430083G14Rik	2.2	1.8	-1.2
RIKEN cDNA 9830147J24 gene	9830147J24Rik	7.8	5.0	-1.6
RIKEN cDNA A030007L17 gene	A030007L17Rik	3.5	5.5	1.6
RIKEN cDNA C920025E04 gene	C920025E04Rik	4.8	7.7	1.6
RIKEN cDNA D930038M13 gene	D930038M13Rik	3.9	-7.6	-29.4
RIKEN cDNA E130201N16 gene	E130201N16Rik	2.8	2.9	1.0
RIKEN cDNA E430036I04 gene	E430036I04Rik	2.0	2.6	1.3
SAM domain and HD domain, 1	Samhd1	3.3	3.5	1.1
SAM domain and HD domain, 1	Samhd1	2.8	2.7	-1.0
SEC8-like 1 (<i>S. cerevisiae</i>)	Sec8l1	2.0	1.5	-1.3
SEC8-like 1 (<i>S. cerevisiae</i>)	Sec8l1	2.1	1.5	-1.4
selenoprotein M	MGI:2149786	4.4	2.5	-1.8
serine (or cysteine) proteinase inhibitor, clade A, member 3G	Serpina3g	3.2	61.4	19.0
serine (or cysteine) proteinase inhibitor, clade B, member 1b	Serpina1b	2.5	2.3	-1.1
sestrin 3	Sesn3	2.2	1.7	-1.3
signal peptide, CUB domain, EGF-like 2	Scube2	0.3	-38.6	-9.8
signal transducer and activator of transcription 1	Stat1	11.3	8.1	-1.4
signal transducer and activator of transcription 1	Stat1	13.0	9.6	-1.4
signal transducer and activator of transcription 1	Stat1	13.1	6.4	-2.1
signal transducer and activator of transcription 2	Stat2	3.1	2.6	-1.2
signal transducer and activator of transcription 2	Stat2	3.3	2.6	-1.3
SLAM family member 8	Slamf8	47.2	100.0	2.1
solute carrier family 11 (proton-coupled divalent metal ion transporters), member 2	Slc11a2	0.4	1.3	3.0
solute carrier family 40 (iron-regulated transporter), member 1	Slc40a1	0.2	-1.7	2.5
solute carrier family 40 (iron-regulated transporter), member 1	Slc40a1	0.3	-1.4	2.1
solute carrier family 5 (sodium/glucose cotransporter), member 1	Slc5a1	0.4	1.1	2.7
sphingomyelin phosphodiesterase, acid-like 3B	Smpd13b	6.5	27.0	4.2
spondin 2, extracellular matrix protein	Spon2	2.6	3.5	1.3
SPRY domain-containing SOCS box 4	MGI:2183445	0.3	1.6	5.1

Appendices

squalene epoxidase	Sqle	0.2	-1.1	3.8
ST3 beta-galactoside alpha-2,3-sialyltransferase 5	St3gal5	3.8	1.5	-2.6
sterol-C4-methyl oxidase-like	Sc4mol	0.3	1.1	3.9
sterol-C5-desaturase (fungal ERG3, delta-5-desaturase) homolog (<i>S. cerevisiae</i>)	Sc5d	0.4	-1.1	2.3
suppressor of cytokine signaling 1	Socs1	9.4	13.3	1.4
TAP binding protein-like	Tapbp1	2.5	2.6	1.0
T-cell specific GTPase	Tgtp	6.1	8.3	1.4
tetraspanin 13	Tspan13	2.0	-3.5	-7.0
tetraspanin 14	Tspan14	0.5	-1.3	1.6
three prime repair exonuclease 1	Trex1	4.0	4.3	1.1
thymidine kinase 1	Tk1	2.3	3.1	1.4
thymidylate kinase family LPS-inducible member	Tyki	4.1	1.3	-3.2
thyroid hormone receptor interactor 13	Trip13	5.4	7.1	1.3
toll-like receptor 3	Tlr3	2.0	1.3	-1.6
transient receptor potential cation channel, subfamily V, member 6	Trpv6	0.5	-1.4	1.4
transmembrane 7 superfamily member 1	Tm7sf1	0.4	1.2	2.8
transmembrane 7 superfamily member 1	Tm7sf1	0.4	1.6	3.9
transmembrane 7 superfamily member 1	Tm7sf1	0.4	2.2	5.9
transmembrane protein 38B	Tmem38b	0.4	-1.1	2.2
transmembrane protein 38B	Tmem38b	0.4	-1.2	2.1
transporter 2, ATP-binding cassette, sub-family B (MDR/TAP)	Tap2	3.3	4.3	1.3
tripartite motif protein 12	Trim12	2.5	2.3	-1.1
tripartite motif protein 21	Trim21	3.3	1.7	-2.0
tripartite motif protein 21	Trim21	3.1	1.9	-1.7
tripartite motif protein 30	Trim30	3.0	3.1	1.0
tripartite motif protein 30 /// tripartite motif protein 30-like	Trim30 /// LOC209387	3.9	4.0	1.0
tripartite motif protein 34	Trim34	2.3	1.3	-1.8
tryptophanyl-tRNA synthetase	Wars	2.8	2.9	1.1
tryptophanyl-tRNA synthetase	Wars	3.5	3.3	-1.0
tryptophanyl-tRNA synthetase	Wars	2.8	2.8	-1.0
tryptophanyl-tRNA synthetase	Wars	4.7	3.7	-1.3
tumor necrosis factor (ligand) superfamily, member 13b	Tnfsf13b	5.1	3.0	-1.7
tumor necrosis factor receptor superfamily, member 22	Tnfrsf22	0.5	1.5	3.3
tumor necrosis factor receptor superfamily, member 5	Tnfrsf5	9.9	4.6	-2.1
tumor necrosis factor receptor superfamily, member 5	Tnfrsf5	5.5	3.6	-1.5
tumor necrosis factor, alpha-induced protein 2	Tnfaip2	2.0	16.9	8.3
type 1 tumor necrosis factor receptor shedding aminopeptidase regulator	MGI:1933403	3.8	3.1	-1.2
ubiquitin D	Ubd	127.6	240.5	1.9
ubiquitin-activating enzyme E1-like	Ube1l	4.5	3.1	-1.4
ubiquitin-activating enzyme E1-like /// RIKEN cDNA D330022A01 gene	Ube1l /// D330022A01Rik	3.9	3.1	-1.2
ubiquitin-conjugating enzyme E2L 6	Ube2l6	6.4	4.2	-1.5
UDP-N-acetyl-alpha-D-galactosamine:polypeptide N-acetylgalactosaminyltransferase 10	Galnt10	2.0	1.9	-1.1
urokinase plasminogen activator receptor	Plaur	0.5	1.6	3.2
vaccinia related kinase 2	Vrk2	2.5	2.4	-1.0
vaccinia related kinase 2	Vrk2	2.2	1.9	-1.2
vascular cell adhesion molecule 1	Vcam1	4.4	2.6	-1.7
vascular cell adhesion molecule 1	Vcam1	3.1	3.2	1.0
Wolfram syndrome 1 homolog (human)	Wfs1	0.4	-1.1	2.4
Z-DNA binding protein 1	Zbp1	11.0	19.8	1.8
Z-DNA binding protein 1	Zbp1	8.8	22.6	2.6
zinc finger CCCH type domain containing 1	Zc3hdc1	3.0	1.7	-1.8

Table 4: Some genes are regulated higher than 2-fold in the lungs of wild-type versus IFN- γ -KO mice. A selection of 327 probe sets differentially expressed in the lungs of C57BL/6 wild-type (WT) and IFN- γ -deficient (KO) mice infected by aerosol with *M. avium* (TM724, 10^5 CFU/mouse). Q value <0.01. The fold change (FC) is the gene expression in infected against uninfected mice, and the cut-off set for differential expression is FC wt/ko >2, showing only highly regulated genes, where the fold change is higher than 2 comparing infected IFN- γ -KO with infected wild-type mice. Repeated probe sets have different numbers and might be alternative splice variants.

Appendix 2

Gene Title	Gene Symbol	FC wt/ko	FC wt	FC ko
---	---	5.5	6.8	1.2
---	---	4.3	8.6	2.0
2'-5' oligoadenylate synthetase-like 1	Oasl1	7.0	7.3	1.0
2'-5' oligoadenylate synthetase-like 2	Oasl2	9.6	5.0	-1.9
Acyl-CoA synthetase long-chain family member 1	Acsl1	4.7	4.5	-1.0
acyl-CoA synthetase long-chain family member 1	Acsl1	9.0	8.7	-1.0
acyl-CoA synthetase long-chain family member 1	Acsl1	7.3	6.9	-1.1
ADP-ribosyltransferase 3	Art3	6.2	-1.0	-6.3
allograft inflammatory factor 1	Aif1	14.5	24.5	1.7
ankyrin repeat and SOCS box-containing protein 11	Asb11	7.2	6.3	-1.1
cathepsin K	Ctsk	0.1	2.3	27.0
CD1d1 antigen	Cd1d1	6.9	8.1	1.2
CD1d1 antigen	Cd1d1	6.0	6.3	1.0
CD72 antigen	Cd72	4.3	7.6	1.8
CD86 antigen	Cd86	4.2	8.5	2.0
cDNA sequence BC010462	BC010462	4.2	5.6	1.3
cDNA sequence BC023105	BC023105	5.5	6.5	1.2
chemokine (C-C motif) ligand 19	Ccl19	8.5	8.9	1.0
chemokine (C-C motif) ligand 3	Ccl3	0.1	22.8	207.5
chemokine (C-X-C motif) ligand 10	Cxcl10	45.9	66.0	1.4
chemokine (C-X-C motif) ligand 11	Cxcl11	10.7	12.3	1.1
chemokine (C-X-C motif) ligand 4	Cxcl4	0.2	-1.1	5.1
chemokine (C-X-C motif) ligand 9	Cxcl9	282.1	325.8	1.2
class II transactivator	C2ta	6.8	8.6	1.3
coatamer protein complex, subunit gamma 2, antisense 2	Copg2as2	0.1	-10.3	-1.2
colony stimulating factor 3 (granulocyte)	Csf3	0.2	1.2	7.8
complement component 2 (within H-2S)	C2	4.7	3.1	-1.5
component of Sp100-rs	Csprs	4.4	5.3	1.2
component of Sp100-rs	Csprs	9.0	18.6	2.1
cystatin F (leukocystatin)	Cst7	12.9	52.7	4.1
cytochrome P450, family 51	Cyp51	0.2	1.0	5.5
deoxyribonuclease 1-like 3	DNase1l3	9.4	10.8	1.1
desmoglein 2	Dsg2	4.3	1.5	-2.9
Diabetic nephropathy-like protein (Dnr12) mRNA, partial sequence	---	6.9	3.5	-2.0
expressed sequence AI132321	AI132321	10.4	6.1	-1.7
expressed sequence AI447904	AI447904	15.8	6.0	-2.7
expressed sequence AI447904	AI447904	7.8	4.3	-1.8
extracellular proteinase inhibitor	Expi	0.2	2.0	8.0
farnesyl diphosphate synthetase	Fdps	0.2	-1.4	2.9
fatty acid binding protein 7, brain	Fabp7	0.1	1.8	15.3
Fc receptor, IgG, high affinity 1	Fcgr1	5.6	13.0	2.3
fibrinogen, alpha polypeptide	Fga	0.1	-1.2	13.5
fibrinogen, gamma polypeptide	Fgg	0.0	-1.4	15.0
fibrinogen-like protein 2	Fgl2	8.7	7.1	-1.2
fibrinogen-like protein 2	Fgl2	10.9	8.6	-1.3
G-protein coupled receptor 65	Gpr65	4.4	12.3	2.8
growth differentiation factor 15	Gdf15	0.2	2.0	10.3
guanylate nucleotide binding protein 1	Gbp1	26.4	29.7	1.1
guanylate nucleotide binding protein 2	Gbp2	17.5	9.7	-1.8
guanylate nucleotide binding protein 2	Gbp2	13.1	8.3	-1.6
guanylate nucleotide binding protein 4	Gbp4	16.2	7.6	-2.1
histocompatibility 2, class II, locus DMA	H2-Dma	9.0	6.6	-1.4
histocompatibility 2, class II, locus Mb2	H2-DMb2	12.0	8.7	-1.4
histocompatibility 2, M region locus 3	H2-M3	4.6	4.3	-1.1
histocompatibility 2, O region alpha locus	H2-Oa	18.0	18.1	1.0
HRAS like suppressor 3	Hrasls3	10.6	5.1	-2.1
hypothetical gene supported by AK018238; AK046289	LOC434002	0.2	-6.5	-1.3
immunoglobulin heavy chain 1a (serum IgG2a)	Igh-1a	57.4	304.9	5.3
immunoglobulin heavy chain 4 (serum IgG1)	Igh-4	0.1	21.9	380.8
immunoglobulin heavy chain 4 (serum IgG1)	Igh-4	0.1	8.9	120.0
immunoglobulin heavy chain 4 (serum IgG1)	Igh-4	0.1	18.5	187.6
immunoglobulin heavy chain 4 (serum IgG1)	Igh-4	0.1	9.4	82.7
indoleamine-pyrrole 2,3 dioxygenase	Indo	25.2	23.0	-1.1
interferon activated gene 203	Ifi203	6.9	3.6	-1.9
interferon activated gene 203	Ifi203	5.3	2.8	-1.9

Appendices

interferon activated gene 203	Ifi203	4.7	3.2	-1.5
interferon activated gene 204	Ifi204	10.7	11.4	1.1
interferon activated gene 205 /// myeloid cell nuclear differentiation antigen	Ifi205 /// Mnda	11.2	13.2	1.2
interferon gamma induced GTPase	Igtp	9.2	9.6	1.0
interferon gamma inducible protein 47	Ifi47	5.6	7.3	1.3
interferon inducible GTPase 1	Iigp1	14.3	15.5	1.1
interferon inducible GTPase 1	Iigp1	10.8	8.2	-1.3
interferon inducible GTPase 2	Iigp2	6.9	3.6	-1.9
interferon inducible protein 1	Ifi1	9.5	8.0	-1.2
interferon regulatory factor 7	Irf7	6.7	5.4	-1.2
interferon, alpha-inducible protein	G1p2	6.1	4.7	-1.3
interferon, alpha-inducible protein 27	Ifi27	16.1	1.4	-11.1
interferon-induced protein 44	Ifi44	14.1	3.3	-4.2
interferon-induced protein with tetratricopeptide repeats 1	Ifit1	6.2	2.8	-2.2
interferon-induced protein with tetratricopeptide repeats 2	Ifit2	13.1	3.5	-3.7
interferon-induced protein with tetratricopeptide repeats 3	Ifit3	5.5	2.2	-2.5
interleukin 1 family, member 9	Il1f9	0.1	2.8	22.8
interleukin 12 receptor, beta 1	Il12rb1	5.2	6.9	1.3
interleukin 18 binding protein	Il18bp	13.4	22.0	1.6
isopentenyl-diphosphate delta isomerase	Idi1	0.2	-2.1	2.2
isopentenyl-diphosphate delta isomerase	Idi1	0.2	-1.4	3.2
killer cell lectin-like receptor subfamily B member 1B	Klrb1b	9.8	5.3	-1.9
killer cell lectin-like receptor subfamily B member 1D	Klrb1d	6.8	5.0	-1.4
killer cell lectin-like receptor, subfamily A, member 2	Klra2	9.8	9.5	-1.0
leukocyte-associated Ig-like receptor 1	Lair1	5.5	11.5	2.1
lymphocyte antigen 6 complex, locus I	Ly6i	8.9	49.8	5.6
macrophage activation 2 like	Mpa2l	25.9	26.0	1.0
mannose receptor, C type 1	Mrc1	0.2	-2.7	2.3
MAS-related GPR, member A2	Mrgpra2	0.1	3.8	25.8
membrane-spanning 4-domains, subfamily A, member 4C	Ms4a4c	12.7	10.6	-1.2
membrane-spanning 4-domains, subfamily A, member 4C	Ms4a4c	4.7	3.9	-1.2
membrane-spanning 4-domains, subfamily A, member 8A	Ms4a8a	0.2	-1.6	3.7
mevalonate (diphospho) decarboxylase	Mvd	0.2	1.7	8.2
myeloid cell nuclear differentiation antigen	Mnda	12.0	8.3	-1.5
myxovirus (influenza virus) resistance 1	Mx1	5.1	5.3	1.1
N-acetylneuraminatase pyruvate lyase	Npl	0.2	1.1	4.5
neuropeptide Y	Npy	0.1	1.7	19.7
nitric oxide synthase 2, inducible, macrophage	Nos2	8.3	15.9	1.9
oncoprotein induced transcript 3	Oit3	0.2	1.0	4.6
phospholipase A1 member A	Pla1a	4.1	23.1	5.6
phospholipase A2, group IVA (cytosolic, calcium-dependent)	Pla2g4a	5.1	6.4	1.2
phospholipase A2, group V	Pla2g5	4.2	4.0	-1.0
proprotein convertase subtilisin/kexin type 5	Pcsk5	0.2	-4.4	1.3
prostaglandin-endoperoxide synthase 2	Ptgs2	26.3	16.0	-1.6
prostaglandin-endoperoxide synthase 2	Ptgs2	20.1	20.1	-1.0
proteasome (prosome, macropain) subunit, beta type 8 (large multifunctional protease 7)	Psmb8	4.2	5.5	1.3
proteasome (prosome, macropain) subunit, beta type 9 (large multifunctional protease 2)	Psmb9	4.8	5.4	1.1
radical S-adenosyl methionine domain containing 2	Rsad2	18.2	9.1	-2.0
radical S-adenosyl methionine domain containing 2	Rsad2	11.1	7.2	-1.5
radical S-adenosyl methionine domain containing 2	Rsad2	8.1	5.9	-1.4
reduced expression 3	Rex3	0.0	-9.4	6.6
RIKEN cDNA 2310016F22 gene /// hypothetical protein LOC223672	2310016F22Rik /// LOC223672	11.7	11.0	-1.1
RIKEN cDNA 4933430F08 gene	4933430F08Rik	5.4	7.7	1.4
RIKEN cDNA 4933430F08 gene	4933430F08Rik	9.3	11.5	1.2
RIKEN cDNA 5830443L24 gene	5830443L24Rik	24.3	36.3	1.5
RIKEN cDNA 5830458K16 gene	5830458K16Rik	10.0	2.1	-4.7
RIKEN cDNA 9830147J24 gene	9830147J24Rik	7.8	5.0	-1.6
RIKEN cDNA C920025E04 gene	C920025E04Rik	4.8	7.7	1.6
selenoprotein M	MGI:2149786	4.4	2.5	-1.8
signal transducer and activator of transcription 1	Stat1	11.3	8.1	-1.4
signal transducer and activator of transcription 1	Stat1	13.0	9.6	-1.4
signal transducer and activator of transcription 1	Stat1	13.1	6.4	-2.1
SLAM family member 8	Slamf8	47.2	100.0	2.1
solute carrier family 40 (iron-regulated transporter), member 1	Slc40a1	0.2	-1.7	2.5
sphingomyelin phosphodiesterase, acid-like 3B	Smpd3b	6.5	27.0	4.2
squalene epoxidase	Sqle	0.2	-1.1	3.8
suppressor of cytokine signaling 1	Socs1	9.4	13.3	1.4
T-cell specific GTPase	Tgtp	6.1	8.3	1.4

three prime repair exonuclease 1	Trex1	4.0	4.3	1.1
thymidylate kinase family LPS-inducible member	Tyki	4.1	1.3	-3.2
thyroid hormone receptor interactor 13	Trip13	5.4	7.1	1.3
tryptophanyl-tRNA synthetase	Wars	4.7	3.7	-1.3
tumor necrosis factor (ligand) superfamily, member 13b	Tnfsf13b	5.1	3.0	-1.7
tumor necrosis factor receptor superfamily, member 5	Tnfrsf5	9.9	4.6	-2.1
tumor necrosis factor receptor superfamily, member 5	Tnfrsf5	5.5	3.6	-1.5
ubiquitin D	Ubd	127.6	240.5	1.9
ubiquitin-activating enzyme E1-like	Ube1l	4.5	3.1	-1.4
ubiquitin-conjugating enzyme E2L 6	Ube2l6	6.4	4.2	-1.5
vascular cell adhesion molecule 1	Vcam1	4.4	2.6	-1.7
Z-DNA binding protein 1	Zbp1	11.0	19.8	1.8
Z-DNA binding protein 1	Zbp1	8.8	22.6	2.6

Table 5: Some genes are regulated higher than 4-fold in the lungs of wild-type versus IFN- γ -KO mice. A selection of 146 probe sets differentially expressed in the lungs of C57BL/6 wild-type (WT) and IFN- γ -deficient (KO) mice infected by aerosol with *M. avium* (TMC724, 10^5 CFU/mouse). Q value <0.01. The fold change (FC) is the gene expression in infected against uninfected mice, and the cut-off set for differential expression is FC wt/ko >4, showing only highly regulated genes, where the fold change is higher than 4 comparing infected IFN- γ -KO with infected wild-type mice. Repeated probe sets have different numbers and might be alternative splice variants.

Appendix 3

Gene Title	Gene Symbol	FC wt/ko	FC wt	FC ko
---	---	5.5	6.8	1.2
2'-5' oligoadenylate synthetase-like 1	Oasl1	7.0	7.3	1.0
2'-5' oligoadenylate synthetase-like 2	Oasl2	9.6	5.0	-1.9
acyl-CoA synthetase long-chain family member 1	Acs11	9.0	8.7	-1.0
acyl-CoA synthetase long-chain family member 1	Acs11	7.3	6.9	-1.1
ADP-ribosyltransferase 3	Art3	6.2	-1.0	-6.3
allograft inflammatory factor 1	Aif1	14.5	24.5	1.7
ankyrin repeat and SOCS box-containing protein 11	Asb11	7.2	6.3	-1.1
cathepsin K	Ctsk	0.1	2.3	27.0
CD1d1 antigen	Cd1d1	6.9	8.1	1.2
CD1d1 antigen	Cd1d1	6.0	6.3	1.0
cDNA sequence BC023105	BC023105	5.5	6.5	1.2
chemokine (C-C motif) ligand 19	Ccl19	8.5	8.9	1.0
chemokine (C-C motif) ligand 3	Ccl3	0.1	22.8	207.5
chemokine (C-X-C motif) ligand 10	Cxcl10	45.9	66.0	1.4
chemokine (C-X-C motif) ligand 11	Cxcl11	10.7	12.3	1.1
chemokine (C-X-C motif) ligand 4	Cxcl4	0.2	-1.1	5.1
chemokine (C-X-C motif) ligand 9	Cxcl9	282.1	325.8	1.2
class II transactivator	C2ta	6.8	8.6	1.3
coatamer protein complex, subunit gamma 2, antisense 2	Copg2as2	0.1	-10.3	-1.2
colony stimulating factor 3 (granulocyte)	Csf3	0.2	1.2	7.8
component of Sp100-rs	Csprs	9.0	18.6	2.1
cystatin F (leukocystatin)	Cst7	12.9	52.7	4.1
cytochrome P450, family 51	Cyp51	0.2	1.0	5.5
deoxyribonuclease 1-like 3	DNase113	9.4	10.8	1.1
Diabetic nephropathy-like protein (Dnr12) mRNA, partial sequence	---	6.9	3.5	-2.0
expressed sequence AI132321	AI132321	10.4	6.1	-1.7
expressed sequence AI447904	AI447904	15.8	6.0	-2.7
expressed sequence AI447904	AI447904	7.8	4.3	-1.8
fatty acid binding protein 7, brain	Fabp7	0.1	1.8	15.3
Fc receptor, IgG, high affinity I	Fcgr1	5.6	13.0	2.3
fibrinogen, alpha polypeptide	Fga	0.1	-1.2	13.5
fibrinogen, gamma polypeptide	Fgg	0.0	-1.4	15.0
fibrinogen-like protein 2	Fgl2	8.7	7.1	-1.2
fibrinogen-like protein 2	Fgl2	10.9	8.6	-1.3
growth differentiation factor 15	Gdf15	0.2	2.0	10.3
guanylate nucleotide binding protein 1	Gbp1	26.4	29.7	1.1
guanylate nucleotide binding protein 2	Gbp2	17.5	9.7	-1.8
guanylate nucleotide binding protein 2	Gbp2	13.1	8.3	-1.6
guanylate nucleotide binding protein 4	Gbp4	16.2	7.6	-2.1
histocompatibility 2, class II, locus DMA	H2-Dma	9.0	6.6	-1.4
histocompatibility 2, class II, locus Mb2	H2-DMb2	12.0	8.7	-1.4
histocompatibility 2, O region alpha locus	H2-Oa	18.0	18.1	1.0
HRAS like suppressor 3	Hras3	10.6	5.1	-2.1
hypothetical gene supported by AK018238; AK046289	LOC434002	0.2	-6.5	-1.3
immunoglobulin heavy chain 1a (serum IgG2a)	Igh-1a	57.4	304.9	5.3
immunoglobulin heavy chain 4 (serum IgG1)	Igh-4	0.1	21.9	380.8
immunoglobulin heavy chain 4 (serum IgG1)	Igh-4	0.1	8.9	120.0
immunoglobulin heavy chain 4 (serum IgG1)	Igh-4	0.1	18.5	187.6
immunoglobulin heavy chain 4 (serum IgG1)	Igh-4	0.1	9.4	82.7
indoleamine-pyrrole 2,3 dioxygenase	Indo	25.2	23.0	-1.1
interferon activated gene 203	Ifi203	6.9	3.6	-1.9
interferon activated gene 203	Ifi203	5.3	2.8	-1.9
interferon activated gene 204	Ifi204	10.7	11.4	1.1
interferon activated gene 205 /// myeloid cell nuclear differentiation antigen	Ifi205 /// Mnda	11.2	13.2	1.2
interferon gamma induced GTPase	Igtp	9.2	9.6	1.0
interferon gamma inducible protein 47	Ifi47	5.6	7.3	1.3
interferon inducible GTPase 1	Iigp1	14.3	15.5	1.1
interferon inducible GTPase 1	Iigp1	10.8	8.2	-1.3
interferon inducible GTPase 2	Iigp2	6.9	3.6	-1.9
interferon inducible protein 1	Ifi1	9.5	8.0	-1.2
interferon regulatory factor 7	Irf7	6.7	5.4	-1.2
interferon, alpha-inducible protein	G1p2	6.1	4.7	-1.3
interferon, alpha-inducible protein 27	Ifi27	16.1	1.4	-11.1

interferon-induced protein 44	Ifi44	14.1	3.3	-4.2
interferon-induced protein with tetratricopeptide repeats 1	Ifit1	6.2	2.8	-2.2
interferon-induced protein with tetratricopeptide repeats 2	Ifit2	13.1	3.5	-3.7
interferon-induced protein with tetratricopeptide repeats 3	Ifit3	5.5	2.2	-2.5
interleukin 1 family, member 9	Il1f9	0.1	2.8	22.8
interleukin 12 receptor, beta 1	Il12rb1	5.2	6.9	1.3
interleukin 18 binding protein	Il18bp	13.4	22.0	1.6
killer cell lectin-like receptor subfamily B member 1B	Klrb1b	9.8	5.3	-1.9
killer cell lectin-like receptor subfamily B member 1D	Klrb1d	6.8	5.0	-1.4
killer cell lectin-like receptor, subfamily A, member 2	Klra2	9.8	9.5	-1.0
leukocyte-associated Ig-like receptor 1	Lair1	5.5	11.5	2.1
lymphocyte antigen 6 complex, locus 1	Ly6i	8.9	49.8	5.6
macrophage activation 2 like	Mpa2l	25.9	26.0	1.0
mannose receptor, C type 1	Mrc1	0.2	-2.7	2.3
MAS-related GPR, member A2	Mrgpra2	0.1	3.8	25.8
membrane-spanning 4-domains, subfamily A, member 4C	Ms4a4c	12.7	10.6	-1.2
membrane-spanning 4-domains, subfamily A, member 8A	Ms4a8a	0.2	-1.6	3.7
myeloid cell nuclear differentiation antigen	Mnda	12.0	8.3	-1.5
myxovirus (influenza virus) resistance 1	Mx1	5.1	5.3	1.1
neuropeptide Y	Npy	0.1	1.7	19.7
nitric oxide synthase 2, inducible, macrophage	Nos2	8.3	15.9	1.9
phospholipase A2, group IVA (cytosolic, calcium-dependent)	Pla2g4a	5.1	6.4	1.2
proprotein convertase subtilisin/kexin type 5	Pcsk5	0.2	-4.4	1.3
prostaglandin-endoperoxide synthase 2	Ptgs2	26.3	16.0	-1.6
prostaglandin-endoperoxide synthase 2	Ptgs2	20.1	20.1	-1.0
radical S-adenosyl methionine domain containing 2	Rsad2	18.2	9.1	-2.0
radical S-adenosyl methionine domain containing 2	Rsad2	11.1	7.2	-1.5
radical S-adenosyl methionine domain containing 2	Rsad2	8.1	5.9	-1.4
reduced expression 3	Rex3	0.0	-9.4	6.6
RIKEN cDNA 2310016F22 gene /// hypothetical protein LOC223672	2310016F22Rik /// LOC223672	11.7	11.0	-1.1
RIKEN cDNA 4933430F08 gene	4933430F08Rik	5.4	7.7	1.4
RIKEN cDNA 4933430F08 gene	4933430F08Rik	9.3	11.5	1.2
RIKEN cDNA 5830443L24 gene	5830443L24Rik	24.3	36.3	1.5
RIKEN cDNA 5830458K16 gene	5830458K16Rik	10.0	2.1	-4.7
RIKEN cDNA 9830147J24 gene	9830147J24Rik	7.8	5.0	-1.6
signal transducer and activator of transcription 1	Stat1	11.3	8.1	-1.4
signal transducer and activator of transcription 1	Stat1	13.0	9.6	-1.4
signal transducer and activator of transcription 1	Stat1	13.1	6.4	-2.1
SLAM family member 8	Slamf8	47.2	100.0	2.1
sphingomyelin phosphodiesterase, acid-like 3B	Smpd13b	6.5	27.0	4.2
suppressor of cytokine signaling 1	Socs1	9.4	13.3	1.4
T-cell specific GTPase	Tgtp	6.1	8.3	1.4
thyroid hormone receptor interactor 13	Trip13	5.4	7.1	1.3
tumor necrosis factor (ligand) superfamily, member 13b	Tnfsf13b	5.1	3.0	-1.7
tumor necrosis factor receptor superfamily, member 5	Tnfrsf5	9.9	4.6	-2.1
tumor necrosis factor receptor superfamily, member 5	Tnfrsf5	5.5	3.6	-1.5
ubiquitin D	Ubd	127.6	240.5	1.9
ubiquitin-conjugating enzyme E2L 6	Ube2l6	6.4	4.2	-1.5
Z-DNA binding protein 1	Zbp1	11.0	19.8	1.8
Z-DNA binding protein 1	Zbp1	8.8	22.6	2.6

Table 6: Some genes are regulated higher than 5-fold in the lungs of wild-type versus IFN- γ -KO mice. A selection of 114 probe sets differentially expressed in the lungs of C57BL/6 wild-type (WT) and IFN- γ -deficient (KO) mice infected by aerosol with *M. avium* (TMC724, 10⁵ CFU/mouse). Q value <0.01. The fold change (FC) is the gene expression in infected against uninfected mice, and the cut-off set for differential expression is FC wt/ko >5, showing only highly regulated genes, where the fold change is higher than 5 comparing infected IFN- γ -KO with infected wild-type mice. Repeated probe sets have different numbers and might be alternative splice variants.

Summary

Granuloma formation is a hallmark of mycobacterial infections. The main function of a granuloma is to contain a microbial invader and to control the infection preventing further dissemination. However, granulomas are double-edged swords. With the progress of infection they increase in size, displace parenchymal tissue and cause organ malfunction. The center of developed granulomas may necrotize, destroy adjacent structures and liquefy, causing erosion into the bronchial system as well as spreading the granuloma contents into the environment. In order to control the pathological consequences without disturbing the protective function of a granuloma, it is necessary to dissect at the molecular level the effector molecules responsible for the development of granuloma necrosis.

The aim of the work presented in this thesis was to capitalize on a published model of *M. avium*-induced pulmonary immunopathology in the mouse in order to (i) identify molecular pathways involved in the development of granuloma necrosis, (ii) test whether these pathways could be modulated to inhibit granuloma necrosis, and (iii) analyze whether the knowledge gained in this model could provide insight into the pathophysiological environment and the metabolic state of *M. tuberculosis* in lung granulomas.

The salient findings of the experiments conducted in this research program are: (i) IFN- γ and the signaling molecules STAT-1 and IRF-1 are responsible for granuloma necrosis. IRF-1 in particular emerged as an effector molecule that could possibly be manipulated to prevent pathology without disturbing protective functions. (ii) Granuloma necrosis is associated with a misbalance between angiogenic and angiostatic mediators in favor of angiostasis. However, in the absence of the angiostatic receptor CXCR3, IFN- γ -induced angiostasis was neither inhibited nor was development of granuloma necrosis reduced. (iii) IFN- γ -mediated granuloma necrosis is associated with severe hypoxia in mice infected with *M. avium* and guinea pigs infected with *M. tuberculosis*, but not in mice infected with *M. tuberculosis*.

These findings have important implications for the use of the mouse and guinea pig models of *M. tuberculosis* infection in developing eradication chemotherapy and for evaluating the mechanisms of chronic persistence and latency of *M. tuberculosis*.

Zusammenfassung

Die Granulombildung ist ein herausragendes Kennzeichen mykobakterieller Infektionen. Die Hauptfunktion eines Granuloms besteht in der Abgrenzung eines Infektionsherds, um eine weitere Streuung der Erreger zu verhindern. Granulome sind jedoch ein zweischneidiges Schwert. Mit fortschreitender Infektion werden sie größer, verdrängen das parenchymale Gewebe und schädigen wichtige Organfunktionen. Das Zentrum des Granuloms nekrotisiert und verflüssigt sich, wobei auch angrenzendes Gewebe zerstört wird, bis der Granulominhalt in das Bronchialsystem einbricht und sich in die Umgebung verbreitet. Um die pathologischen Folgen zu beherrschen, ohne die Schutzfunktionen des Granuloms zu beeinträchtigen, ist es nötig, auf molekularer Ebene die Effektor-Moleküle zu analysieren, die für die Entwicklung einer Granulomnekrose verantwortlich sind.

Das Ziel dieser Arbeit war, anhand eines publizierten Mausmodells der *M. avium*-vermittelten pulmonaren Immunpathologie in der Maus, (i) molekulare Signalwege zu identifizieren, die für die Entwicklung der Granulomnekrose verantwortlich sind; (ii) herauszufinden, ob diese Signalwege modulierbar sind, um eine Granulomnekrose zu verhindern; (iii) Erkenntnisse aus diesem Model für Einblicke in die pathophysiologische Umgebung und den metabolischen Zustand von *M. tuberculosis* im Lungengranulom zu nutzen.

Die wesentlichen Befunde der in diesem Forschungsansatz durchgeführten Experimente sind: (i) IFN- γ und die Signalmoleküle STAT-1 und IRF-1 sind an der Granulomnekrose beteiligt. Insbesondere IRF-1 stellte sich als ein Effektor-Molekül heraus, das einen therapeutischen Ansatz bietet, um die Pathologie zu verhindern, ohne den Schutz zu beeinträchtigen. (ii) Granulomnekrose geht mit einem geänderten Gleichgewicht zwischen angiogenetischen und angiostatischen Mediatoren einher, sodass Angiostase überwiegt. Bei Abwesenheit des Rezeptors CXCR3 war jedoch weder die IFN- γ -vermittelte Angiostase noch die Entwicklung einer Granulomnekrose aufgehoben. (iii) Die IFN- γ -vermittelte Granulomnekrose weist eine starke Hypoxie in mit *M. avium* infizierten Mäusen und in mit *M. tuberculosis* infizierten Meerschweinchen auf, nicht jedoch in Mäusen, die mit *M. tuberculosis* infiziert sind.

Diese Befunde haben wichtige Konsequenzen für die Nutzung von Tiermodellen der Tuberkulose, wenn es darum geht, neue Chemotherapeutika zu testen und die Mechanismen der Latenz und Persistenz des Tuberkuloseerregers zu definieren.

Acknowledgement

It is a pleasure to find the chance to show my gratitude and all my regards to my supervisor Prof. Dr. med. Stefan Ehlers for proposing this interesting subject, his instructive supervision, his kind help, his continuous encouragement as well as for the great work conditions in the division of Molecular Infection Biology.

I would like to express my cordial thanks and gratitude to Prof. Dr. Dr. h.c. Ernst Theodor Rietschel for his valuable suggestions, his fruitful discussions, his unforgettable support and for the excellent work facilities at the Research Center Borstel.

Many thanks for the friendly cooperation to PD Dr. Tamás Laskay and Birgit Hansen, University of Lübeck, for their help and support in carrying out the Ribonuclease Protection Assays, Prof. Dr. med. Klaus Wagner, University of Lübeck, for performing the oxygen measurements with the micro-electrode, Dr. med. Roland Lang and Dr. Jörg Mages, Technical University of München, for conducting the micro-array analysis and evaluation, Dr. Jörg Mages for helping a lot with the statistical analysis of the arrays, Prof. Dr. Ian Orme, Colorado State University, USA, for providing lungs and lymph nodes from TB-infected guinea pigs, Prof. Dr. Christoph Hölscher und Dr. Christine Keller, Research Center Borstel, for providing TB-infected mice, PD Dr. Sven Brandau and Gabriele Bentien, Research Center Borstel, for providing tumor cells.

I would like to thank my lab-group for the nice time I spent with them, for their help and assistance whenever I needed it. A special appreciation to Alexandra Hölscher, who introduced me to the techniques of Infection Biology with a lot of patience and a deep insight, I will never forget her critical eye, her keen observation and her assistance, whenever I asked for it.

Special thanks also to Maike Kohlmorgen for her help and support in good times and bad times.

Finally, I would like to thank my small very scientific family, my father, my mother and my sister, who were always there for me, especially my parents, who supported me and made it possible for me to set my own goals and to reach them.

Thank you!

Danksagung

Ich freue mich, diese Gelegenheit nutzen zu können, um meinem Betreuer Prof. Dr. med. Stefan Ehlers Achtung und Dank zu erweisen für seine lehrreiche Betreuung, seine freundliche Hilfe, seine ununterbrochene Unterstützung sowie für die großartigen Arbeitsbedingungen in der Laborgruppe Molekulare Infektiologie.

Herrn Prof. Dr. Dr. h.c. Ernst Theodor Rietschel möchte ich meinen herzlichsten Dank aussprechen für seine hilfreichen Vorschläge und die fruchtbaren Diskussionen, seine unvergessliche Unterstützung und die hervorragenden Arbeitsbedingungen am Forschungszentrum Borstel.

Ich bedanke mich auch sehr für die freundliche Kooperation bei PD Dr. Tamás Laskay und Birgit Hansen, Universität zu Lübeck, für ihre Hilfe und Unterstützung bei der Durchführung der Ribonuclease Protection Assays, Prof. Dr. med. Klaus Wagner, Universität zu Lübeck, für die Ausführung der Sauerstoffmessungen mit der Mikro-Elektrode, Dr. med. Roland Lang und Dr. Jörg Mages, Technische Universität München, für die Durchführung der Mikro-Array Analysen und der Auswertung, Dr. Jörg Mages für seine große Hilfe bei den statistischen Analysen der Arrays, Prof. Dr. Ian Orme, Colorado State Universität, USA, für die Bereitstellung von Lungen und Lymphknoten aus TB-infizierten Meer-schweinchen, Prof. Dr. Christoph Hölscher und Dr. Christine Keller, Forschungszentrum Borstel, für die Bereitstellung von TB-infizierten Mäusen, PD Dr. Sven Brandau und Gabriele Bentien, Forschungszentrum Borstel, für die Bereitstellung von Tumorzellen.

Bei meiner Laborgruppe möchte ich mich bedanken für die schöne Zeit, die ich mit allen verbracht habe und für ihre Hilfsbereitschaft, wenn ich sie gebraucht habe. Ein besonderer Dank geht an Alexandra Hölscher, die mich in die Methoden der Infektionsbiologie mit viel Geduld und Verständnis eingeführt hat. Ihr kritisches Auge, ihre lebhaftige Beobachtung und ihre Hilfe, wenn ich sie brauchte, werde ich nie vergessen.

Ein besonderer Dank auch an Maike Kohlmorgen für ihre Hilfe und Unterstützung in guten und in schlechten Zeiten.

Am Ende, will ich mich bei meiner kleinen, sehr wissenschaftlichen Familie bedanken, meinem Vater, meiner Mutter und meiner Schwester, die immer für mich da waren, besonders meine Eltern, die mich unterstützt und es mir ermöglicht haben, meine eigenen Ziele zu setzen und sie zu erreichen.

Vielen Dank!

Curriculum

NAME : Sahar El-Sayed Hassan Abbas Aly
DAY OF BIRTH : 20th of March 1970 in Alexandria, Egypt
NATIONALITY : Egyptian

COURSE OF EDUCATION

- Heusteigschule, from 1976-1980, Stuttgart, Germany
- Deutsche Schule der Borromäerinnen, from 1980-1985, Alexandria, Egypt
- Manarat El-Riyadh, from 1985-1988, Riyadh, Saudi-Arabia
- Graduation with secondary school certificate, 1988
- Department of Biology, from 1989-1991, Faculty of Science, Alexandria University, Egypt
- Department of Biochemistry, from 1991-1993, Faculty of Science, Alexandria University, Egypt
- Graduation with Bc. Sc. in biochemistry, grade good, 1993
- Post-graduate studies, from 1993-1999, Faculty of Science, Alexandria University, Egypt
- Post-graduate diploma in biochemistry, grade very good, 1994
- First part of M. Sc. degree in biochemistry, grade very good, 1995
- Receiving the M. Sc. degree in biochemistry, 1999
- Post-graduate studies, since 2003, Faculty of Science, University of Lübeck, Germany

EXTRA-CURRICULAR STUDIES

- Intensive English course, from 1988-1989, King-Saud University, Saudi-Arabia
- Intensive computer course, Computer Center of the Alexandria University, grade distinction, 1995, Alexandria, Egypt
- Preparatory course at the Goethe-Institut Alexandria for the specialized diploma in German language KDS in Cairo, from 1996-1997, Alexandria, Egypt
- KDS exam, 1997, Cairo, Egypt
- Receiving the KDS certificate from the Ludwig-Maximilians-University München with best grades of the year, 1998, München, Germany

SCIENTIFIC EXPERIENCE

- Training in the laboratory of the Alexandria Insurance Hospital, 1993, Alexandria, Egypt
- Working in the laboratory of the German Hospital, from 1993-1994, Alexandria, Egypt
- Training in the central laboratory of the Alexandria University Hospital, from 1994-1997, Alexandria, Egypt
- Working on the practical part of the M. Sc. degree in the Main Hospital of the Alexandria University Faculty of Medicine, from 1995-1999, Alexandria, Egypt
- Obtaining the license for practicing the profession of Medical Analysis from the Egyptian Ministry of Health
- Ph.D. student at the Research Center Borstel, Leibniz-Center for Medicine and Biosciences, Department of Immunochemistry and Biochemical Microbiology, Division of Molecular Infection Biology, since May 2003, Borstel, Germany

EXTRA-SCIENTIFIC ACTIVITIES

- General and scientific translation from and into German, English, French and Arabic, since 1993, Alexandria, Egypt
- Teaching German at the Alexandria University, Faculty of Science, Faculty of Engineering, Faculty of Tourism and Hotels, Community Development Center CDC, as well as at the Institute of the Egyptian Organization for Tourism and Hotels EGOH, from 1995-2001, Alexandria, Egypt
- General Secretary of the Regional Office of the Euro-Arab Cooperation Center VEA (Headquarters located in Köln, Germany), from June 1999 till May 2000, Alexandria, Egypt
- Translator and simultaneous translator at the Bibliotheca Alexandrina, from September 2001 till June 2002, Alexandria, Egypt
- Head of the Specialized Translation Unit at the Manuscript Center of the Bibliotheca Alexandrina, from June 2002 till April 2003, Alexandria, Egypt

MEMBERSHIPS

- Member of the German for Specific Purposes GSP Center, since 1995, Alexandria, Egypt
- Member of the Egyptian-German Society North ADGN, since 2004, Hamburg, Germany
- Member of the New York Academy of Sciences, since 2005, New York, USA

CONFERENCES

- Attending the conference: German Language in Science and Technology, 1996, Alexandria, Egypt
- Simultaneous translation and public relation at the 9th, 10th and 11th international conference: Environmental Protection Is A Must, 1999, 2000 and 2001, Alexandria, Egypt
- Attending the conference: German Translation, 2000, 2001 and 2002, Cairo, Egypt
- Attending the 34th Annual Meeting of the German Society of Immunology, September 2003, Berlin, Germany
- Attending the 55th Meeting of the German Society for Microbiology and Hygiene, October 2003, Dresden, Germany
- Attending the 8th Symposium of the German Society for Immunology: Infection and Immune Defense, March 2004, Burg Rothenfels, Germany
- Attending BioVision Alexandria, April 2004, Alexandria, Egypt
- Presenting a poster at the International Symposium: Inflammation and Immune Response, special research program SFB 367 of the German Research Foundation DFG, September 2004, Lübeck, Germany
- Holding a presentation at the 9th Symposium of the German Society for Immunology: Infection and Immune Defense, March 2005, Burg Rothenfels, Germany
- Attending The World Life Sciences Forum BioVision, as a member of the BioVision Next delegation, April 2005, Lyon, France
- Attending the IVth Autumn Seminar on Pathology and Biomedicine, September 2005, Borstel, Germany
- Attending the 36th Annual Meeting of the German and Scandinavian Societies of Immunology, September 2005, Kiel, Germany

WORKSHOPS

- Simultaneous translation at the match-making workshop of the German Arab Chamber of Industry and Commerce, 2001, Alexandria, Egypt
- Attending the 26th and 27th workshop of the Northern German Immunologists, November 2003 and 2004, Borstel, Germany

EXHIBITIONS

- Main member of the Egyptian Delegation representing the Guest of Honor, The Arab World, 22 Arabic Countries of the Arab League as well as the Bibliotheca Alexandrina at the International Book Fair, October 2004, Frankfurt, Germany

PUBLICATIONS

- Eissenhauer, S.; Aly, S., A Reading Course in German for Scientists - Deutsch für Naturwissenschaftler - Eine Einführung in die Strukturen des Deutschen, DAAD, Bonn, 1997
- Balbaa, M.; Abbas, S.; El-Deen, S.; Hassab, A.; Awad, O., Some hydrolases in human schistosomiasis with special reference to arylsulfatase B, International Journal of Environmental Studies, December 2003, vol. 60, no. 6, pp. 563-573
- Ehlers, S.; Aly, S., Tuberculosis Research: The Promise of Genetics and Biotechnology – Scientific and Ethical Issues, In Discovery to Delivery: BioVision Alexandria 2004, I. Serageldin and G. J. Persley (eds.), Bibliotheca Alexandrina, Alexandria, 2005, pp. 227-251
- Schreiber, T.; Ehlers, S.; Aly, S.; Hölscher, A.; Hartmann, S.; Lipp, M.; Lowe, J. B.; Hölscher, C., Selectin ligand-independent priming and maintenance of T cell immunity during airborne tuberculosis, The Journal of Immunology, January 2006, vol. 176, pp. 1131–1140
- Aly, S.; Wagner, K.; Keller, C.; Malm, S.; Malzan, A.; Basaraba, R. J.; Orme, I.; Brandau, S.; Bange, F.; Ehlers, S., Granulomatous lesions in the lungs of mice chronically infected with Mycobacterium tuberculosis are not severely hypoxic, submitted for publication
- Aly, S.; Laskay, T.; Vestweber, D.; Malzan, A.; Lu, B.; Gerard, C.; Lang, R.; Ehlers, S., Imbalance of angiogenic vs. angiostatic mediators as a possible cause for granuloma necrosis in mycobacterial infections, to be submitted

Lebenslauf

NAME : Sahar El-Sayed Hassan Abbas ALY
GEBURTSTAG : 20. März 1970 in Alexandria, Ägypten
NATIONALITÄT : Ägypterin

BILDUNGSGANG

- Heusteigschule, von 1976 bis 1980, Stuttgart, Deutschland
- Deutsche Schule der Borromäerinnen, von 1980 bis 1985, Alexandria, Ägypten
- Manarat El-Riyadh, von 1985 bis 1988, Riyadh, Saudi-Arabien
- Abschluss: secondary school certificate, 1988
- Abteilung der Biologie, von 1989 bis 1991, Naturwissenschaftliche Fakultät, Universität Alexandria, Ägypten
- Abteilung der Biochemie, von 1991 bis 1993, Naturwissenschaftliche Fakultät, Universität Alexandria, Ägypten
- Abschluss: Bc. Sc. in Biochemie, Note: gut, 1993
- Postgraduale Studien, von 1993 bis 1999, Naturwissenschaftliche Fakultät, Universität Alexandria, Ägypten
- Postgraduales Diplom in Biochemie, Note: sehr gut, 1994
- Erster Teil des M. Sc. Grades in Biochemie, Note: sehr gut, 1995
- Erteilung des M. Sc. Grades in Biochemie, 1999
- Postgraduale Studien, seit 2003, Naturwissenschaftliche Fakultät, Universität zu Lübeck, Deutschland

ZUSATZQUALIFIKATIONEN

- Intensiver Englischkurs, von 1988 bis 1989, King-Sauds-Universität, Saudi-Arabien
- Intensiver Computerkurs, Computerzentrum der Universität Alexandria, Note: exzellent, 1995, Alexandria, Ägypten
- Vorbereitungskurs am Goethe-Institut Alexandria auf die Prüfung des Kleinen Deutschen Sprachdiploms KDS in Kairo, von 1996 bis 1997, Alexandria, Ägypten
- KDS-Prüfung, 1997, Kairo, Ägypten
- Erteilung des KDS-Zertifikats der Ludwig-Maximilians-Universität München mit der besten Leistung des Jahres, 1998, München, Deutschland

WISSENSCHAFTLICHE ERFAHRUNGEN

- Praktikantin im Labor des Alexandriner Versicherungskrankenhauses, 1993, Alexandria, Ägypten
- Laborärztin im Labor des Deutschen Krankenhauses, von 1993 bis 1994, Alexandria, Ägypten
- Praktikantin im Zentrallabor des Alexandriner Universitätskrankenhauses, von 1994 bis 1997, Alexandria, Ägypten
- Bearbeitung des praktischen Teiles des M. Sc. Grades im Hauptkrankenhaus der Medizinischen Fakultät der Universität Alexandria, von 1995 bis 1999, Alexandria, Ägypten
- Erteilung der Lizenz zur Ausübung der Medizinischen Analyse vom ägyptischen Gesundheitsministerium
- Doktorandin am Forschungszentrum Borstel, Leibniz-Zentrum für Medizin und Biowissenschaften, Abteilung Immunchemie und Biochemische Mikrobiologie, Laborgruppe Molekulare Infektiologie, seit Mai 2003, Borstel, Deutschland

AUSSERWISSENSCHAFTLICHE TÄTIGKEITEN

- Allgemeine und wissenschaftliche Übersetzung von und in die deutsche, englische, französische und arabische Sprache, seit 1993, Alexandria, Ägypten
- Deutschlehrerin an der Universität Alexandria, an der Naturwissenschaftlichen Fakultät, an der Ingenieurwissenschaftlichen Fakultät, an der Fakultät für Tourismus und Hotels, am Gesellschaftsentwicklungszentrum sowie am Institut der ägyptischen Gesellschaft für Tourismus und Hotels EGOH, von 1995 bis 2001, Alexandria, Ägypten
- Generalsekretärin der Filiale des Vereins für Europäisch-Arabische Zusammenarbeit VEA (Hauptsitz in Köln, Deutschland), von Juni 1999 bis Mai 2000, Alexandria, Ägypten
- Übersetzerin und Dolmetscherin an der Bibliotheca Alexandrina, von September 2001 bis Juni 2002, Alexandria, Ägypten
- Leiterin der spezialisierten Übersetzungsabteilung am Manuskriptzentrum der Bibliotheca Alexandrina, von Juni 2002 bis April 2003, Alexandria, Ägypten

MITGLIEDSCHAFTEN

- Mitglied des German for Specific Purposes GSP Center, seit 1995, Alexandria, Ägypten
- Mitglied der Ägyptisch-Deutschen Gesellschaft Nord ADGN, seit 2004, Hamburg, Deutschland
- Mitglied der New York Academy of Sciences, seit 2005, New York, USA

KONGRESSE

- Teilnahme an der Konferenz "Deutsche Sprache in Wissenschaft und Technik", 1996, Alexandria, Ägypten
- Dolmetscherin und Public Relations auf dem 9., 10. und 11. internationalen Kongress "Umweltschutz ist dringend", 1999, 2000 und 2001, Alexandria, Ägypten
- Teilnahme an der Konferenz "Deutsche Übersetzung", 2000, 2001 und 2002, Kairo, Ägypten
- Teilnahme an der 34. Jahrestagung der Deutschen Gesellschaft für Immunologie, September 2003, Berlin, Deutschland
- Teilnahme an der 55. Tagung der Deutschen Gesellschaft für Mikrobiologie und Hygiene, Oktober 2003, Dresden, Deutschland
- Teilnahme am 8. Symposium der Deutschen Gesellschaft für Immunologie "Infektion und Immunabwehr", März 2004, Burg Rothenfels, Deutschland
- Teilnahme an BioVision Alexandria, April 2004, Alexandria, Ägypten
- Posterpräsentation im Rahmen des internationalen Symposiums "Inflammation and Immune Response", Sonderforschungsbereich SFB 367 der Deutschen Forschungsgesellschaft DFG, September 2004, Lübeck, Deutschland
- Vortrag im Rahmen des 9. Symposiums der Deutschen Gesellschaft für Immunologie "Infektion und Immunabwehr", März 2005, Burg Rothenfels, Deutschland
- Teilnahme am World Life Sciences Forum BioVision, als Mitglied der BioVision Next Delegation, April 2005, Lyon, Frankreich
- Teilnahme am IV. Herbstseminar für Pathologie und Biomedizin, September 2005, Borstel, Deutschland
- Teilnahme an der 36. Jahrestagung der Deutschen und der Skandinavischen Gesellschaft für Immunologie, September 2005, Kiel, Deutschland

WORKSHOPS

- Dolmetscherin auf dem match-making Workshop der Deutsch-Arabischen Industrie- und Handelskammer, 2001, Alexandria, Ägypten
- Teilnahme am 26. und 27. Arbeitstreffen der Norddeutschen Immunologen, November 2003 und 2004, Borstel, Deutschland

AUSSTELLUNGEN

- Hauptmitglied der ägyptischen Delegation in Vertretung des Ehrengasts, Die Arabische Welt, 22 arabische Länder der Arabischen Liga sowie die Bibliotheca Alexandrina auf der Internationalen Buchmesse, Oktober 2004, Frankfurt, Deutschland

VERÖFFENTLICHUNGEN

- Eissenhauer, S.; Aly, S., A Reading Course in German for Scientists - Deutsch für Naturwissenschaftler - Eine Einführung in die Strukturen des Deutschen, DAAD, Bonn, 1997
- Balbaa, M.; Abbas, S.; El-Deen, S.; Hassab, A.; Awad, O., Some hydrolases in human schistosomiasis with special reference to arylsulfatase B, International Journal of Environmental Studies, December 2003, vol. 60, no. 6, pp. 563-573
- Ehlers, S.; Aly, S., Tuberculosis Research: The Promise of Genetics and Biotechnology – Scientific and Ethical Issues, In Discovery to Delivery: BioVision Alexandria 2004, I. Serageldin and G. J. Persley (eds.), Bibliotheca Alexandrina, Alexandria, 2005, pp. 227-251
- Schreiber, T.; Ehlers, S.; Aly, S.; Hölscher, A.; Hartmann, S.; Lipp, M.; Lowe, J. B.; Hölscher, C., Selectin ligand-independent priming and maintenance of T cell immunity during airborne tuberculosis, The Journal of Immunology, January 2006, vol. 176, pp. 1131–1140
- Aly, S.; Wagner, K.; Keller, C.; Malm, S.; Malzan, A.; Basaraba, R. J.; Orme, I.; Brandau, S.; Bange, F.; Ehlers, S., Granulomatous lesions in the lungs of mice chronically infected with Mycobacterium tuberculosis are not severely hypoxic, submitted for publication
- Aly, S.; Laskay, T.; Vestweber, D.; Malzan, A.; Lu, B.; Gerard, C.; Lang, R.; Ehlers, S., Imbalance of angiogenic vs. angiostatic mediators as a possible cause for granuloma necrosis in mycobacterial infections, to be submitted